A STABLE ISOTOPE STUDY of the KAAP VALLEY TONALITE, BARBERTON MOUNTAIN LAND, SOUTH AFRICA.

by
KEVIN FAURE

Thesis submitted in fulfilment of the requirements
for the degree of
Master of Science

Department of geochemistry
University of Cape Town
September, 1989

DECLARATION

I hereby declare that all the work presented in this thesis is my own, except where otherwise stated.

Signed by candidate

K. FAURE

Signature removed

CONTENTS

ABSTRACT

The Kaap Valley Tonalite (KVT) was a homogenous hornblende + biotite tonalite that had been subjected to overall propylitic and potassic alteration. Petrographic studies reveal that carbonate alteration and increased proportions of hydrous minerals occur along the KVT and Barberton greenstone belt contact zone, and along major shear zones within the KVT.

Oxygen isotope analysis of silicate minerals indicate that subsolidus hydrothermal exchange occurred with all the KVT minerals except perhaps quartz. Mineral-mineral fractionations are varied for each mineral pair and open system conditions are indicated from δ-δ, "isotherm" diagrams and petrographic evidence. Mineral disequilibria are fairly small, indicating reasonably low water/rock ratios. Chlorite cation thermometry indicates that they formed at temperatures between 150 and 300 °C (mean, 252 °C). The generally constant $\delta^{18}O$ values of plagioclase (+7.4 ‰) at varying degrees of alteration, indicates that plagioclase $\delta^{18}O$ values were buffered by the alteration. At 250 °C $\Delta_{plag-H2O}$ is ~ +7 ‰, so a $\delta^{18}O_{H2O}$ of ~ 1 ‰ would account for the constant plagioclase values. The average chlorite formed at 250 °C would have been in equilibrium with water having $\delta^{18}O$ values of ~ +2 ‰. Hence the plagioclase and chlorite $\delta^{18}O$ values are consistent with exchange with an aqueous fluid of $\delta^{18}O$ of +1 to +2 ‰ at 250 °C. This fluid has a $\delta^{18}O$ slightly heavier than possible meteoric fluid and may represent meteoric fluid that had exchanged ^{18}O with the wall-rocks, or a mixture of meteoric and magmatic fluid, where the meteoric component is dominant.

The carbonates from the carbonated KVT can be subdivided into two groups on the basis of their $\delta^{18}O$ and $\delta^{13}C$ data. Group A has $\delta^{18}O$ between +6 and +9 ‰ and $\delta^{13}C$ between -6 and -2 ‰ and group B has $\delta^{18}O$ between +11 and +25 ‰ and $\delta^{13}C$ between -3 and 0 ‰. Two models can explain the carbonate data. (1) The CO_2-bearing fluid precipitated group A carbonates at high temperatures (~ 250 °C) and group B carbonates at lower temperatures (< 250 °C). (2) The two

groups can be modelled as coming from two different sources. The group A carbonates precipitated from fluids at ~ 250 °C containing magmatic carbon; a second generation of carbonates precipitated at low temperatures (< 50 °C), from fluids which had dissolved carbon from Archaean carbonate sediments. Group B carbonates are mixtures of this second group and group A. It is suggested that model (2) involving two generations of calcite is more likely.

On the basis of its mineralogy the KVT is an I-type granitoid but the molecular $Al_2O_3/(Na_2O+K_2O+CaO)$ ratio indicates that the KVT is an S-type granitoid. The $\delta^{18}O$ value of the KVT magma was +9.7 ‰, estimated from the average quartz $\delta^{18}O$ values. This value is ~ 3 ‰ heavier than mantle melts, and the KVT must represent a contaminated mantle magma or a crustal melt.

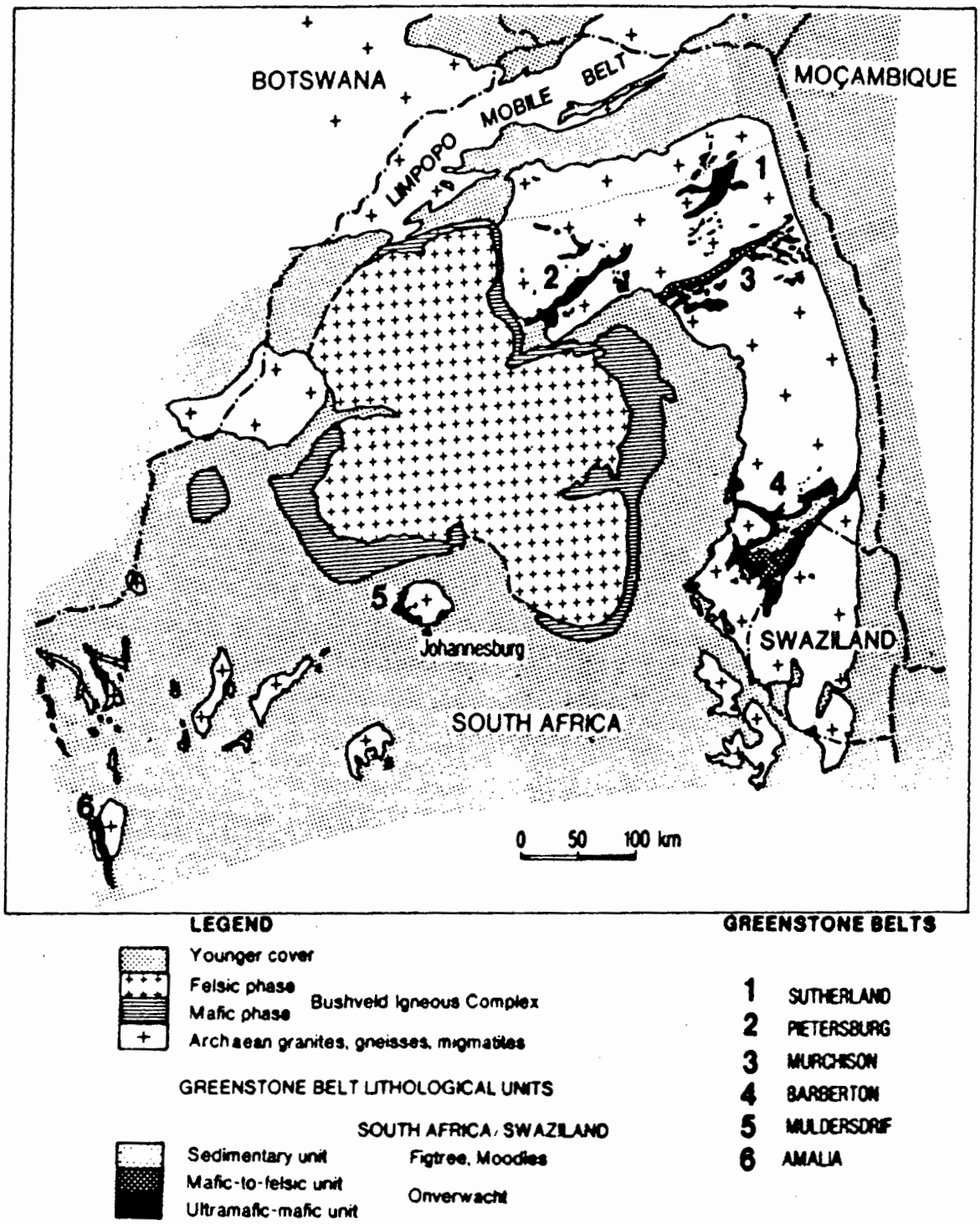

Figure 1.1 Map illustrating the exposed granite-greenstone terrain of the Kaapvaal Craton, South Africa. After Anhaeusser, 1986.

Table 1.1:
Selected isotopic ages for some units of the Barberton granite-greenstone terrain, discussed in this study. The isotopic ages are in Ma.

Rock Types	Units	Pb/Pb, Whole Rock	U/Pb, Zircons *Ion Microprobe	Rb/Sr, @Sm/Nd, Whole Rock
Mafic/ Umafic	Onverwacht Group	3460+70[a]		@3560±240[c] @3510±60[c]
Bimodal Suite	Ancient Gneiss Complex(Swazil.)			@3590±75[d] @3417±34[e]
Tonalite/ Trond-hjemite	Kaap Valley Pluton	$3211^{+94\ b}_{-102}$	*3223±8[f] *3223±5[g] 3270±80[i]	3491±166[h,b]
	Stentor Gneiss		$*3347^{+60g}_{-67}$	
	Stentor Pluton		*3250±30[g]	2755±51[h]
	Theespruit Pluton		*3437±3[b]	3432±135[h]

Data from: a, Brevart et al.,1986; b, Robb et al.,1986; c, Hamilton et al.,1979; d, Tegtmeyer et al.,1985; e, Carlson et al.,1983; f, de Wit et al.,1987; g, Tegtmeyer and Kroner 1987; h, Barton et al., 1983 i, Oosthuisen, 1970 recalculated"

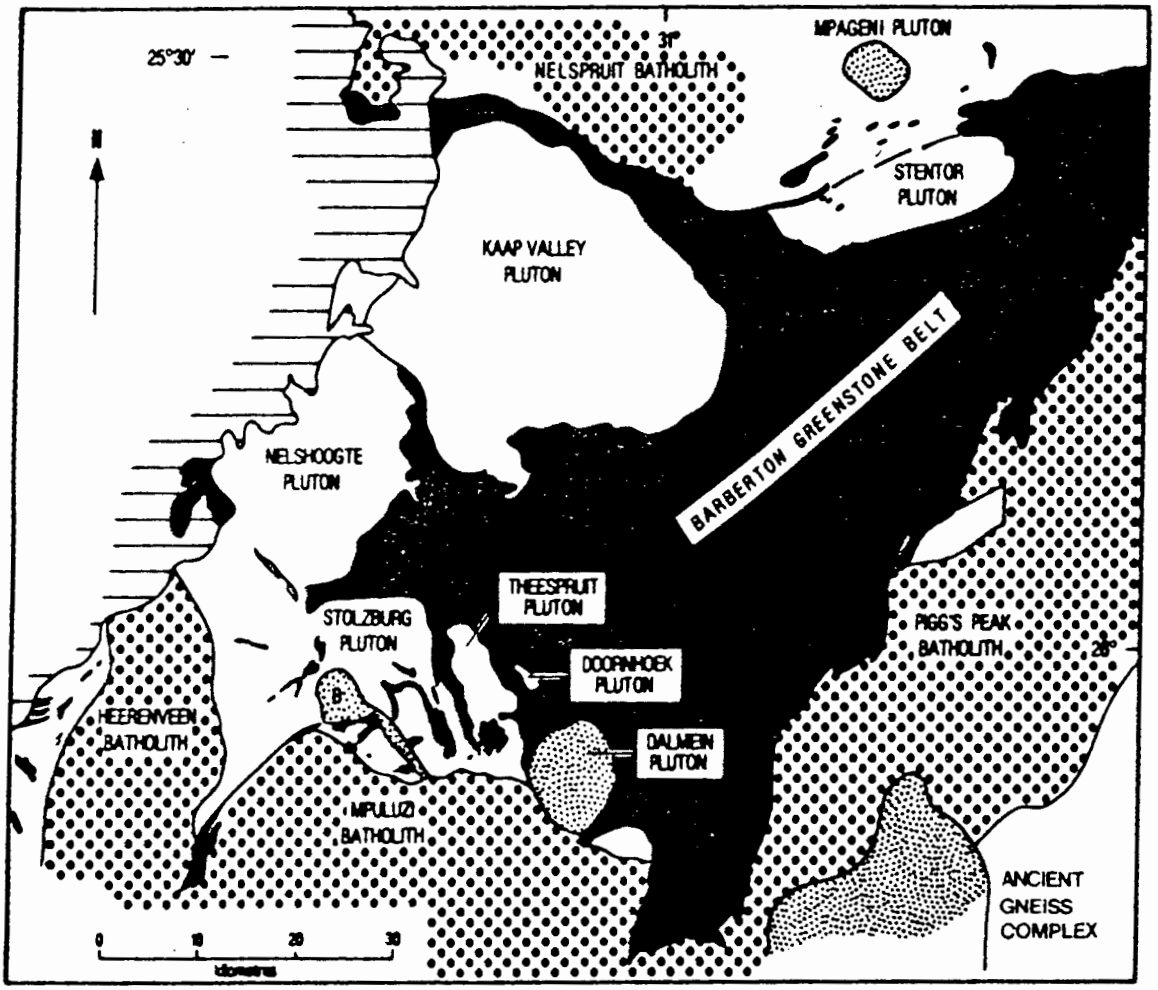

Figure 1.2 Map illustrating a portion of the Barberton granite-greenstone terrain. The black shows the greenstone belt succession and the horizontal stripes represent the Proterozoic cover rocks. The heavy dotted pattern shows a portion of the early potassic batholiths and the fine dotted patterns the distribution of some of the late potassic plutons. The white areas are the tonalite-trondhjemite plutons. After Barton, 1983.

geological relationship between the Ancient Gneiss Complex and the Barberton greenstone belt is uncertain as they have been intruded at their contacts by later TTG plutons (Anhaeusser, 1986;Fig. 1.2).

Two entirely different regional models for the Barberton Mountain Land have been suggested. The first model considers the BGB to be composed of a "layer-cake" stratigraphy, ca. 20 km thick, of extrusive ultramafic(komatiitic)-mafic-felsic lavas overlain by a pile of sedimentary sequences. TTG diapirs, especially in the northwest and southwest flank of the Barberton greenstone belt, caused vertical deformation and disrupted the broad regional pattern of the volcano-sedimentary pile (Anhaeusser, 1969, 1986; Anhaeusser and Robb, 1980; Robb and Anhaeusser, 1983; Viljoen and Viljoen, 1969b; Viljoen et al., 1983; Smith and Erlank, 1980, 1982).

The second model suggested by de Wit et al. (1987b) proposed that the lower ultramafic to mafic part of the greenstone succession contains an ophiolite-like stratigraphy and formed as oceanic crust (ca. 3 km thick) by processes similar to those operating at mid-oceanic ridges today. De Wit et al. (1987b) suggest that thrusting and nappe formation within the greenstone belt have resulted in much of the supposed "layer-cake" successions being due to tectonic repetition.

Magmatic cycles have been proposed by Viljoen and Viljoen (1969b), Robb and Anhaeusser (1983) and Anhaeusser (1981) to categorise TTG plutons in the Barberton Mountain Land. Broadly, they envisage an initial sodic granitoid emplacement (ca. 3.5 Ga) represented by the Ancient Gneiss Complex of Swaziland and the tonalite-trondhjemite plutons adjacent to the Barberton greenstone belt (Fig. 1.2). This was followed by an extensive second cycle of potassium-rich granite batholiths (ca. 3.2 Ga) and a third cycle (ca. 2.9 Ga) of mainly potassium-rich granites and syenitic plutons (Fig. 1.2).

The TTG plutons on the west and south-west portions of the Barberton greenstone belt (Fig. 1.2) have been described by Visser et al. (1956), Anhaeusser (1966), Viljoen and Viljoen (1969b) and Robb and Anhaeusser (1983). The hornblende-bearing tonalites and the leucocratic biotite-

bearing rocks of trondhjemitic composition account for the greatest proportion of the TTG outcrop. The most prominent of these, the Kaap Valley Tonalite (KVT) near Barberton, has U-Pb zircon ages of 3.22 Ga and a $^{207}Pb/^{206}Pb$ whole-rock minimum age which does not agree with a Rb-Sr whole-rock isochron age of about 3.5 Ga (Table 1.1). U-Pb zircon ages show that the trondhjemitic Stentor (3.3 Ga) and Theespruit plutons (3.4 Ga) pre-date the KVT which was previously considered to be one of the oldest TTG plutons (Robb et al., 1986; Barton et al., 1983).

Archaean tonalite-trondhjemite plutons form an integral part of the typical granitoid-greenstone terrain of the Barberton Mountain Land. Most studies of the TTG are either of a reconnaissance nature or consider the plutons collectively because of the difficulty in delineating their individual extent. However, the KVT pluton is largely surrounded by the Barberton greenstone belt (Fig. 1.2) and has therefore been part of many regional studies of the Barberton Mountain Land (Hall 1918; Visser et al., 1956; Ramsay, 1963; Viljoen and Viljoen, 1969b; Anhaeusser, 1966, 1969; Condie and Hunter, 1976; Barton et al., 1983; Robb and Anhaeusser, 1983; Layer, 1986; Robb et al., 1983; Tegtmeyer and Kroner, 1987; de Beer et al., 1988) and of one detailed study (Robb et al., 1986).

The BGB immediately adjacent to the KVT, hosts small to moderately sized gold deposits. Regionally, more than 95% of the gold has been recovered from the north-west flank of the BGB, of which over 90% of the gold and silver has come from greenstone belt rocks within 10 km of the KVT contact (Anhaeusser, 1976). Structural influences (fold, fault and shear zones) appear to have played a dominant role in the localisation of gold mineralisation. Most of the mineralisation is considered to have been precipitated from hydrothermal fluids and the source of the gold to have been syngenetic with the greenstones (Anhaeusser, 1986).

1.3 SCOPE of THESIS

It is well known that granites play an important role in establishing hydrothermal systems. Structures associated with granite emplacement may also aid the migration and deposition of gold and other elements

(Anhaeusser, 1969, 1976, 1986; Foster et al., 1985; Burrows and Spooner, 1988; Smith et al., 1988; Stott and Smith, 1988; Colvine et al., 1988). Even though the altered nature of the KVT was recognised by Visser et al. (1956) and Viljoen and Viljoen (1969b) and Anhaeusser (1976 and 1986) has pointed out the proximity and spatial distribution of the gold mineralisation within the greenstones to the KVT, suggesting a genetic link, no detailed study regarding the alteration or mineralisation aspects, so far, have been undertaken for the KVT.

In other areas, e.g. Skaergaard, Skye, etc., oxygen and hydrogen isotopes have been utilised to establish the existence of fossil hydrothermal systems (Taylor, 1968, 1977; Taylor and Forester, 1979; Magaritz and Taylor 1976a, b) and to investigate aspects of rock alteration and ore deposition (Taylor, 1973, 1974). This study presents petrographic, mineralogical, oxygen and carbon stable isotope data for KVT rocks, mineral separates and vein-quartz, and some Au analyses. These will be used to attempt evaluation of the following:

1. the style and extent of the alteration,
2. the nature of any hydrothermal system set up by the intrusion of the pluton,
3. the stable isotope composition and possible sources of the alteration fluid,
4. to constrain the role of KVT fluids in the development of the surrounding greenstone belt gold deposits and
5. the petrogenesis of the KVT magma.

Although oxygen isotope data exist for some of the Onverwacht Group rocks of the Barberton Sequence (Smith et al., 1984; Hoffman et al., 1986) and for a regional investigation of the Barberton Mountain Land granitoids (Taylor and Magaritz, 1975), no detailed oxygen and carbon stable isotope investigation has been reported for an individual pluton in the BGB, or indeed in southern Africa.

Oxygen isotope studies of plutonic rocks elsewhere are generally of Mesozoic or younger age and therefore an isotopic study of the KVT and prevailing fluids during the Archaean is necessary.

2. GEOLOGY of the KVT

2.1 INTRODUCTION

The KVT is surrounded by the metavolcanics of the BGB in the north, east and south and overlain by the Lower Proterozoic Transvaal Supergroup to the west (Fig. 2.1). The KVT forms the floor of the relatively flat, roughly circular Kaap Valley (ca. 400 km^2) which is broken by low ridges formed by north-west trending Proterozoic dolerite dykes. Outcrop, which takes the form of flat or slightly domed pavements, is generally restricted to river beds, road cuttings and dolerite dyke contact zones. The western half of the pluton is particularly poorly exposed because of extensive en-forestation.

In the most recent study of the KVT, Robb et al. (1986) mapped the KVT as a variably foliated, two-phase tonalite containing:

1. a dominant hornblende tonalite **with** biotite phase, and
2. a smaller, but distinct, hornblende tonalite **without** biotite phase (Fig. 2.1).

Robb et al. (1986) used trace element data to suggest that the KVT parental magma was a trondhjemite derived by partial melting of average komatitic basalt composition, but was contaminated prior to magma emplacement by a mafic component to account for its isotope and distinct mafic character (Condie and Hunter, 1976; Robb and Anhaeusser, 1983). Robb et al. (1986) envisaged "a subdued form of crystal fractionation" which resulted in the formation of discrete hornblende and hornblende + biotite tonalite phases. The KVT was considered to have crystallised ca 3500 Ma ago (Rb-Sr whole-rock isochron: Barton et al., 1983; Robb et al., 1986) and subsequently diapirically emplaced into its present position ca 3200 Ma ago (Rb-Sr biotite whole-rock, Pb-Pb whole-rock, Robb et al., 1986). Diapirism was then thought to have deformed the surrounding greenstone belt and an original sub-horizontal compositional zoning of the KVT (Robb et al., 1986). More recent U-Pb zircon dating, however, indicates a crystallisation age for the KVT of ca 3220 Ma

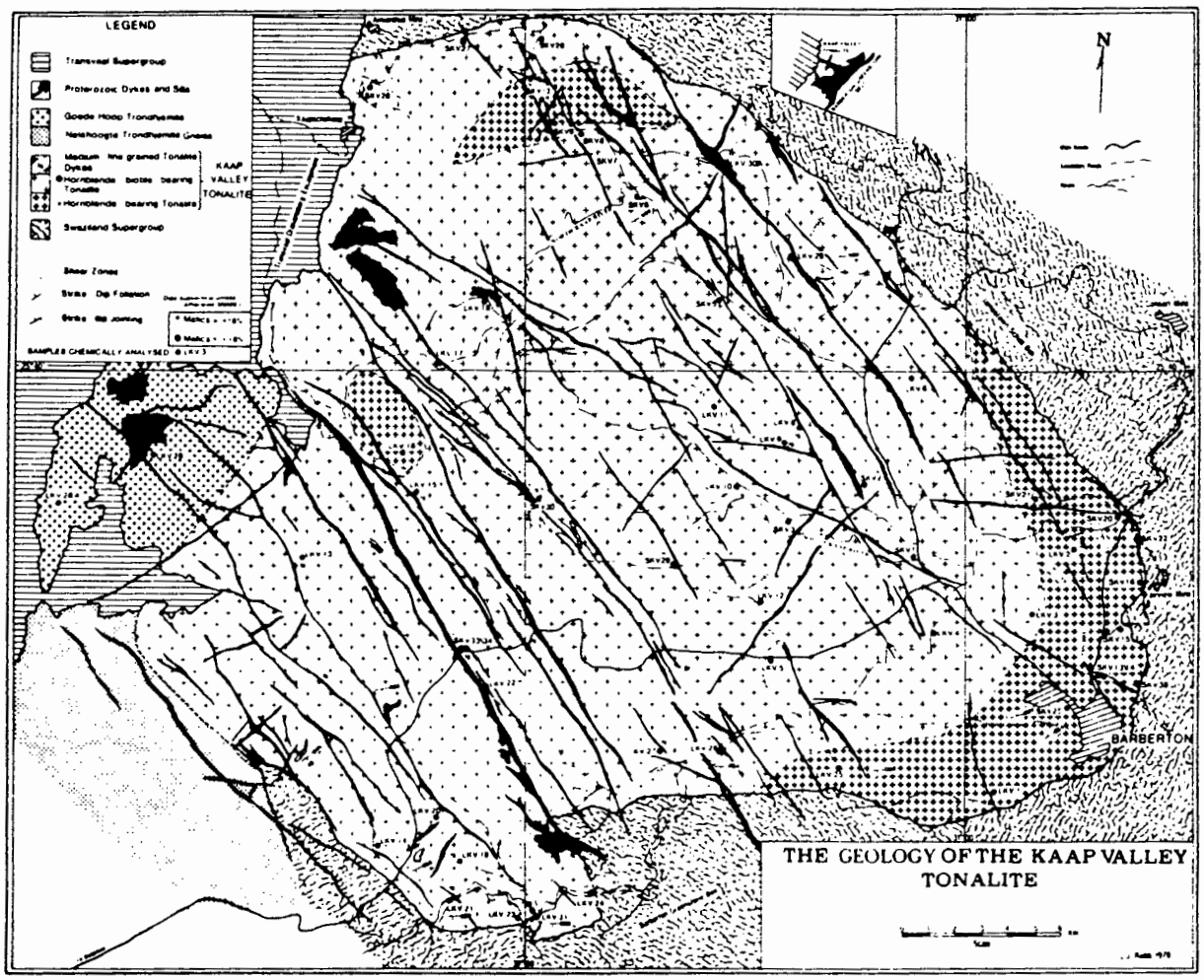

Figure 2.1 The geology of the Kaap Valley Tonalite pluton, after Robb et al., 1986. The KVT was interpreted to consist of (1) a hornblende and (2) a hornblende + biotite phase.

(Tegtmeyer and Kroner, 1987; de Wit et al., 1987a) which demands a later diapiric emplacement in the Robb et al. (1986) model.

It has been suggested that processes analogous to those operating in modern subduction zones were also active in Archaean time (de Wit et al., 1987b; Taylor and McLennan, 1985). Objections to this suggestion arise primarily from compositional differences between Archaean rocks and their modern day equivalents (calc-alkaline volcanics). Thermal evolution models of subducting oceanic plates during the Archaean, however, suggest that tholeiitic basalts in the subducting wet crust melted at depths of 50 to 80 km and produced viscous Archaean tonalitic magmas, that diapirically intruded the lithosphere, as laterally spreading plutons (Arkani-Hamed and Jolly, 1989).

2.2 FIELD RELATIONSHIPS

A well developed foliation and accompanying mineral lineation is present along the enveloping tonalite/greenstone contact but is absent in the centre of the pluton. The mineral lineation and fabric generally dip steeply towards the greenstones, and sub-parallel to the fabric developed in the schists of the adjacent BGB, suggesting contemporaneous deformation of both units (Anhaeusser, 1966, 1969, 1976; Fripp et al., 1980; Viljoen and Viljoen, 1969b).

The contact between the BGB and the KVT is not well exposed. Nevertheless, Anhaeusser (1969, 1966) reported evidence of tonalite crosscutting the greenstones along the southern margin of the Jamestown Schist Belt and a variable, narrow contact-metamorphic halo in the surrounding greenschists (hornblende-hornfels to greenschist facies).

An exposure of the KVT/BGB contact was studied along the Havelock road just north of Barberton (Fig. 2.2, 2.3). Intense shearing of the KVT is limited to a zone of ~5m next to the BGB contact. A petrographic study of this zone shows that it is essentially a cataclastic rock medium- to coarse-grained KVT and has no obvious chill-phase. This shearing is observed at other KVT/Barberton greenstone contacts and is consistent with either a near solid-state emplacement i.e diapirism (Anhaeusser, 1969, 1976; Viljoen and Viljoen, 1969b; Robb and Anhaeusser, 1983; Robb

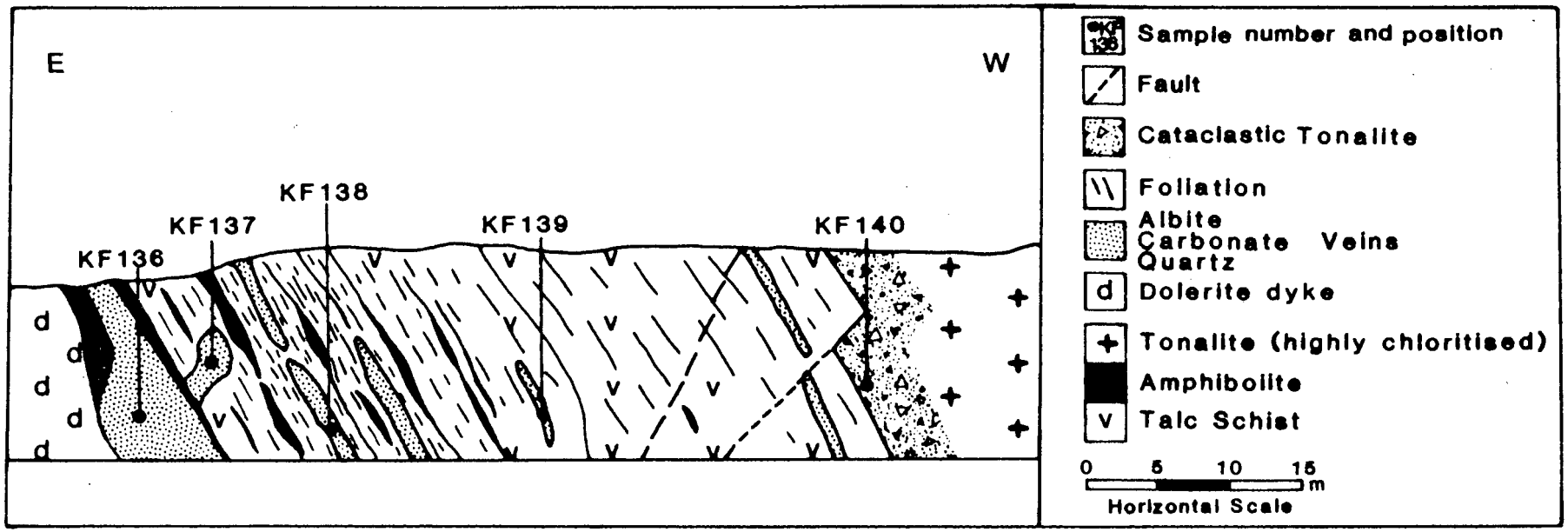

Figure 2.2 A cross-section of the KVT/BGB contact along the Havelock road, immediately north of Barberton. The greenstones have a strong foliation parallel to the plane of the KVT/BGB contact and numerous veins of albite, quartz and carbonate, mostly ankeritic. The KVT/BGB contact at this locality dips towards the tonalite but generally it dips steeply towards the greenstone belt. The KVT has an ~ 5m cataclastic contact and a 100m zone of highly chloritised tonalite from the contact (see Fig. 2.4).

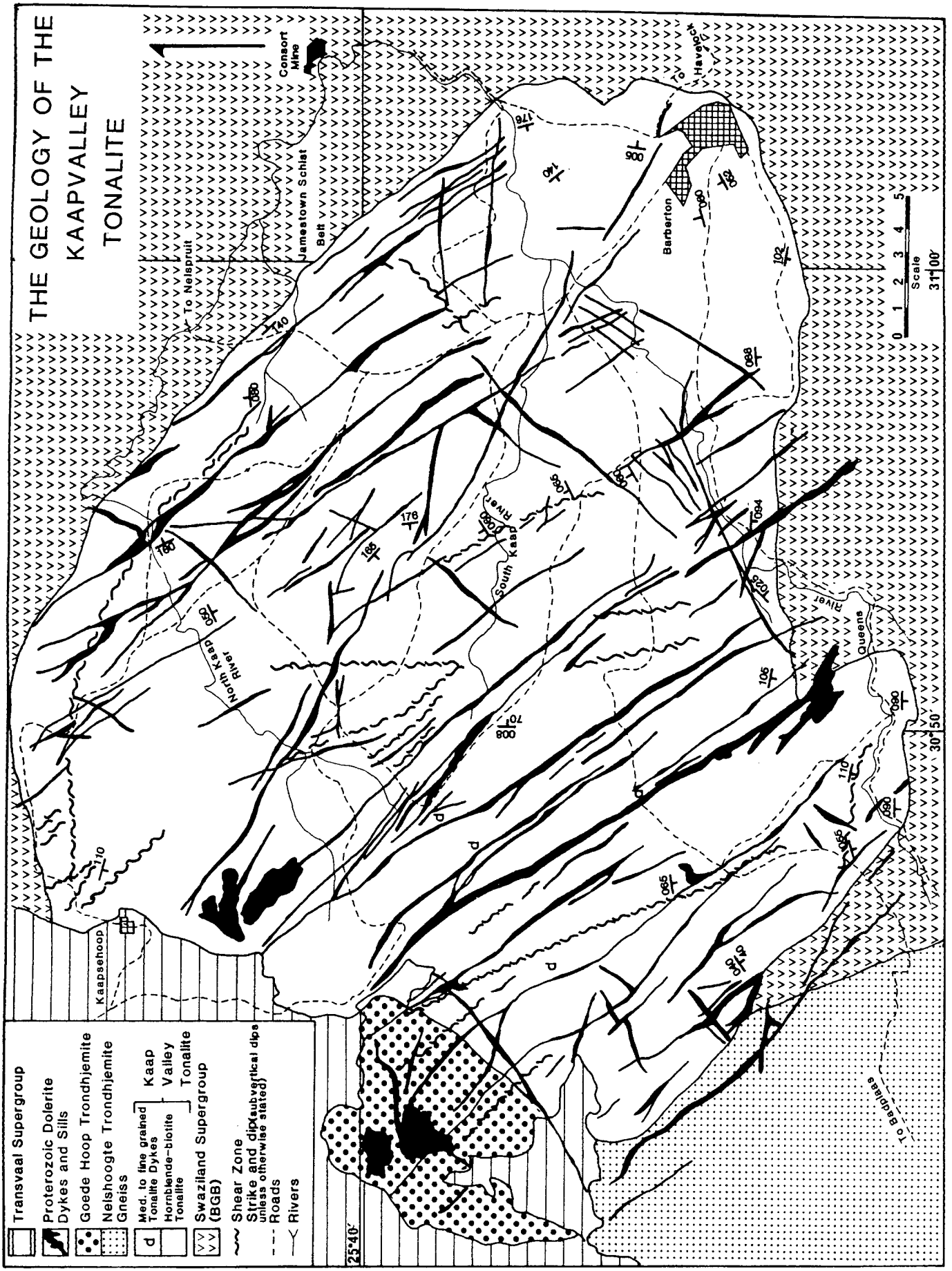

Figure 2.3 The geology of the KVT showing the major doleritic dykes and major shear zones across the pluton. Modified after Visser et al., 1951 and Robb et al., 1986). The KVT is considered to originally have been homogenous in terms of its mineral abundances and therefore a two phase tonalite is not envisaged in this study.

et al., 1986) or deformation along the contact after emplacement (Visser et al., 1956; de Wit 1983a, b). No evidence was found to suggest that the KVT was intrusive into the BGB. The KVT has a ~100 m zone from the KVT/BGB contact, that shows evidence of quartz recrystallisation and extensive chloritisation (Fig. 2.4). This confirms Anhaeusser's (1966) observations of increased chlorite near the contact zone elsewhere in the KVT. The adjacent sheared BGB metavolcanic schists have disseminated pyrite and, parallel to the plane of schistosity, numerous veins of ankerite, albite and quartz. The preponderance of these veinlets, chloritisation and quartz recrystallisation are indicative of hydrothermal activity in the KVT/BGB contact zone (Fig. 2.2).

Dykelets of fine- to medium-grained tonalite have intruded the KVT pluton in several places and possess similar mineralogies and chemistry to their medium- to coarse-grained host. While they appear to be volumetrically insignificant, the dykes occur over a large area in the centre of the pluton (Robb et al., 1986). The tonalite dykelets do not have chill margins but have sharp contacts with the host. A small quartz-porphyry occurs within the KVT just east of Barberton and is probably a marginal phase of the KVT which intrudes the BGB (Visser et al., 1956). No aplites, pegmatites or evidence of greisenisation was observed within the KVT. Amphibolite and serpentinite xenoliths which have reacted to varying degrees with the tonalite, occur intermittently across the pluton and could represent roof-pendants or cognate inclusions derived from the source region (i.e restite).

Major shear zones trend mostly in a northwest-southeast direction except in the north-eastern portion of the KVT where they have a curvature parallel to the KVT/greenstone contact (Fig. 2.3). The shear zones parallel the dolerite dyke swarm and are perpendicular to general BGB structural trends which trend northeast-southwest. Visser et al. (1956) noted these shear zones and observed that they were often accompanied by sericite schists and in some cases continued for distances up to 45 km with a width of 0.5 km. The exact age of the shear zones is uncertain particularly in view of their probable reactivation and exploitation of dolerite dykes along pre-existing shear zones. (Visser et al., 1956).

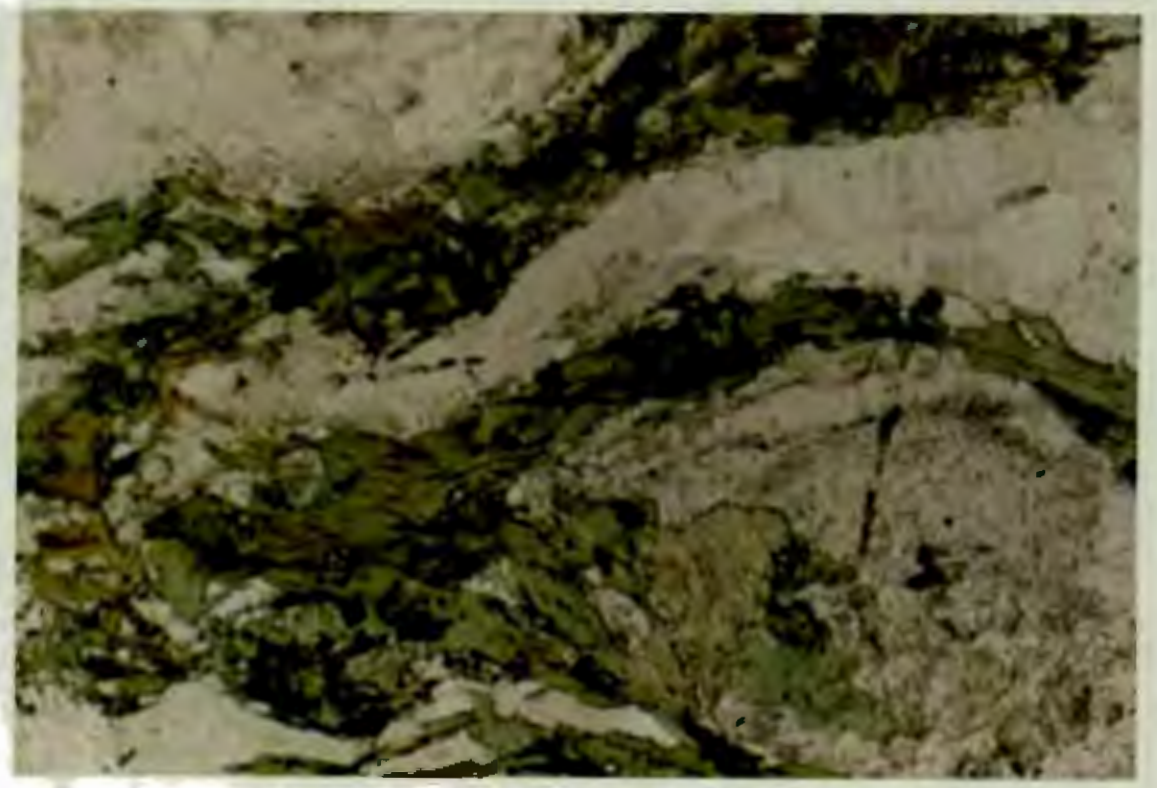

0.5mm

Figure 2.4 Chlorite veinlets/stringers within the 100m zone from the KVT/BGB contact. Plane polarised light.

The shear zones are restricted to the KVT, Nelshooghte Pluton and the Nelspruit Batholith. The alteration associated with the shear zones is varied and includes alteration products such as sericite, chlorite, quartz veins, pyrite, migmatites and kaolinite. Kaolinite has been mined on the farm Snymansbult 550KQ, in the north-central KVT, along a shear zone.

2.3 DOLERITE DYKES

The tonalitic-trondhjemitic plutons surrounding the BGB are cut by three sets of dolerite, quartz diorite and quartz gabbro dykes and sheets which vary in age from late Archaean to Karoo (Visser et al., 1956) (Fig. 2.3). Comparatively few dykes cut through the basic rocks of the Barberton greenstones, probably because the dykes are more difficult to identify in the greenstones due to their similarity in composition.

1. Dolerite dykes of late Archaean to early Proterozoic age constitute the majority of the dykes in the KVT. They generally strike in a northwest-southeast direction and were intruded after the orogenic movements related to the Barberton Mountain Land but did not intrude the overlying Transvaal age sequences (ca 2200 Ma, S.A.C.S., 1980). These dykes generally parallel the major shear zones.

2. Less prominent doleritic dykes, strike in approximately northeast-southwest directions and cross-cut the dolerite dykes described above and cut through the overlying Transvaal rocks. Visser et al. (1956) considers these dykes to be genetically related to the Bushveld igneous activity.

3. Dolerite dykes that cross-cut both of the previous types are correlated with the hypabyssal rocks of Karoo age and trend in a northeast-southwest direction (Visser et al., 1956).

Dykes of widths of a few metres or less generally have sharp contacts with the host tonalite and show a chill margin. The contact zone in the tonalites with the dolerite dykes show only a small zone of alteration. The margins of wider dykes are generally less well defined and often

xenoliths of tonalite are incorporated into the marginal zone of the dykes. In these cases, the tonalite shows small quartz veining which was taken as evidence of partial melting.

2.4 GRAVITY SURVEYS

A geophysical study showed that the rocks in the BGB and the surrounding granitoid terrain have distinctive resistivity and density properties (de Beer et al., 1988). The BGB is interpreted to be less than 8 km thick and not ~20 km as previously thought (Viljoen and Viljoen, 1969a) and that large areas of granitoid terrain (e.g. Nelspruit Batholith) are underlain by greenstone material (de Beer et al., 1988).

There are some variations in the geophysical properties within the granitoid terrain. Distinctive in this respect is the KVT pluton which has both the highest density and resistivity of all these rocks. The high density is considered to be a function of its distinctive mafic geochemistry (de Beer et al., 1988). The high resistivities are interpreted by de Beer et al. (1989) to indicate that the pluton is largely unfractured. This is considered by de Beer et al. (1988) to be consistent with the interpretation that the KVT was "emplaced in its present position as a large solid pluton rather than by a tectonic process associated with large scale fracturing". This, however, would also be consistent with a diapirically intruded melt which subsequently crystallised. Notably, to fit the available gravity data, de Beer et al. (1988) have to model the Stentor and KVT plutons as structures sloping southeastward underneath the BGB. The KVT interpretations of de Beer et al. (1989) are largely based on the work and maps of Robb et al. (1986) which do not report or discuss the shear zones first reported by Visser et al. (1956).

2.5 POSSIBLE COGENETIC TONALITES

Felsic igneous rocks within the ca 3.5 Ga Onverwacht Group of the BGB have traditionally been mapped as recurring volcanic units within a continuous stratigraphic succession. These felsic units are part of several mafic to felsic volcanic cycles making up this succession (Anhaeusser 1966, 1969; Viljoen and Viljoen, 1969a). De Wit et al.

(1987a) have suggested that the field and geochemical data indicate that the felsic rocks are cogenetic with the surrounding tonalite-trondhjemite plutons and may have been emplaced contemporaneously with them. De Ronde et al. (1988) have recently mapped a number of high-level porphyries intruded up thrust fault contacts within the BGB near the KVT contact. Geochemical data combined with zircon U-Pb age constraints (ca. 3230 Ma) suggest that the porphyries are compositionally similar, and temporally related, to the nearby KVT pluton (3223 ±8 Ma, de Wit et al., 1987a). Dykelets of fine- to medium-grained tonalite that have intruded the host KVT, and possess similar mineralogies and chemistry to the KVT, are possibly cogenetic to the KVT or the porphyries within the surrounding BGB.

2.6 ECONOMIC GEOLOGY

The economic significance of the BGB lies in some 350 gold deposits and/or prospects that occur in the Barberton area. During the period 1884 to 1983 the recorded production figures indicate that 251 553 kg gold and 8 875 kg of silver have been recovered from these deposits of which ~100 kg was mined from the KVT (Anhaeusser, 1986). Anhaeusser (1986) also pointed out that 95% of the gold was mined along the north-western flank of the BGB and that many of the more significant deposits are located within 6 km of the tonalite-trondhjemite contacts or are located adjacent to major regional faults and deformation which can be ascribed to diapiric emplacement. Anhaeusser et al. (1969, 1976), Anhaeusser (1986), Viljoen and Viljoen (1969b), Saager et al. (1982) and Saager and Meyer (1984) considered that gold in the deposits of the Archaean greenstone belt of the Rhodesian and Kaapvaal Cratons (including the Barberton Mountain Land) was initially present in the mafic and ultramafic lavas and was mobilised and concentrated in dilatant zones during metamorphic events attendant with granitoid intrusion.

Thirty-five samples from the KVT were assayed for Au and included relatively unaltered, highly chloritised and carbonated tonalite, quartz and carbonate veins. The assay results are presented in Table 2.1. The highest Au value of 0.52 ppm was obtained from sample KF81, a quartz

Table 2.1: Au analysis of samples from the KVT were done at Scientific Services, Cape Town using the fire assay technique (100g samples, 0.01 ppm detection limit). Sample locations are presented in Figure 4.3.

Sample No.	Au (ppm)	Sample discription
KF10	nd	KVT + carb. veinlets
KF15	nd	KVT + carb., qtz, chl. and epi. veinlets
KF31	0.06	KVT
KF36	0.09	KVT + chl and qtz recrystallisation
KF37	0.05	KVT + carb. and epi.
KF38	0.08	KVT + carb., epi. and secondary sphene
KF40	0.15	KVT + chl., epi. and sphene
KF43	0.05	KVT + carb. and chl.
KF44	0.04	KVT highly chl., seri. and carb. altered
KF45	0.06	KVT highly chl. and seri. altered
KF46	0.02	KVT highly chl. and carb. altered
KF47	0.06	KVT highly carb. and chl. altered
KF48	0.06	KVT highly chl. and seri. altered
KF58	nd	KVT + epi.
KF67	nd	KVT + chl.
KF69	0.02	KVT + chl.
KF77	0.02	KVT + chl. and seri.
KF78	nd	KVT + chl.
KF80	0.07	KVT + chl.
KF81	0.52	Qtz, chl. and limonite vein in KVT
KF86	0.05	KVT + chl. and carb. veinlets,wall-rock of KF81
KF89	0.05	KVT + epi. veinlets
KF95	0.18	Siderite vein in KVT
KF97	0.04	KVT highly seri. altered
KF102	0.04	KVT + epi.

Table 2.1: continued....

Table 2.1: continued.....

Sample No.	Au (ppm)	Sample discription
KF106	0.04	KVT + epi. and sphene
KF116	0.06	KVT + seri.
KF126	0.05	KVT + qtz recrystallisation (shear zone)
KF127	0.05	KVT + qtz + disseminated py. (shear zone)
KF128	0.40	KVT + qtz + disseminated py. (shear zone)
KF131	0.03	KVT + chl
KF132	0.05	KVT + qtz recrystallised

vein in the northern portion of the pluton and a value of 0.40 ppm Au from sample KF128, a recrystallised tonalite with disseminated pyrite. No gold was detected in relatively unaltered KVT samples (KF78 and KF67). The distribution of the gold values and previous gold mining sites indicate that mineralisation is strongly correlated with major shear zones in the KVT, especially in the north-western portion of the pluton (Fig. 2.5).

2.7 SUMMARY

It has been suggested elsewhere that processes analogous to those operating in modern subduction zones were also active in Archaean times, in the Barberton Mountain Land. Young subducting oceanic crust melted at depths of 50 to 80 km and produced buoyant, viscous Archaean tonalitic magmas, that rose and intruded the lithosphere and spread out laterally as gravitational equilibrium was approached. Isotopic age dating indicates that the BGB is older than the KVT by ca 200 Ma (± analytical errors) and that the KVT is not the oldest tonalite intruding the BGB. Evidence from the KVT and the KVT/BGB contact indicates that the KVT pluton was either diapirically emplaced in a subsolidus state and/or it intruded as a melt to its present level, crystallised and acted as a resistant mass, against which the BGB was deformed. The lack of large scale cross-cutting contacts and general concordant nature of the contacts with the BGB as well as gravity modelling, suggests that the KVT was originally a stratiform intrusion which was subsequently deformed at its contacts.

Fine- to medium-grained tonalite dykelets intruded the KVT but the petrogenetic relationship between the tonalites is not known. The finer-grained tonalite could, however, be related to some of the tonalitic apophyses within the BGB that have been thought to be cogenetically related to the KVT.

The relative timing of intrusion of the early Proterozoic dolerite dyke swarm and major shear zones which both generally trend in a northwest-southeast direction, is equivocal. The persistent shear zones resulted in local intense sericitisation, chloritisation, silicification,

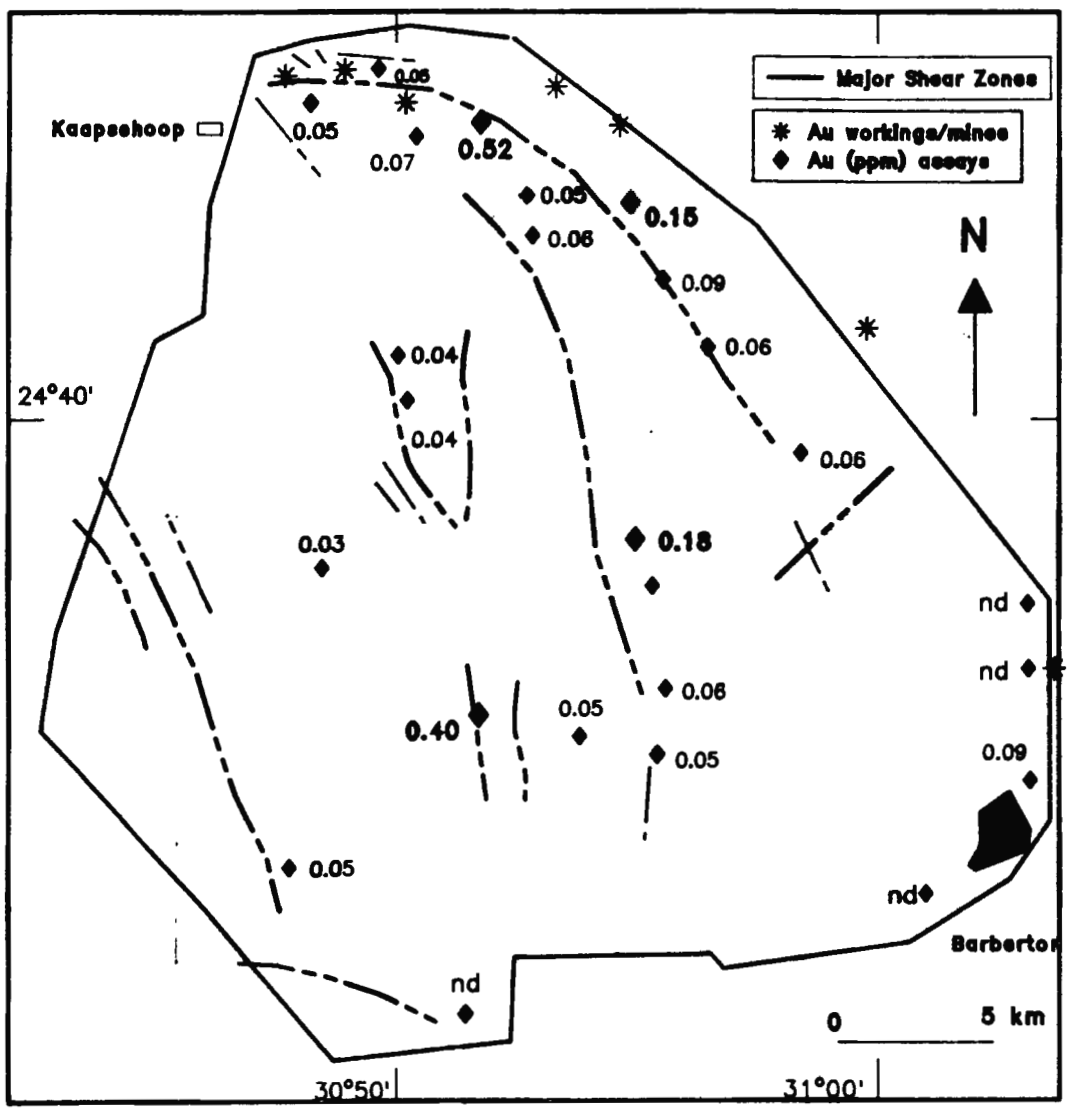

Figure 2.5 Localities and results of samples assayed for gold (ppm), gold mines and pitting within and immediately adjacent to the KVT are presented in this map. Gold mineralisation is closely associated with the KVT/BGB contact zone and major shear zones within the KVT, especially in the north and northwestern portion of the pluton.

pyritisation and kaolinitisation of the KVT. Au assay values and previous gold mining are closely associated with these major shear zones. The shear zone paralleling the KVT/BGB contact in the north of the pluton, in particular, is favourable for gold mineralisation.

3. TECHNICAL and ANALYTICAL DETAILS

3.1 CONTOURING

The data from modal point-counting and stable isotope analysis obtained in this study, were contoured using the SACLANTS GRAPHICS PACKAGE, at the University of Cape Town in the Department of Computer Science. The package was originally developed at the Department of Energy, Mines, and Resources, Ottawa, Canada. The local version is an adaptation of a package which was obtained from the NATO SACLANT ASW Research Centre Spezia, Italy.

The Saclants Graphics Package will plot a perspective picture of a single-valued surface Z defined over a rectangular grid in X and Y. The data may be given as a set of points arbitrarily placed over the region of the grid, as is the case in this study, or as already gridded data. The ungridded or randomly spaced data is interpolated onto a grid and then treated as gridded data. The Z surface may then be represented by means of contours.

The method for two-dimensional interpolation consists of an initial assignment of values to the grid points followed by a process whereby the grid values are iteratively improved until the surface through the original data points has attained a satisfactory state of " smoothness". Once the data points have been gridded, contour lines can be drawn by linear interpolation between grid points. Smoothing of the linear contour lines can be achieved by using a combination of various parameters.

3.2 ELECTRON MICROPROBE ANALYSIS

Minerals were analysed in the Department of Geochemistry at U.C.T. using a 4-channel, fully automated Cameca Camebax Microprobe. Samples were prepared as polished carbon-coated thin sections.

3.2.1 *Routine analysis*

The following instrumental conditions were observed:
beam current: 40 nA
accelerating voltage: 15 kV

counting time: 10 seconds
analyte line: K_α
analysing crystals: TLAP for Na, Mg, Si and Al
LiF(200) for Fe, Mg and Ni
PET for Ca, K, Ti and Cr
detectors: flow counters with Ar/CO_2 gas mixture
beam: diameter 8 - 10 micro m

Standards used:

Element	Amphibole	Mica	Feldspar	Epidote
Si	K-H	K-H	NUNI	K-H
Ti	RUT	RUT	-	RUT
AL	K-H	K-H	NUNI	K-H
Fe	K-P	K-H	K-P	K-H
Mn	RHOD	RHOD	-	RHOD
Mg	K-H	K-H	K-H	K-H
Ca	K-H	K-H	LACO	K-H
Na	K-H	K-H	NUNI	K-H
K	K-H	K-H	OR-1	K-H
Cr	CHRO	CHRO	-	CHRO

APAT - apatite
CHRO - chromite 52nlll
K-H - Kakanui hornblende
LACO - labradorite, LakeCo.,Ore.
NUNI - Nunivak Is. plagioclase
RHOD - rhodonite
RUT - synthetic rutile

Raw counts were corrected for dead time and background, and nominal concentrations calculated using the standards. Nominal concentrations were corrected for interelement matrix affects using the method of Bence and Albee (1968) for amphiboles and the ZAF procedure used at UCT (modified after Henoc et al., 1973) for all other minerals.

3.3 STABLE ISOTOPE GEOCHEMISTRY

Theoretical background to stable isotope geochemistry is detailed in Appendix 1.

3.3.1 *Notation*

Data are reported in the δ notation where

$$\delta_x = [(R_x - R_{std})/R_{std})] * 10^3 \text{ ‰}$$

and $R_x = {}^{18}O/{}^{16}O, {}^{13}C/{}^{12}C$

R_{std} = corresponding ratio in standard e.g. V-SMOW

3.3.2 *Oxygen Isotope Ratios of Silicate Minerals - Sample preparation*

Whole rock samples were reduced to -60 to -80 mesh size by splitting, crushing (Mn-steel jaws) and sieving. The -60 to -80 mesh grains were stripped of magnetite with a hand-held magnet. The mafic mineral fractions were roughly separated from the quartz and plagioclase using a Frantz Isodynamic Magnetic Separator. Individual mineral grains were then handpicked while viewed under a binocular microscope. To help distinguish between quartz and plagioclase a thin layer of the non-magnetic fraction was suspended within a Pt-pan and etched with HF vapours for ~2 minutes. The minerals are placed in an electric furnace for ~5 minutes to fix the etch-residue, resulting in clean and "sparkly" quartz and a "milky" coloured plagioclase. It has been shown that the HF treatment does not affect the $\delta^{18}O$ of the plagioclase (unzoned) and quartz minerals (T. Venneman, personal communication) . Any impurities in either the quartz or plagioclase are now easily identified. All mineral separates are considered to have been ~98 % pure except the hornblende which can sometimes be poikilitic and is at times probably only ~90 % pure. The separated minerals were then crushed to a fine powder using an agate mortar and pestle and dried at 50 °C for at least 48 hours before analysis.

3.3.3 *Oxygen Extraction and Sample analysis*

Oxygen was extracted from minerals and whole rocks using facilities in the Department of Geochemistry at the University of Cape Town. Samples

were loaded into Ni-reaction vessels and degassed at 200 °C for 2 hours in order to remove adsorbed moisture. For silicates and whole rocks ~10mg sample were reacted with about 35 kpa ClF_3 and oxygen extracted by the method described by Borthwick and Harmon (1982). The reaction temperatures were 550 °C for quartz and plagioclase and 600 °C for all other samples. Runs were for at least twelve hours and all analyses were run in duplicate.

The extracted oxygen was converted to CO_2 via a heated carbon rod and analysed for $^{18}O/^{16}O$ using a VG 602E mass spectrometer. Oxygen isotope data are reported relative to the V-SMOW (Vienna-Standard Mean Ocean Water) standard. During this work 59 analyses of the quartz standard NBS-28 gave an average $\delta\ ^{18}O$ of + 9.65 ‰ with a standard deviation of 0.15 ‰. The yields for most minerals were between 97-102 % but for chlorite lower yields of 90-97 % were obtained and even lower yields of ~80 % were obtained for epidote. The low yields could be related to the volatile contents or incomplete oxygen liberation from these minerals. The difference between duplicate analyse was < 0.1 ‰ unless otherwise stated. The fractionation factors were related to temperature using equations given in Appendix 1.

3.3.4 *C- and O-Isotope Ratios of Carbonates - Sample Preparation*

Rocks that contained thin veins or disseminated carbonate were analysed for their $\delta^{13}C$. The crushed whole rocks (Mn-steel jaws) were ground to < -90 mesh by an agate mortar and dried for at least 48 hours before analysis. The samples (1.25g) dried at 50 °C for at least 48 hours were placed in glass reaction vessels with 20ml of 100 % H_3PO_4 (in a separate arm of the reaction vessels). The sample and acid in the reaction vessels were degassed under vacuum, then removed from the line and left overnight in a water-bath at 25.2 °C (McCrea, 1950). The acid is then poured onto the sample as quickly as possible to ensure that the reaction takes place at 25.2 °C and left in the water-bath until it reaches completion. The following reaction scheme:

$$3\ CaCO_3 + 2\ H_3(PO_4) = 3\ CO_2 + 3\ H_2O + Ca_3(PO_4)_2$$

shows that both water and carbon dioxide is liberated from the carbonate

which will fractionate oxygen isotopes. The H_2O-CO_2 isotope fractionation has been experimentally determined at 25.2 °C and it is therefore important to maintain this temperature during the carbonate phosphoric acid reaction.

The released CO_2 was analysed on a VG 602E mass spectrometer. Both $\delta^{18}O$ and $\delta^{13}C$ were calculated from mass spectrometer measurements. All analyses were done in duplicate and isotope data are reported in δ notation with $\delta^{18}O$-values reported relative to the V-SMOW standard and the $\delta^{13}C$-values reported relative to the PDB (Peedee Belimnite) standard. The difference between duplicate samples were all better than 0.15 ‰. The in-house standard (Namaqualand marble) gave an average $\delta^{18}O$ of + 25.1 ‰ and $\delta^{13}C$ of + 1.7 ‰ for 9 analyses with a standard deviation of less than 0.1 ‰.

4. PETROGRAPHY and MINERAL CHEMISTRY of the KVT

4.1 INTRODUCTION

The KVT has plagioclase, quartz, hornblende and chlorite as its dominant minerals. Modal biotite content is very variable between 0-15% but more typically 0-2%. A petrographic study shows that all the tonalites have undergone some degree of alteration. Slightly altered samples have plagioclase phenocrysts that are turbid while in extreme cases, altered samples show only a relict outline of the plagioclase and a few pale grains of chlorite indicating the existence of a previous mafic mineral. Fig. 4.1 and 4.2 illustrate examples of unaltered and highly altered KVT.

The modal distribution of primary and altered minerals was determined by point-counting. A total of 900 counts was done on each of 78 thin-sections and results are tabled in Appendix 3. Sample positions and a brief sample description are presented in Figure 4.3 and Appendix 2 respectively. The modal percentages have been contoured using the Saclants Graphics Package described in Chapter 3 and contour plots presented in Appendix 3.

Minerals from the KVT were analysed using a microprobe (Chapter 3), to establish the mineral compositions and whether the minerals are in chemical equilibrium. This information is also important when interpreting the stable isotope geochemistry of the KVT minerals in Chapter 5. Analytical results are presented in Appendix 3.

4.2 MINERALOGY

4.2.1 *Feldspar*

Plagioclase occurs as large, subeuhedral laths (3-8mm) that characteristically exhibit oscillatory zoning and albite twinning (Fig. 4.4). The KVT is locally porphyritic with plagioclase phenocrysts up to 18mm in length. The average modal percentage plagioclase for 78 thin-sections is 58.1%.

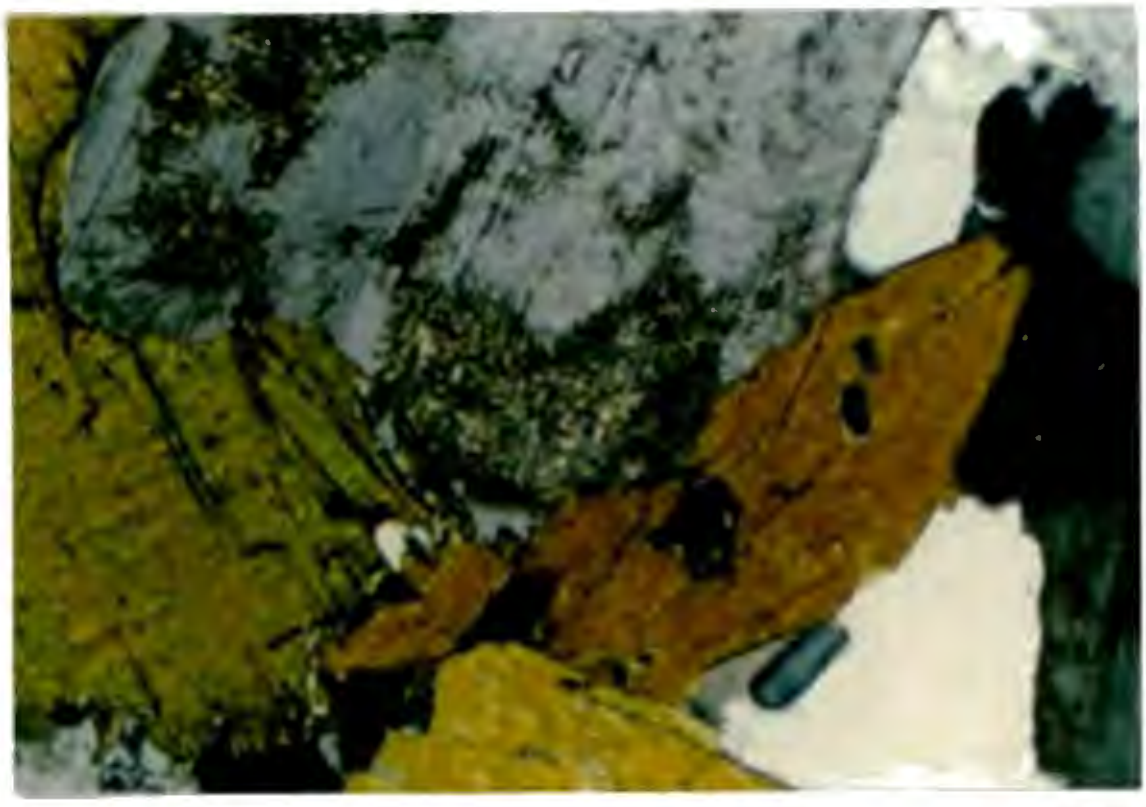

Figure 4.1 "Unaltered" KVT (KF65) consisting of plagioclase, euhedral hornblende with inclusions, biotite and quartz. Cross-polars.

0.5mm

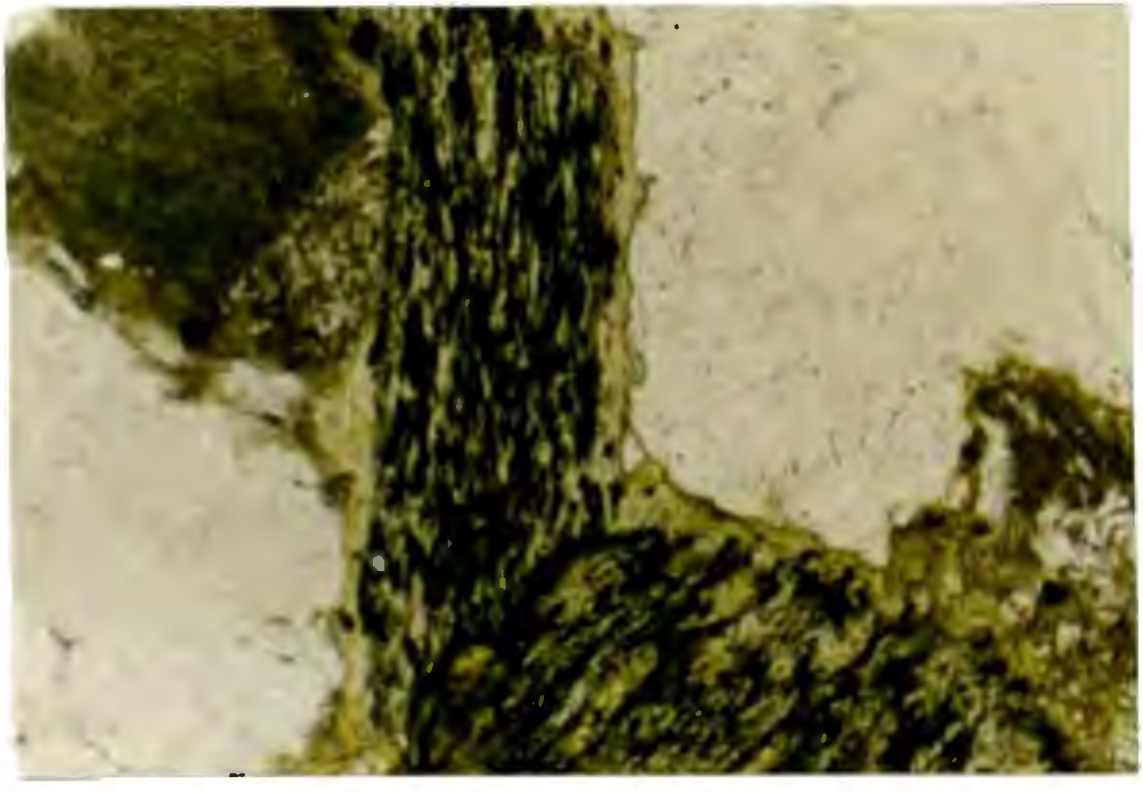

Figure 4.2 Highly altered KVT (KF77) with remnants of previous plagioclase (top left of photograph) and mafic minerals. Quartz does not appear to have been affected by the hydrothermal alteration. Plane polarised light.

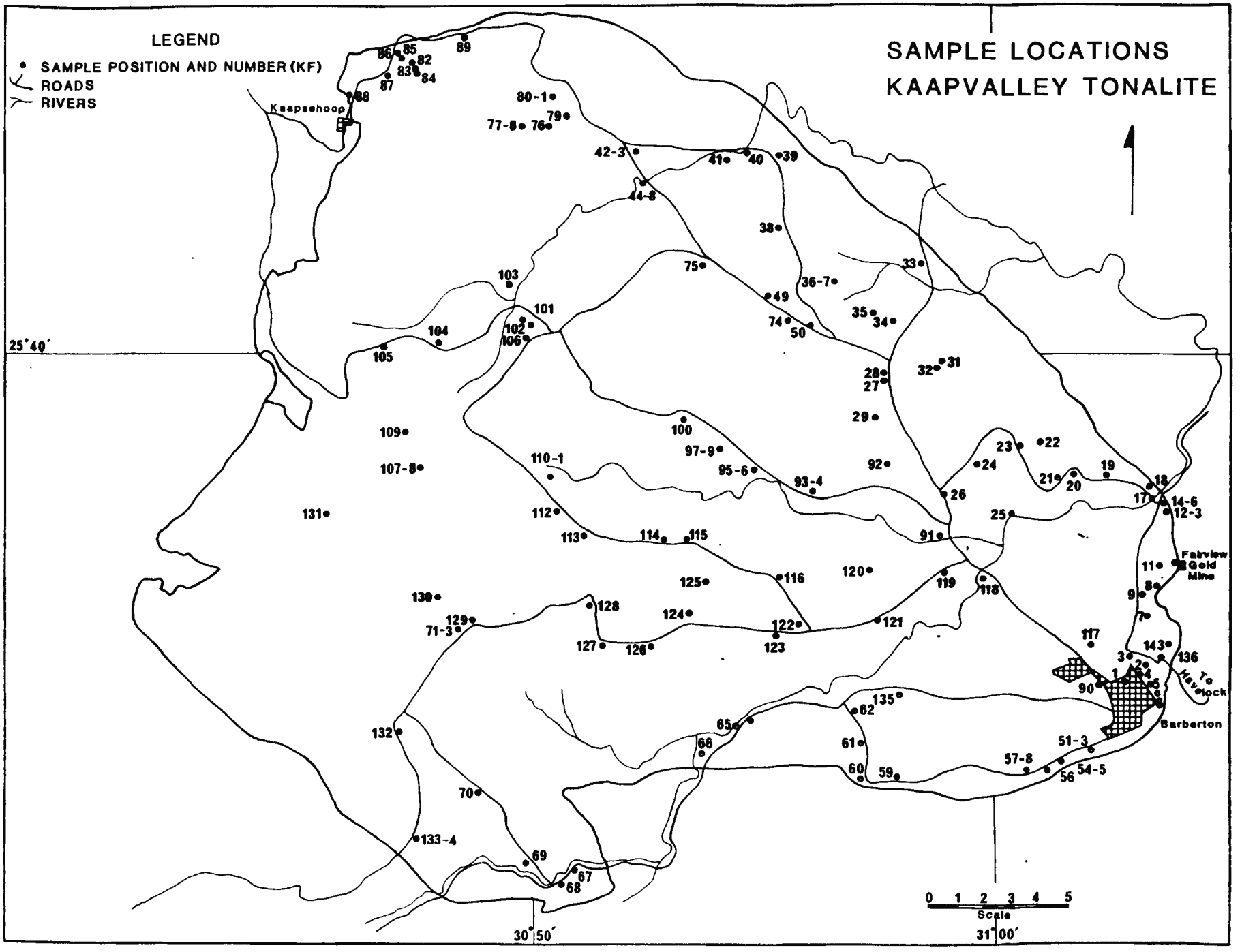

Figure 4.3 KVT sample locations.

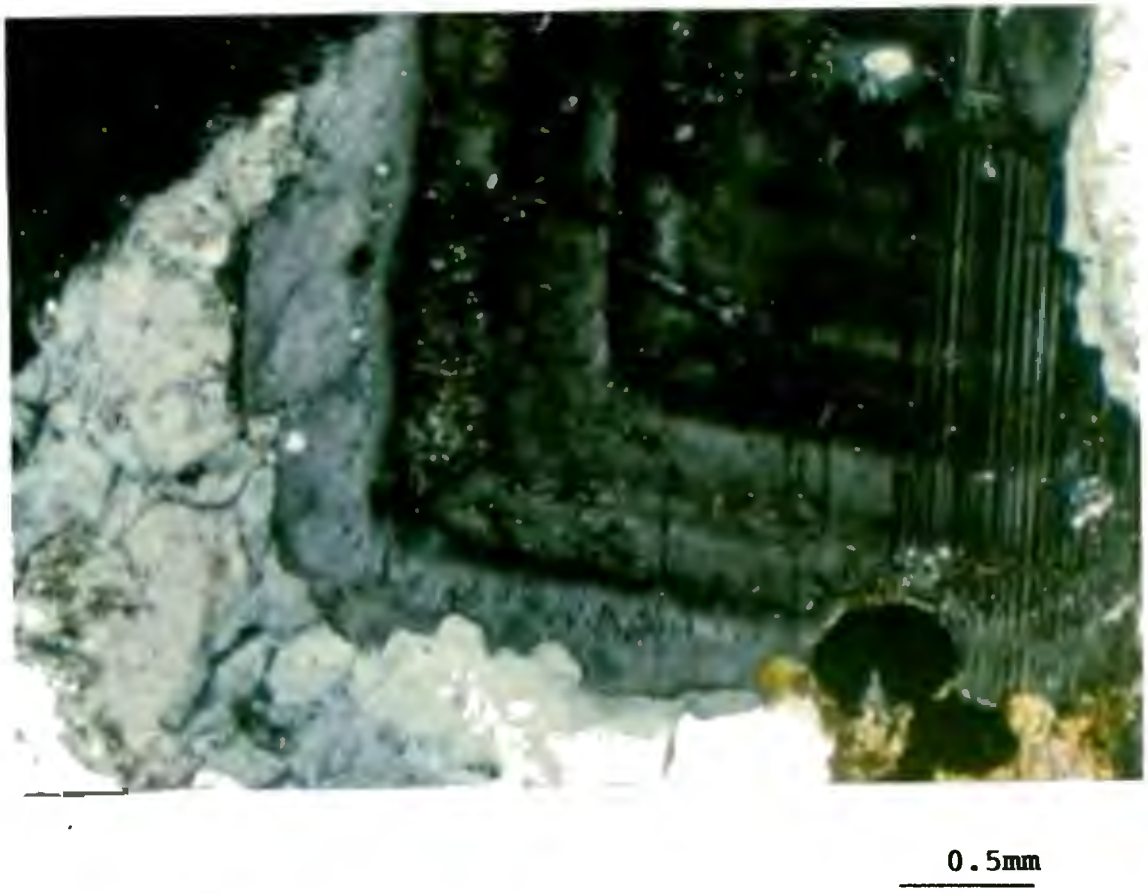

Figure 4.4 Zoned plagioclase with albite twinning. The plagioclase minerals have a sodic-rich rim (An_{15-20}), zoned intermediate and core portions that range between An_{20} and An_{30}. Core and intermediate portions cannot be distinguished from their chemistry. Crossed polarised light.

The least altered plagioclases have turbid cores or turbid concentric zones around a less altered core. The feldspar turbidity is often due to the presence of small sericite crystals within the host. At advanced stages of alteration, the plagioclase is completely turbid and/or sericitised and commonly with accompanying quartz and epidote. In hand-specimen the altered plagioclases have a green to white "chalky" appearance. The mean altered plagioclase (turbid/sericitised) is 80 %. Trace amounts of microcline are found in some samples in the northern portion of the pluton.

A number of analyses were done on each plagioclase grain to determine the range in composition existing between margins, cores and intermediate portions of unaltered plagioclase. Microprobe data from the plagioclase minerals are plotted in Figure 4.5 and show that their composition ranges from albite (An_2) to andesine (An_{40}). The majority of the analyses, however, plot in the oligioclase range (An_{15} to An_{30}). The mineral margins are clearly more sodic than the internal portions of the plagioclase. The intermediate and cores of the plagioclase which show oscillatory zoning cannot be distinguished from their chemistry. This was also observed in the petrographic study where altered plagioclases have both the intermediate concentric zones and cores, which are turbid/sericitised.

4.2.2 *Quartz*

The quartz is inequigranular (0.5-5mm), subhedral and usually exhibits undulose extinction. Some samples have much finer equidimensional neoblasts which are associated with areas of major shearing (Fig. 4.6). The average modal percentage quartz for 78 thin-sections is 22.0%.

4.2.3 *Hornblende*

Hornblende occurs as green subhedral/euhedral, commonly twinned and poikilitic (2-5mm) crystals (Fig. 4.1). Distribution within the pluton is even and regular with no evidence of "clotting" or reaction with the tonalite. Inclusions of plagioclase, magnetite and minor quartz occur in the hornblende. Alteration minerals associated with hornblende are commonly epidote and calcite and less frequently chlorite and sphene

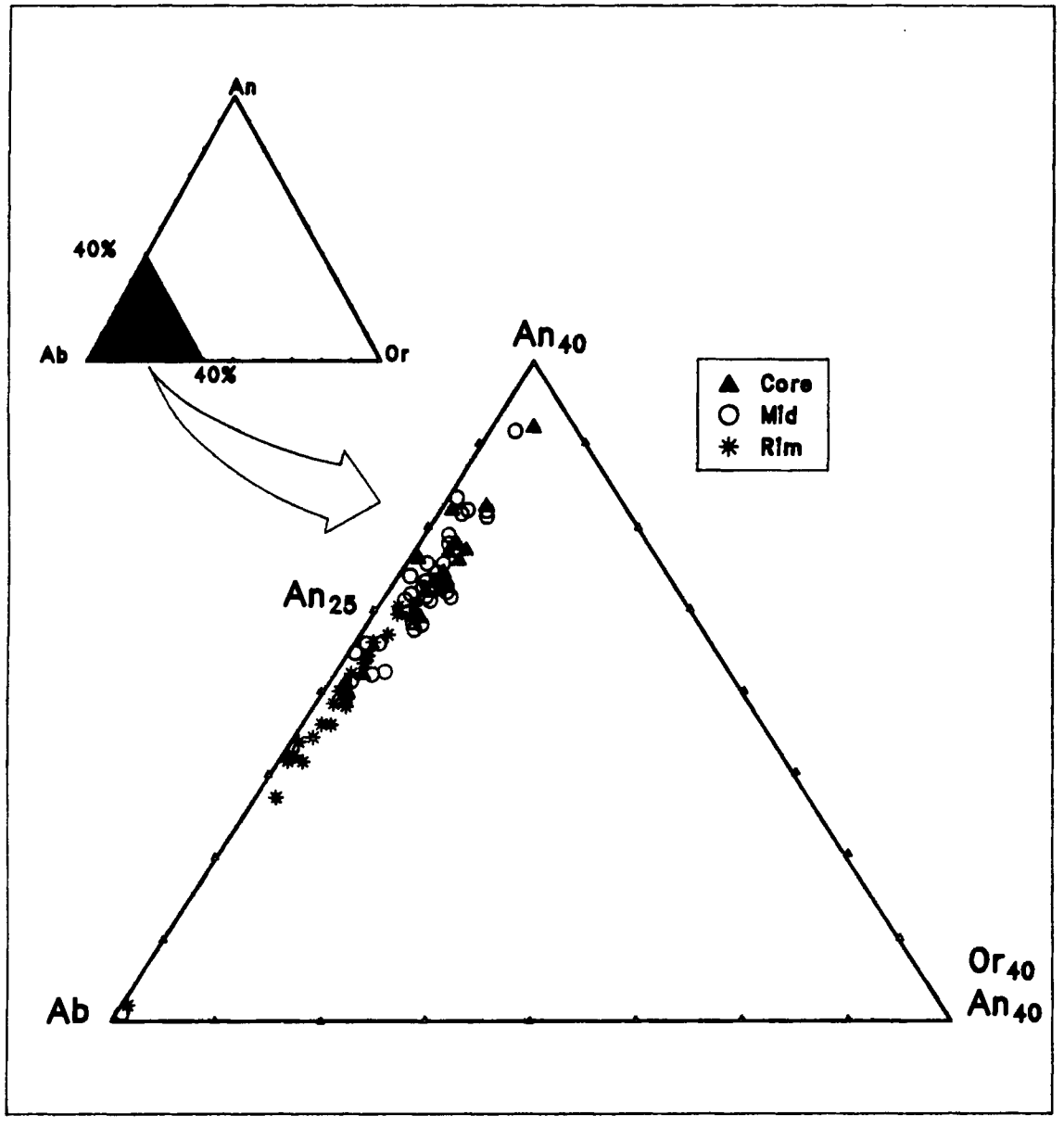

Figure 4.5 Microprobe data for plagioclase minerals (least turbid/sericitised) from the KVT. The majority of the analysis plot in the oligioclase range (An_{15-30}). The margins of the plagioclase minerals are more sodic but the "mid" and core portions cannot be distinguished from their An contents.

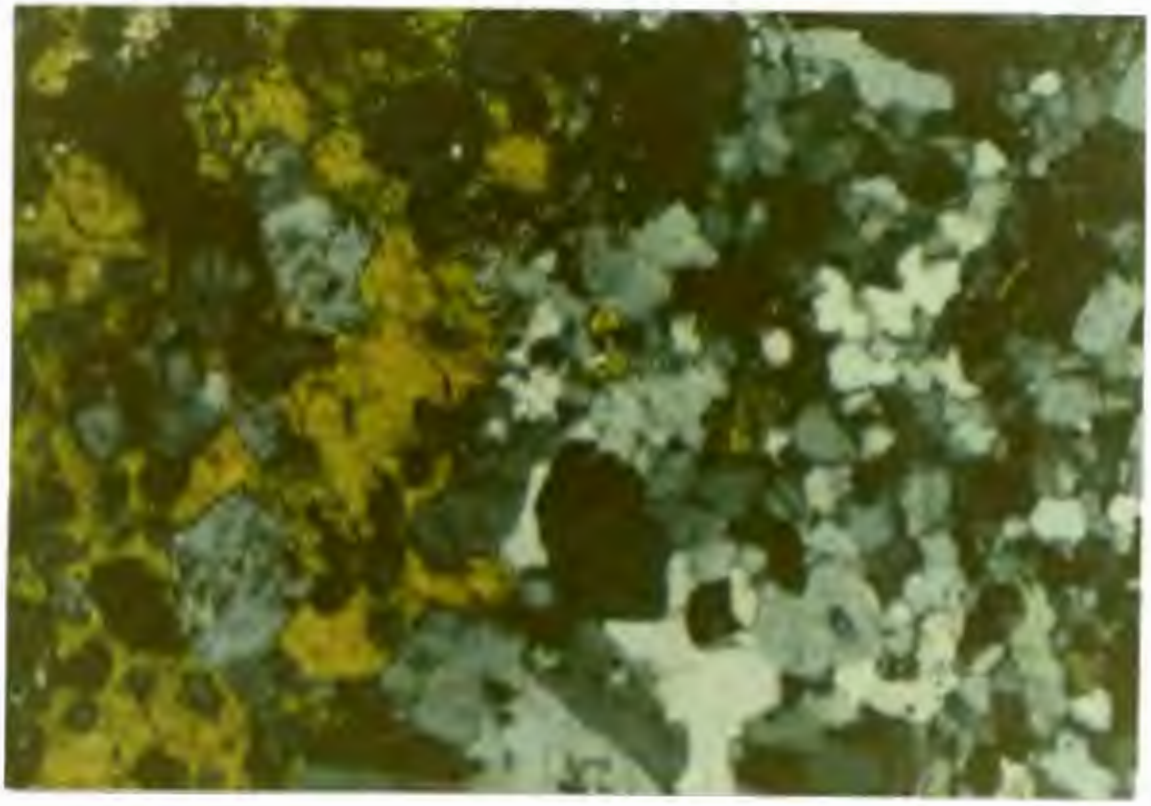

Figure 4.6 Recrystallised quartz and hornblende (KF126), from a shear zone. Crossed polarised light.

0.5mm

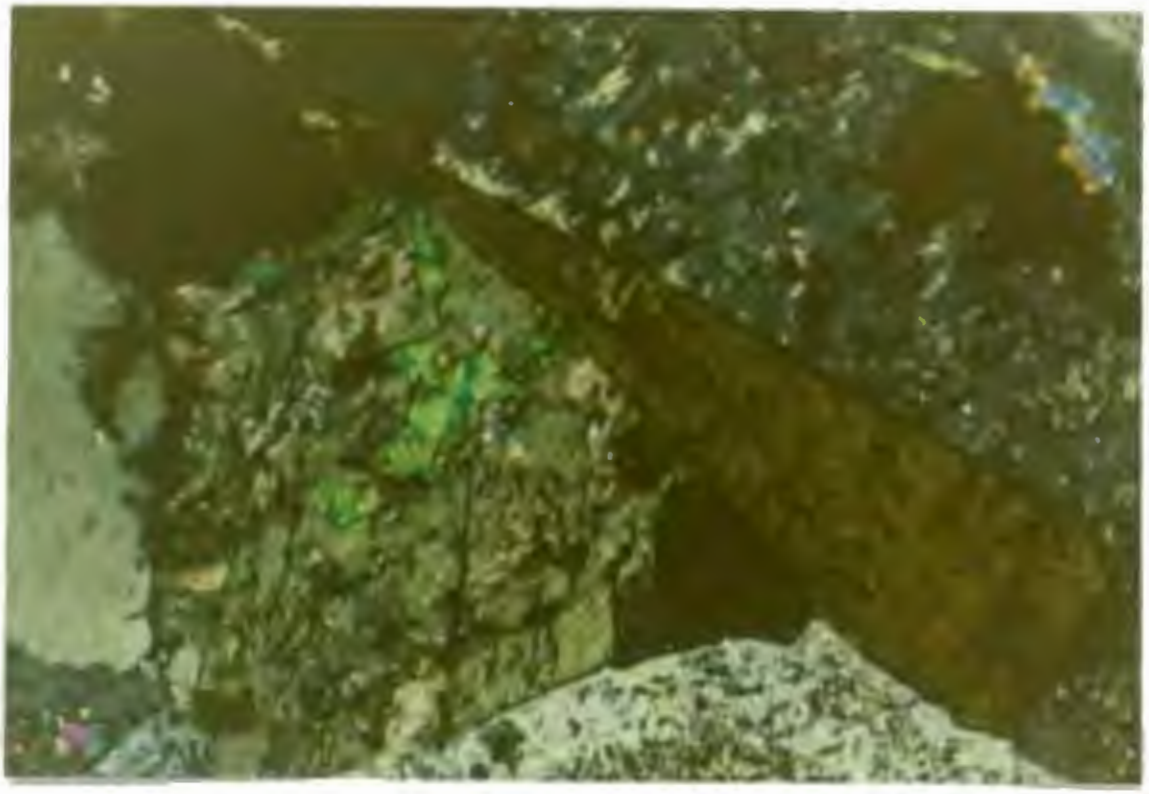

Figure 4.7 Hornblende is generally altered to epidote, calcite, chlorite and less frequently sphene. This photograph shows the initial stages of hornblende alteration, sericite in plagioclase, and euhedral sphene (primary). Crossed polarised light.

(Fig. 4.7). The average modal percentage hornblende for 78 thin-sections is 5.8%, while in relatively unaltered samples (e.g. KF65) the modal proportion of hornblende is ~20%.

In an Al^{4+} vs $(K^{+}+Na^{+})$ plot (Fig. 4.8) the calcium-rich amphiboles plot in a linear array, well within the common hornblende field as defined by Deer et al. (1979). The hornblendes of metabasaltic xenoliths from the KVT and other parts of the Barberton Greenstone Belt (data Robb, 1981) are also plotted on this graph. The hornblendes from metabasaltic xenoliths plot in a broader field than the KVT hornblendes but they nevertheless overlap appreciably. The KVT hornblendes generally exhibit igneous textures but on the basis of chemistry cannot be unequivocally distinguished from the metabasaltic xenolith hornblendes. Systematic microprobe analysis across one unaltered hornblende indicated that no significant chemical zoning is present in the KVT hornblendes.

4.2.4 *Biotite*

The KVT generally contains very little or no biotite but it may be locally as abundant as hornblende (Fig. 4.1). Biotite occurs as primary brown, rectangular flakes which are generally equigranular (~4mm). Biotite alteration to chlorite proceeds along cleavage planes and grain boundaries of the biotite. In hand-specimen this conversion is marked by a distinct decrease in "lustre" of the biotite grains, and in extreme cases by the dull olive-green colour of chlorite. In relatively unaltered rocks the mode of biotite is ~10% while the average modal percentage biotite for 78 thin-sections is 1%. Biotite is primarily altered to chlorite (Fig. 4.9) and to a lesser extent epidote and quartz. Secondary biotite which is greener in colour and finer grained than the primary biotite, is occasionally present in some veinlets along with epidote.

Biotite analysed from the KVT have compositions typical of magmatic biotite (Deer et al. 1979). Secondary biotite cannot be distinguished from primary biotite on the basis of its chemistry (Appendix 3, KF110). The average biotite and hornblende in samples where the two minerals coexist, are plotted on a Al^{4+} vs $Mg^{2+}/(Mg^{2+} + Fe_{total})*100$ plot

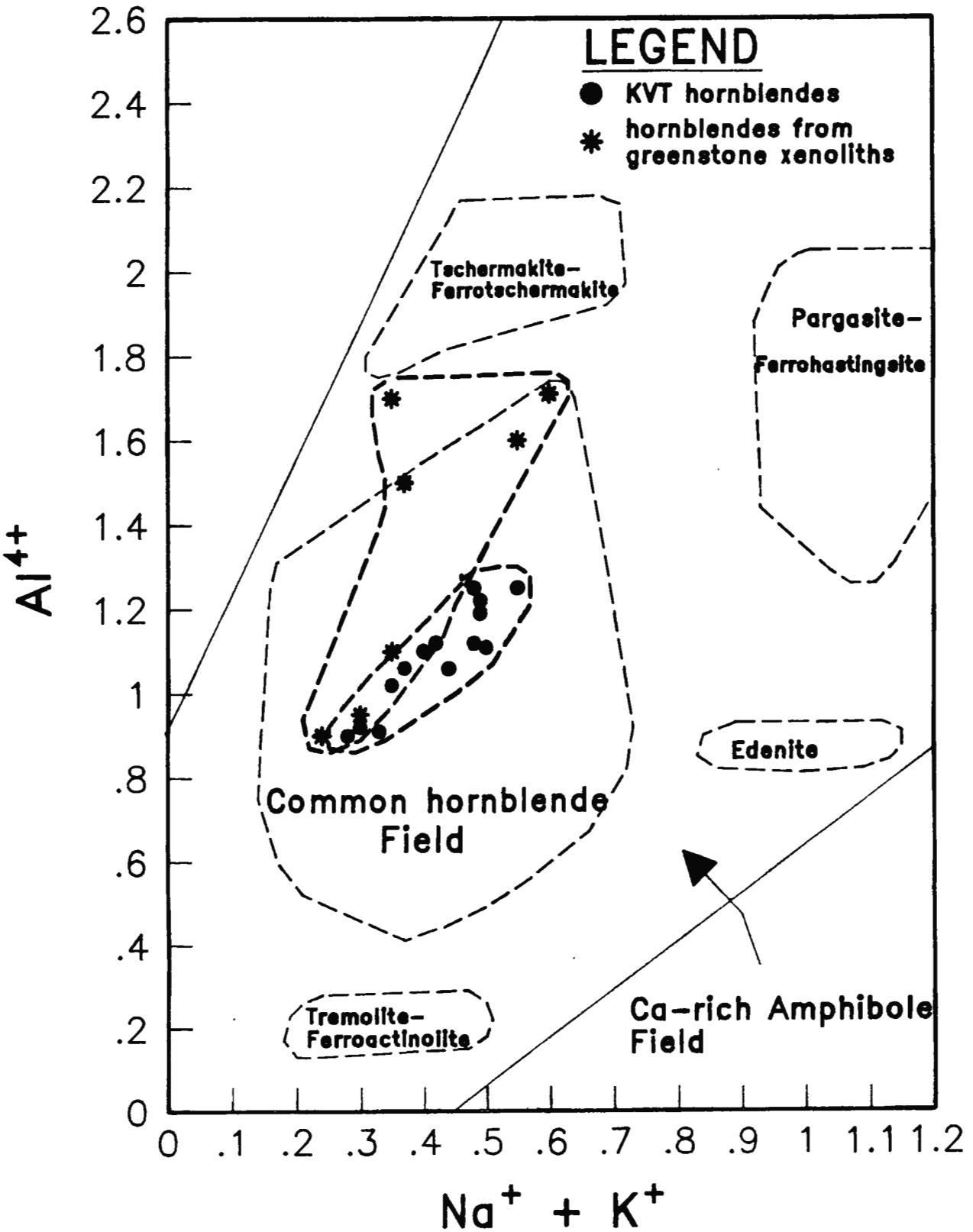

Figure 4.8 The KVT hornblendes plot well within the common hornblende field (after Deer et al., 1977). The KVT hornblendes partially overlap with the hornblendes from the greenstone xenolith field (xenolith data, Robb et al., 1986).

(Fig. 4.10). The hornblende and biotite appear to be in chemical equilibrium except for two samples. These can be recognised in Figure 4.10 by their tie-lines which cross those of the other biotite-hornblende pairs. The samples which have crossing tie-lines do not show any petrographic evidence of hydrothermal alteration. The hornblendes from metabasaltic xenoliths are also plotted and again cannot be unequivocally separated from the KVT hornblendes.

4.2.5 *Chlorite*

Green chlorite is ubiquitous in all the samples studied. Chlorite occurs as an alteration product of biotite and hornblende but also occurs in veinlets with epidote, muscovite and calcite. Alteration of biotite results in the formation of chlorite which also usually pseudomorphs the characteristic rectangular shapes of the biotite (Fig. 4.9). The chlorite associated with the alteration of hornblende is easily distinguished from the chlorite after biotite because alteration of hornblende is usually accompanied by more than one alteration mineral, chlorite is generally of minor abundance and the prismatic shape of hornblende is generally preserved after alteration. Samples collected from zones which have been delineated by Robb et al. (1986) as the hornblende (without biotite) tonalite phase all have chlorite which have been interpreted to be secondary after biotite. Biotite is more susceptible to alteration than hornblende. The average modal percentage chlorite for 78 samples is 10.1%.

The analytical results of chlorite are represented on a Si^{4+} vs Fe_{total} plot (Fig. 4.11). The chlorites are tightly grouped in the corundophyllite field as defined by Hey (1954). The vein chlorites also plot in the same field and are chemically indistinguishable from the other chlorites.

Cathelineau and Nieva (1985) have devised a chlorite solid-solution geothermometer from the empirical relationship between the chlorite chemical variables and temperature of crystallisation from different geothermal fields. The chemical changes are mainly related to the changes of the molar fraction of the Si_{IV} and the variation of Al_{IV}

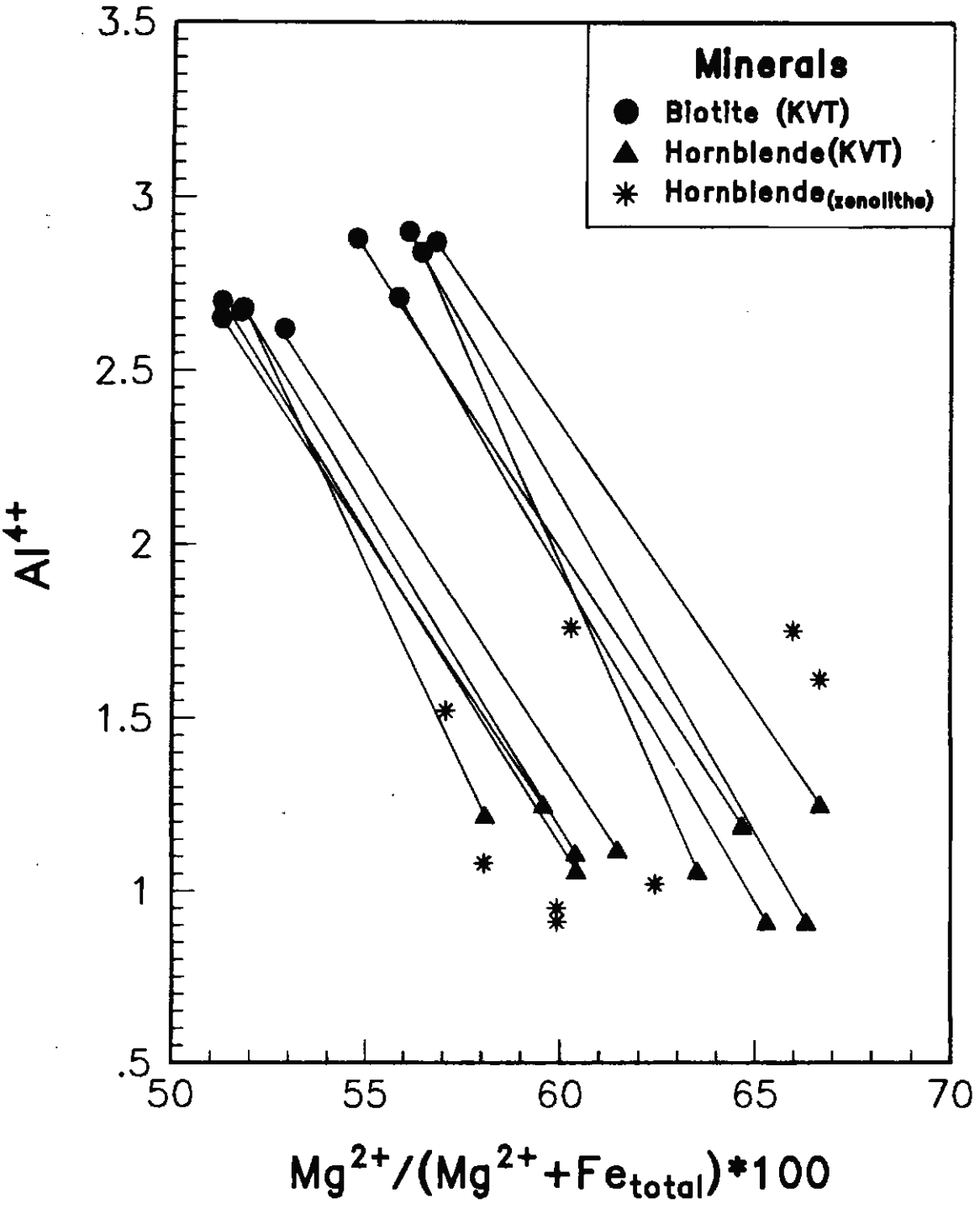

Figure 4.10 The hornblendes and biotites of the KVT are in chemical equilibrium except for two samples which have crossing-tie lines. The hornblendes from the metabasaltic xenoliths, again, cannot be unequivocally distinguished from the KVT hornblendes.

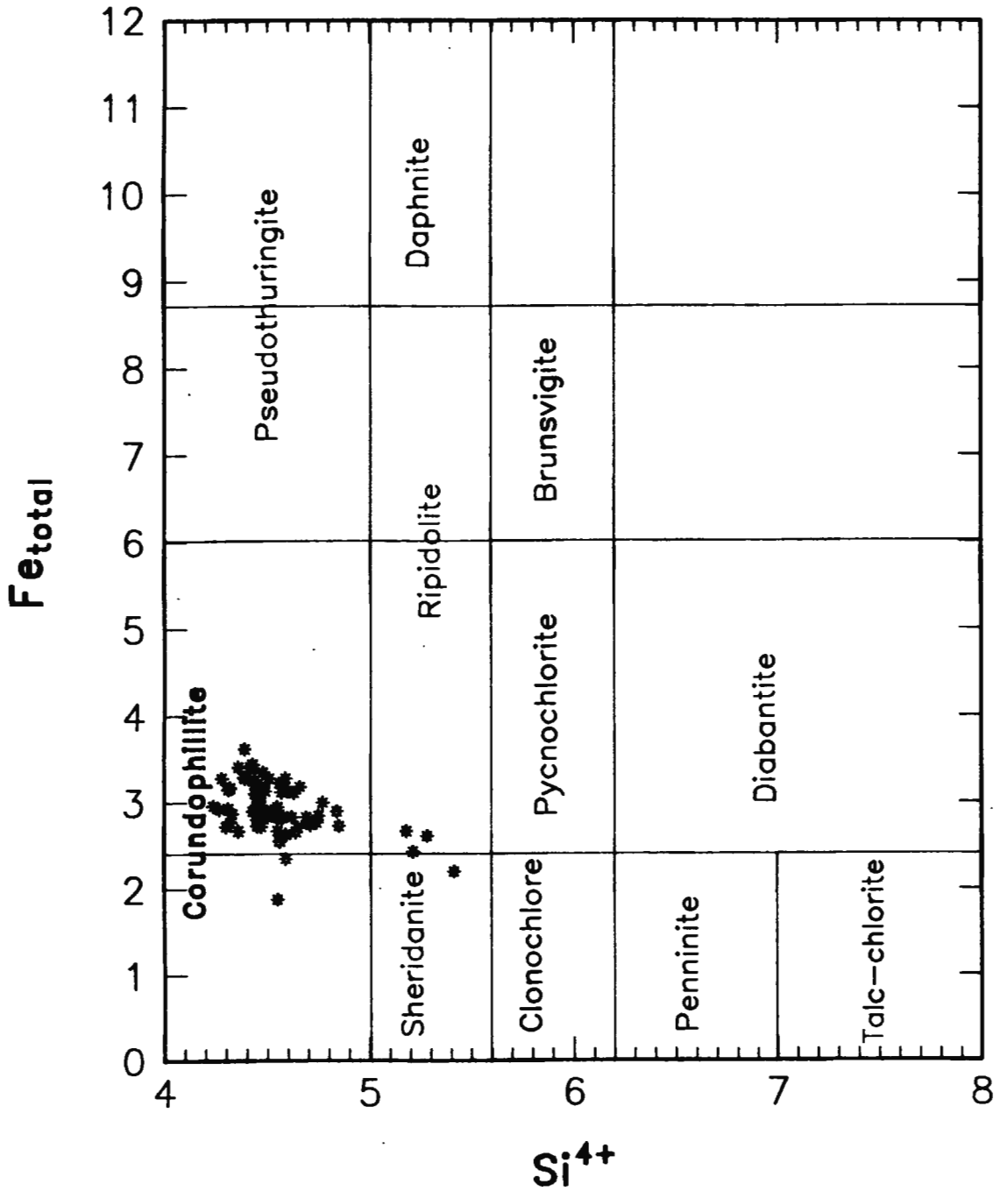

Figure 4.11 Analyses of KVT chlorites plotted on a nomenclature diagram defined by Hey (1954), generally plot in the corundophyllite field.

in the tetrahedral site of chlorites which are considered to be mainly temperature dependent. The chlorite geothermometer has, however, only been calibrated for temperatures ranging from 150 to 300 °C but extrapolations at lower and higher temperatures seem promising (Cathelineau, 1988). The Fe/Fe+Mg ratio correlates very poorly with temperature and is considered to be mainly dependent on the host-rock composition. The temperature-composition relationship is represented by the general formula:

$$Al_{IV} = 4.71*10^{-3}*T - 8.26*10^{-2}$$

Al_{IV} is atomic proportions based on 14 oxygens and T is in °C. The crystallisation temperatures of the chlorites based on this geothermometer range from 150°C to 300°C and average ~ 250 °C (Table 4.1). The average Al(IV) atomic proportions (based on 14 oxygens) for the KVT chlorites are presented in Appendix 3.

4.2.6 *Epidote*

Epidote occurs mainly as an alteration mineral after hornblende and to lesser extend after plagioclase but is also present in chlorite and calcite veinlets. The two styles of epidote occurrence are chemically indistinguishable from each other. The average modal percentage for epidote in 78 samples is 2.0%.

4.2.7 *Carbonate*

Carbonate occurs in the KVT as calcite in veinlets with or without epidote, chlorite and muscovite. as siderite veins (KF95) or ankerite veins (KF138) and as very fine calcite grains in altered hornblende. The carbonate veinlets and disseminations do not cross-cut and are not cross-cut by any of the other alteration minerals. The KVT can be replaced by as much as 40% carbonate (extreme case), normally calcite (Fig 4.12). The average modal percentage carbonate for 78 samples is 0.9%.

4.2.8 *Sphene*

Sphene is an accessory mineral in a few rocks and can be euhedral or

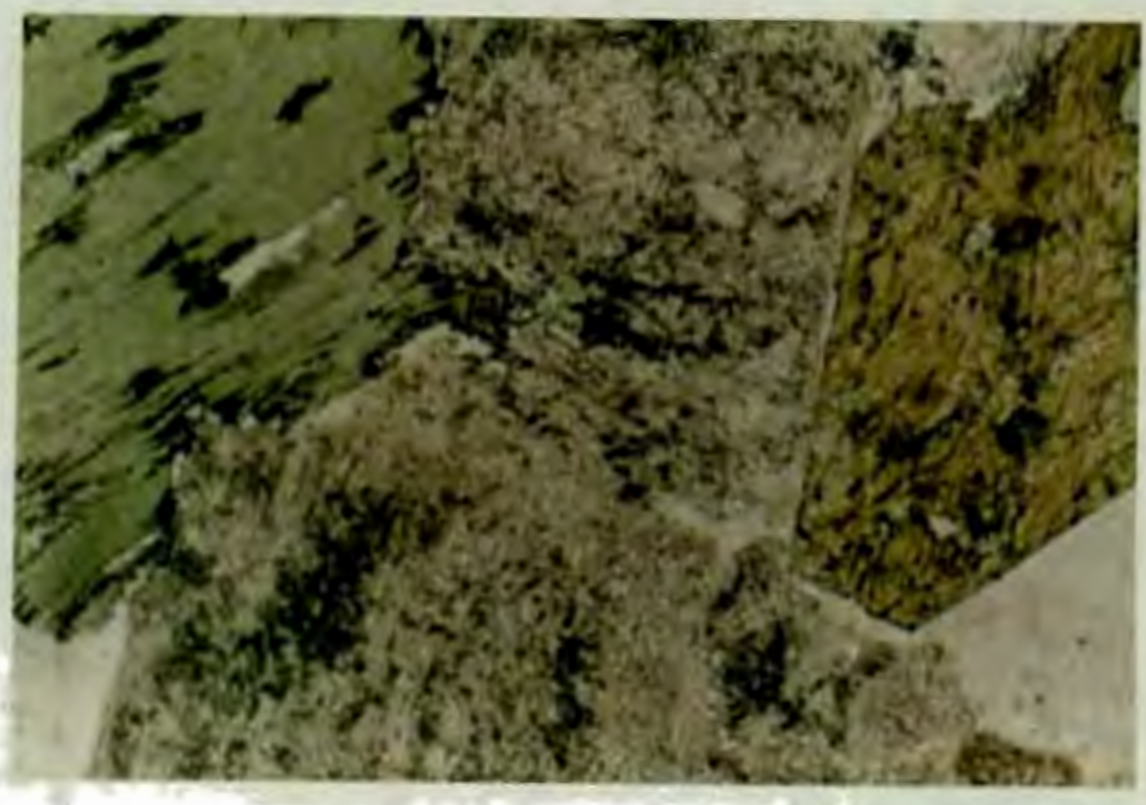

0.5mm

Figure 4.9 Biotite is mostly altered to chlorite (fresh biotite Fig. 4.1). The chlorite after biotite has rectangular shapes and can usually be distinguished from chlorite which formed after prismatic hornblende. The chlorites after hornblende are smaller and accompanied by Ca-rich alteration minerals. Plane polarised light.

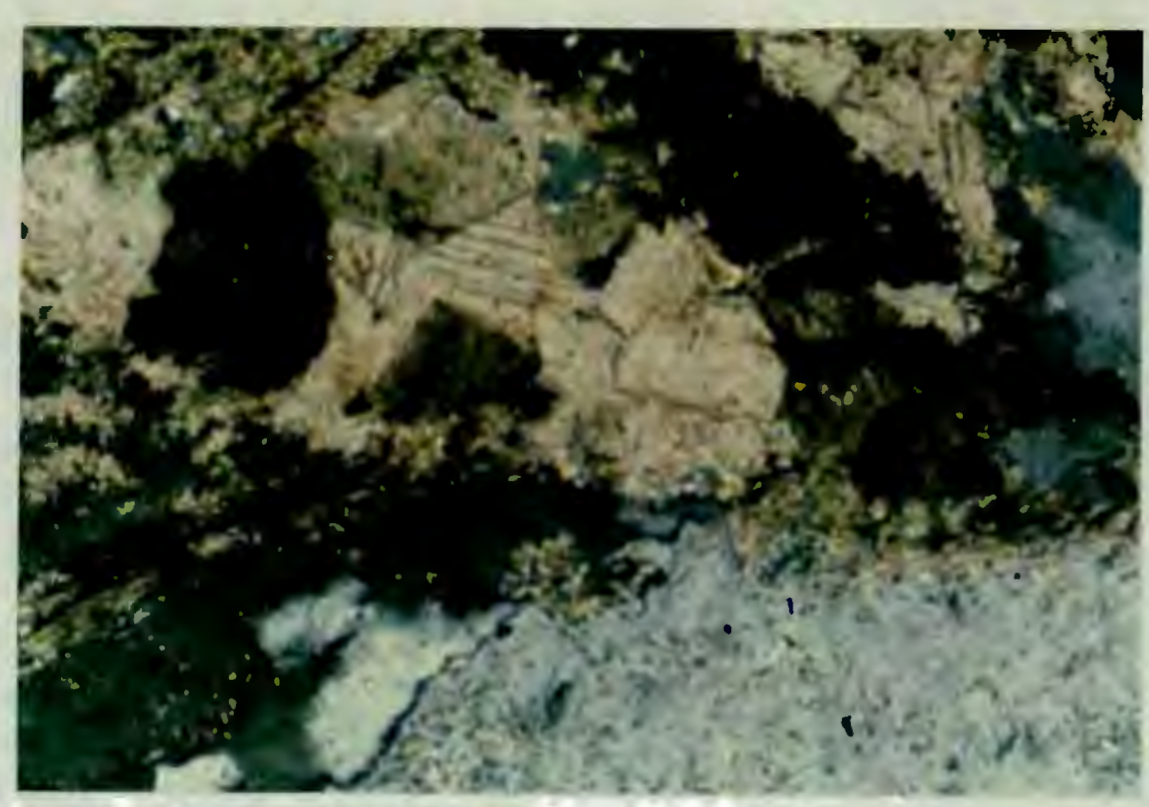

Figure 4.12 Carbonate alteration within KVT (KF11). The carbonate, generally calcite, occurs mostly within veinlets or less frequently as small disseminated calcite grains predominantly in hornblendes. Crossed polarised light.

0.5mm

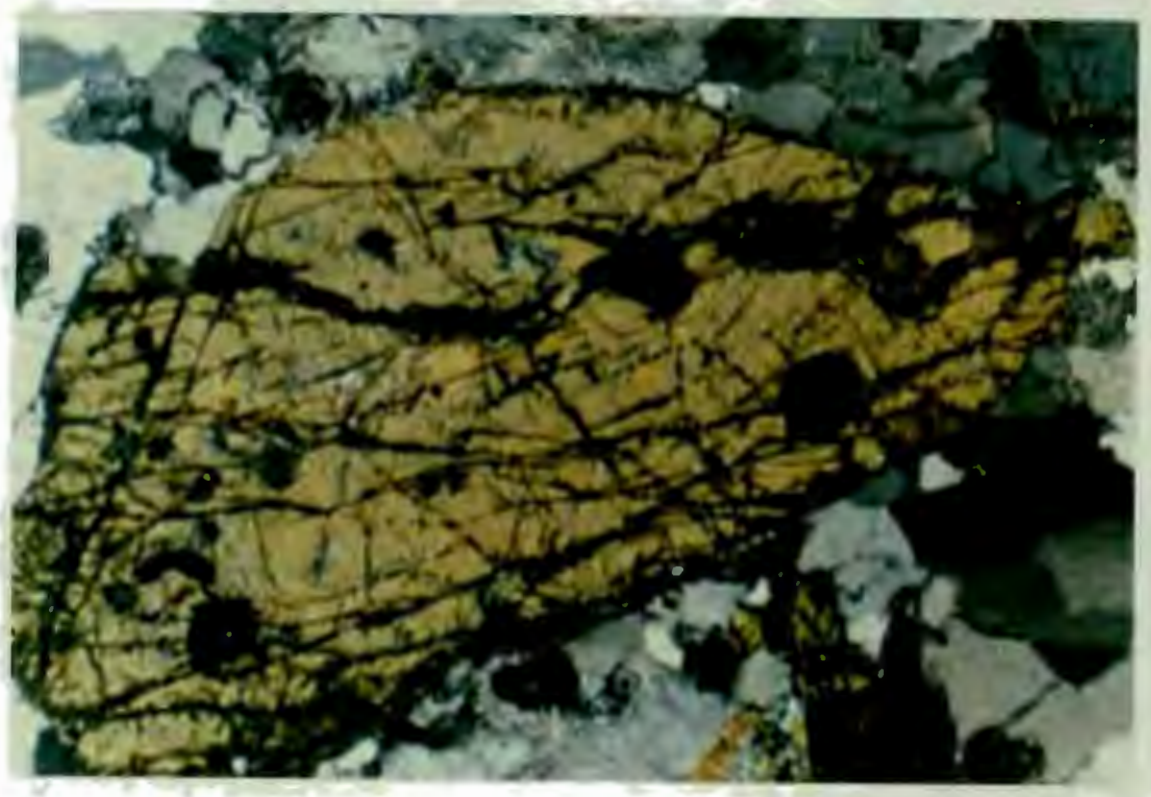

Figure 4.13 Anhedral, secondary sphene within a fractured hornblende. Euhedral sphene (primary) is shown in Figure 4.7. Crossed polarised light.

Table 4.1: Chlorite Temperatures based on the Cathelineau and Nieva (1985) Geothermometer. Chlorites are alteration products of biotite and hornblende unless otherwise indicated.

	Temperature°C	No. Chlorites	Range °C	Comment
KF19	285	1	-	-
KF28	260	5	251-266	-
KF32	251	1	-	-
KF39	205	4	153-166	vein chl.
KF40	205	4	136-283	vein chl.
KF68	262	5	249-290	-
KF87	235	4	223-247	-
KF93	253	5	241-264	-
KF93	259	4	245-279	xenolith
KF96	261	4	249-270	-
KF97	255	5	249-266	-
KF100	266	10	234-287	-
KF104	236	3	225-246	-
KF110	271	3	268-274	-
KF112	272	4	268-293	-
KF119	262	2	251-272	-
mean	252		150-300	
1 std Dev.	22			

anhedral. Euhedral sphene (~1mm in diameter) appears to be primary but the finer anhedral sphene occurs as a replacement mineral and are obviously secondary (Fig. 4.7, 4.13).

4.3 GEOGRAPHICAL ASSOCIATION of MINERALS

The modal percentage contour plots (Appendix 3) are discussed with reference to Figures 4.14. The diagrams of Figure 4.14 have been constructed from the zonations highlighted by contour plots (Appendix 3), using cut-off values that are approximately greater or lesser than the modal percentage mean ± standard deviation (Table A.1, Appendix 3). It is important to note that the zonations defined are not strict but only generalised trends to highlight the areas where the KVT has increased proportions of secondary, often hydrous, minerals and concomitant decreasing hornblende which is less susceptible to alteration than biotite.

Modal percentage contours show that **plagioclase** is evenly distributed across the pluton except for a local depletion in the northern part. Eighty percent of the KVT plagioclases are turbid and/or sericitised. The areas in which samples have plagioclase altered beyond 90 % occur along three trends (Fig. 4.14):

1. a northwest-southeast high following the Jamestown Schist Belt.
2. two approximate north-south trends through the south-central portion of the pluton.

Modal percentage contours of **quartz** show:

1. an increase (>27%) along the Jamestown Schist Belt contact
2. two other quartz "highs" in the south and south-central parts.

The quartz contours parallel the other alteration mineral enrichment trends and thus there appears to have been a secondary quartz input along the alteration zones .

Hornblende modal percentage contours show distinct zones of depletions.

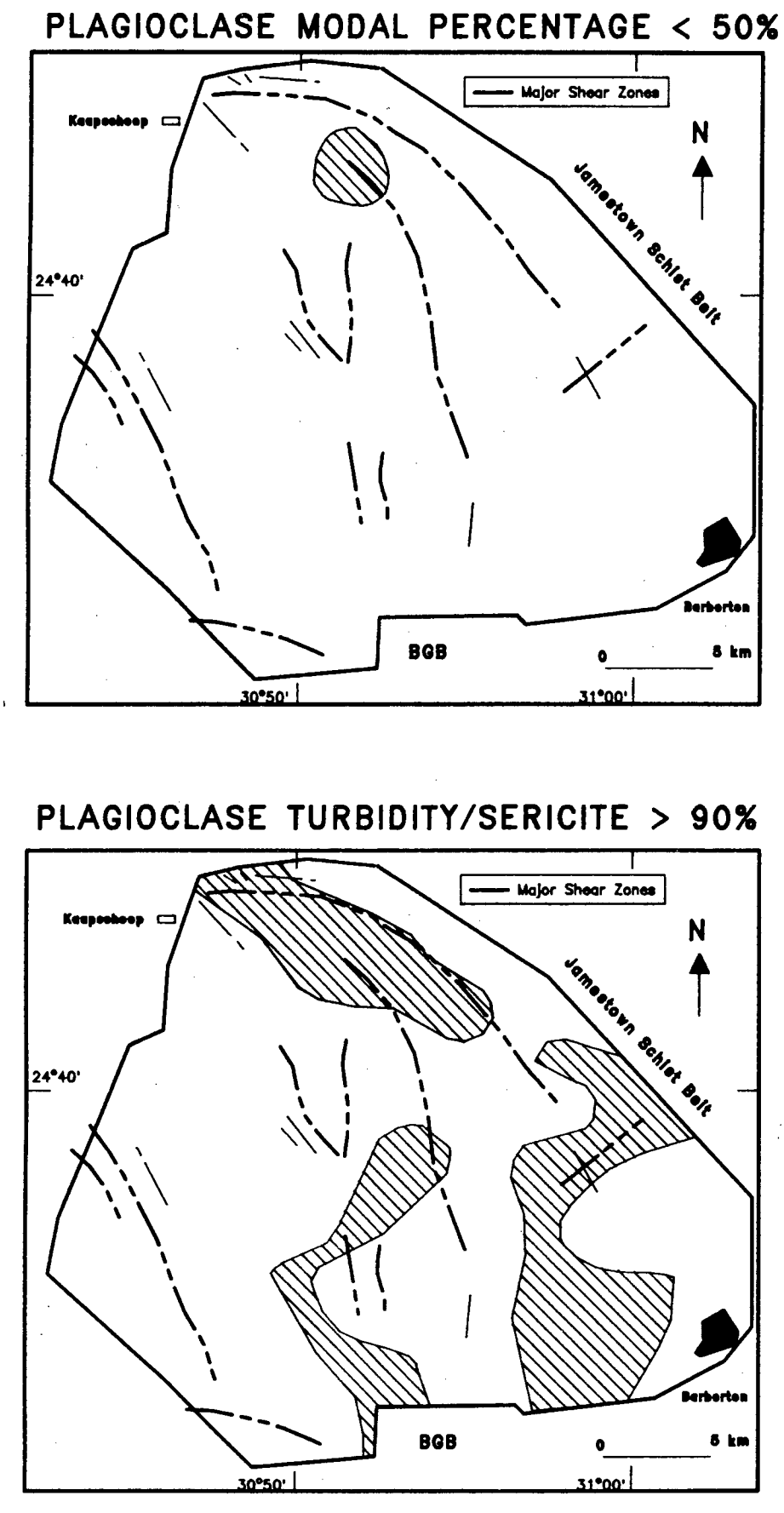

Figure 4.14 KVT mineral volume (%) diagrams (hatched areas) constructed from contour plots in Appendix 2. The cut-off values, indicated above each diagram, are approximately greater or less than the mean modal percentages for each mineral delineated from a point-counting survey (Appendix 1). See text for discussion. Continued.....

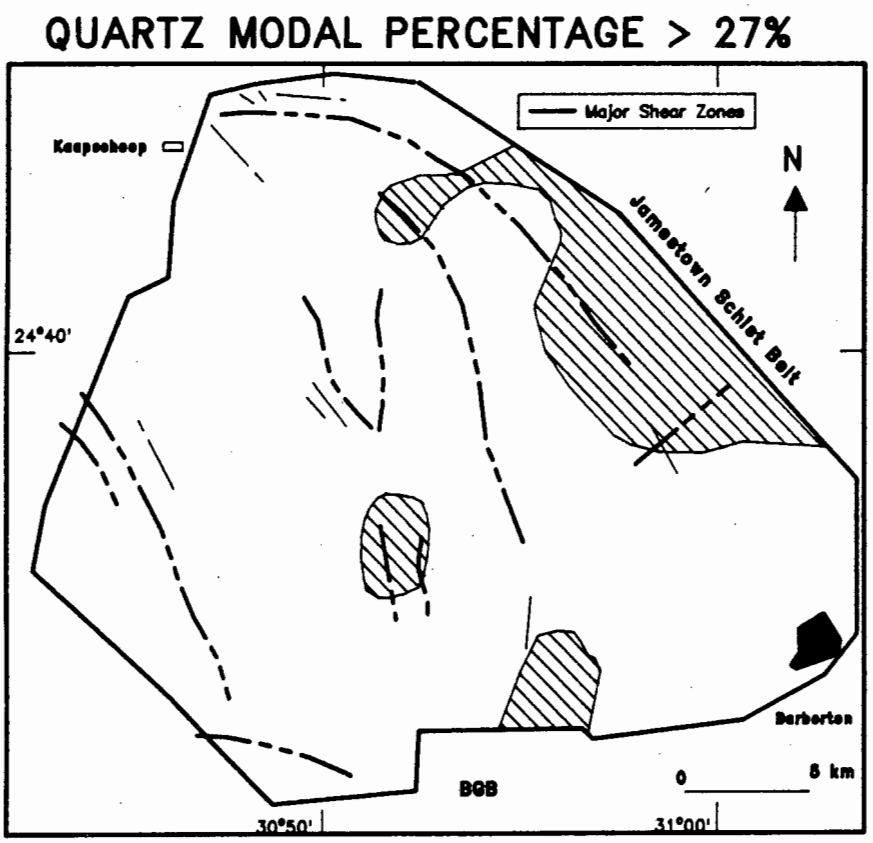

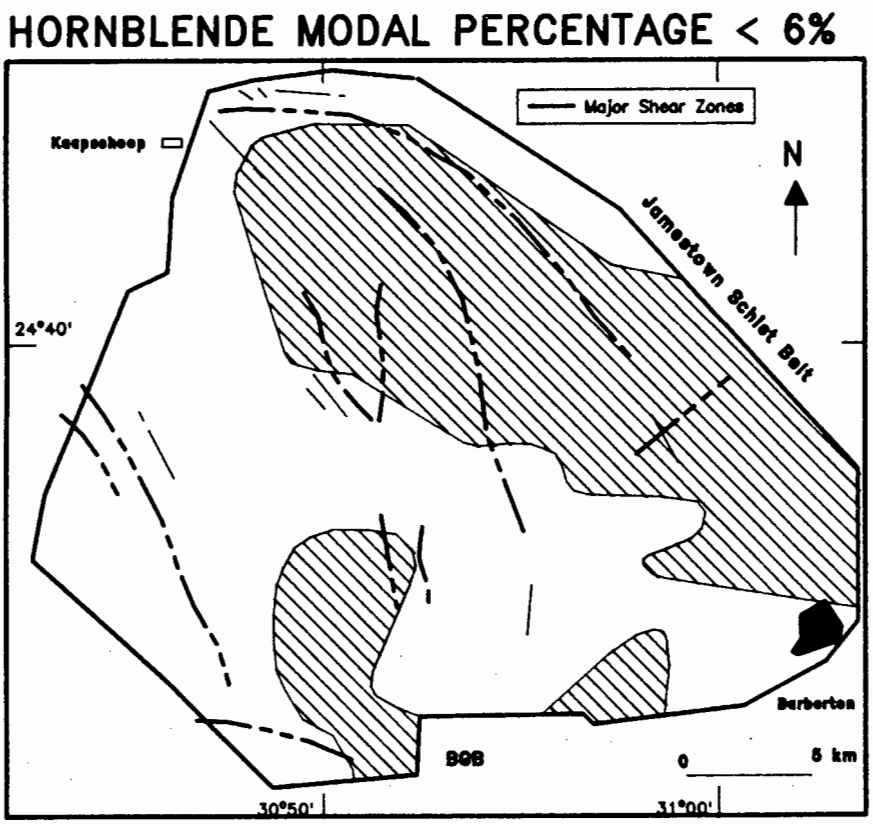

Figure 4.14 Continued.....

1. a prominent northwest-southeast low abundance trend stretches along the Jamestown Schist Belt

2. two smaller north-south trends in the southern part.

The hornblende < 6% contours broadly coincide with the zones of quartz, sericite, chlorite, carbonate and sphene enrichment zones.

Biotite modal percentage contours indicate that the mineral is present in only a few isolated areas.

Chlorite modal percentage contours indicate four high chlorite trends.

1. a zone in the north-central portion of the KVT

2. a northeast-southwest trend in the eastern part of the KVT, coinciding with a major shear

3. two near north-south trends along the southern edge of the pluton

4. the perimeter of the KVT along the east and southern KVT/BGB contact (as was noted in Chapter 2).

These high chlorite zones (> 10%) correspond broadly with increased amounts of other alteration minerals and a decrease in hornblende.

Epidote modal contours show two high north-south trends in the southern portion pluton.

Carbonate (mainly calcite) alteration present in the KVT has trends:

1. that parallel shears along the KVT/Jamestown Schist Belt contact zone

2. a zone along the BGB contact in the southeastern and southern portion and

3. two north-south trends within the center of the pluton.

The **sphene** modal contours indicate a strong zoning along:

1. the Jamestown Schist Belt and

2. a weaker zone in the eastern side of the KVT.

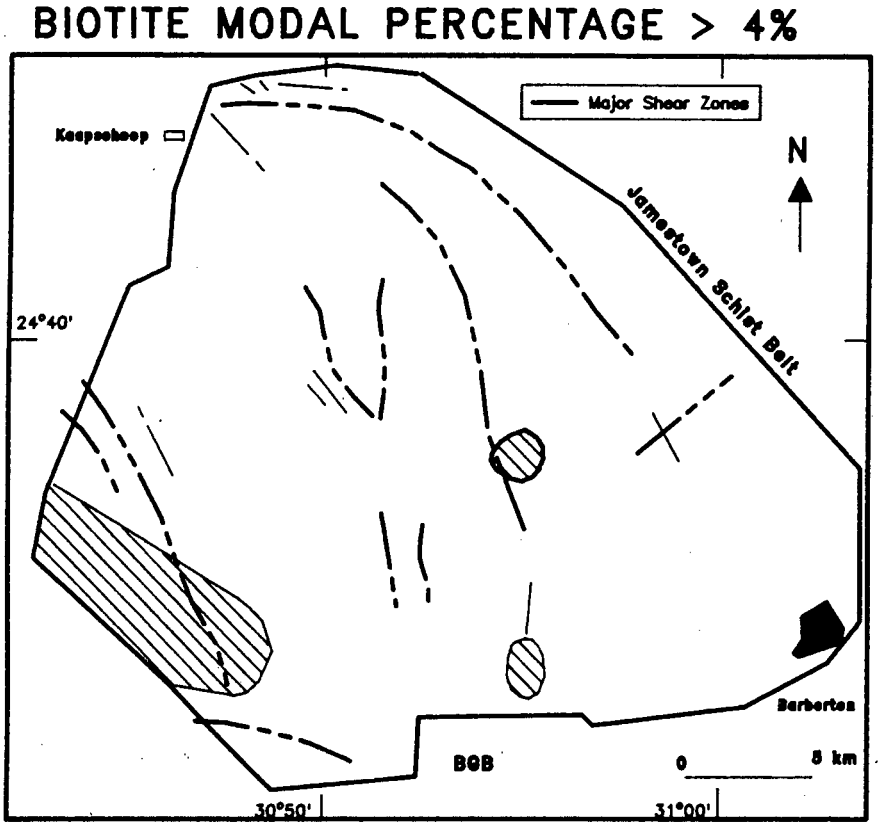

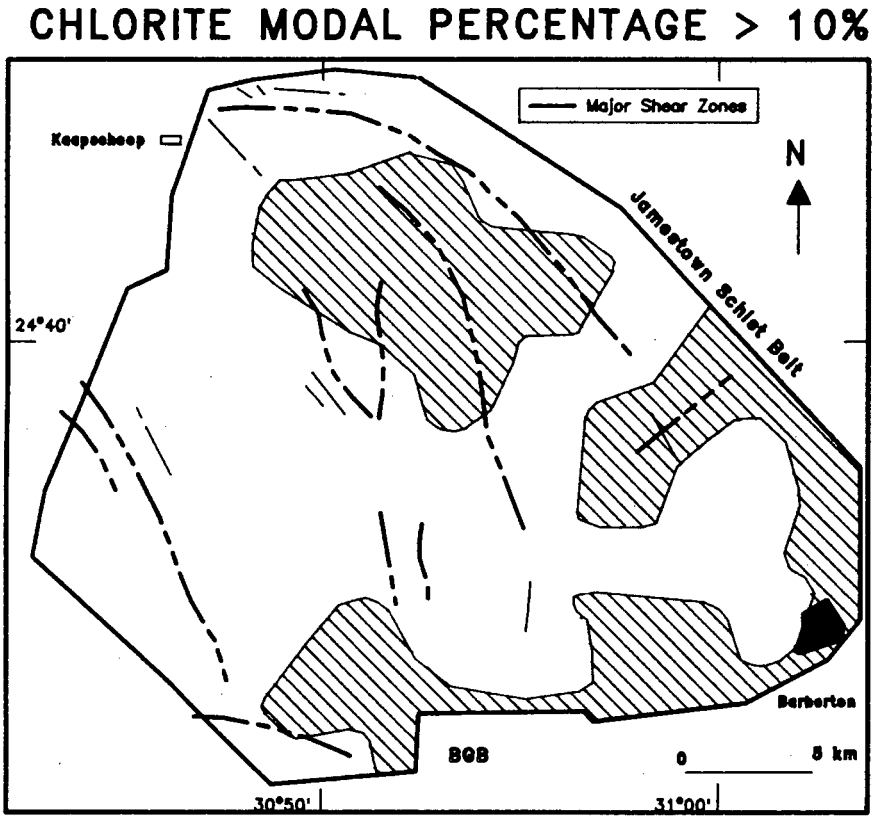

Figure 4.14 Continued.....

EPIDOTE MODAL PERCENTAGE > 3%

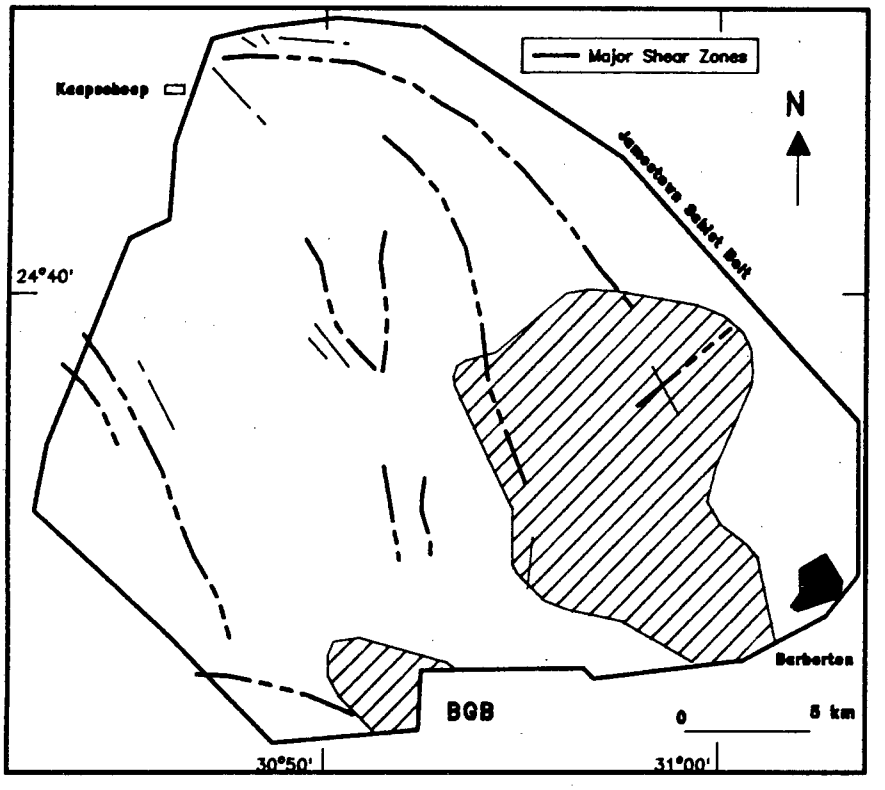

CARBONATE ALTERATION PRESENT in the KVT

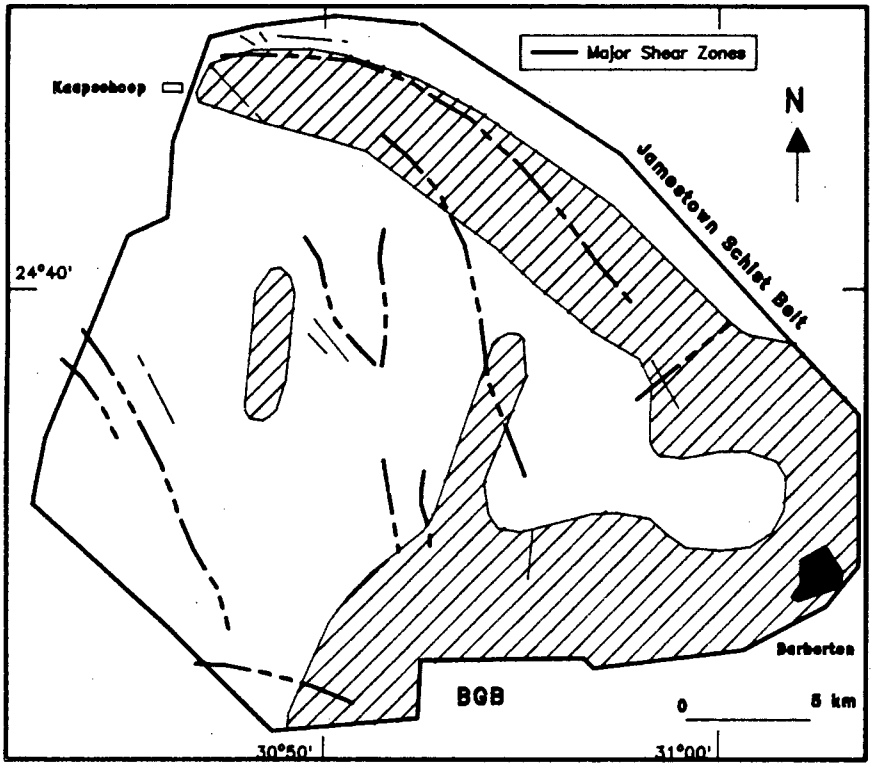

Figure 4.14 Continued.....

The zone paralleling the Jamestown Schist Belt Contact is strongly associated with other zones of intense mineral alteration.

Petrographic observations therefore indicate that the KVT does have specific areas that have increased percentages of chlorite, turbidity/sericite and quartz, the presence of carbonate and decreased proportions of hornblende. These broadly overlap along zones following the KVT/Jamestown Schist Belt, the southern KVT/BGB contact and two north-south trends in the southern part of the KVT. These zones overlap with some of the major shear zones within the KVT and the KVT/BGB contact, which could have been conduits along which alteration fluids were channelised to cause the intense propylitic, sericitic and carbonate alteration (Fig. 4.15).

4.4 SUMMARY

Plagioclase feldspars which characteristically exhibit oscillatory zoning, are predominantly oligioclase (mean = An_{25}) in composition. The plagioclase rims are more sodic than the internal portions but the intermediate and core portions cannot be distinguished from their chemistry. The variation in plagioclase composition can be attributed to systematic changes in the composition of the liquid from which it crystallised. The more calcic portions have subsequently altered to sericite or become turbid.

It has been suggested that in the KVT, hornblende is xenocrystic and derived from assimilated wall-rock metavolcanics (Condie and Hunter, 1976 ;Anhaeusser, 1969). The hornblende however does not exhibit resorption textures and generally has euhedral to subeuhedral shapes. Petrographic evidence from the KVT hornblendes suggest that they are primary. Robb et al. (1986) from petrographic and chemical evidence also consider the hornblende to be primary.

The hornblende of the KVT overlap chemically with hornblendes of metabasaltic xenoliths. The hornblende and biotite of the KVT are generally in chemical equilibrium with two exceptions which may indicate that some of the hornblende and/or biotite is xenocrystic. Petrographic observations indicate that they are not visibly altered.

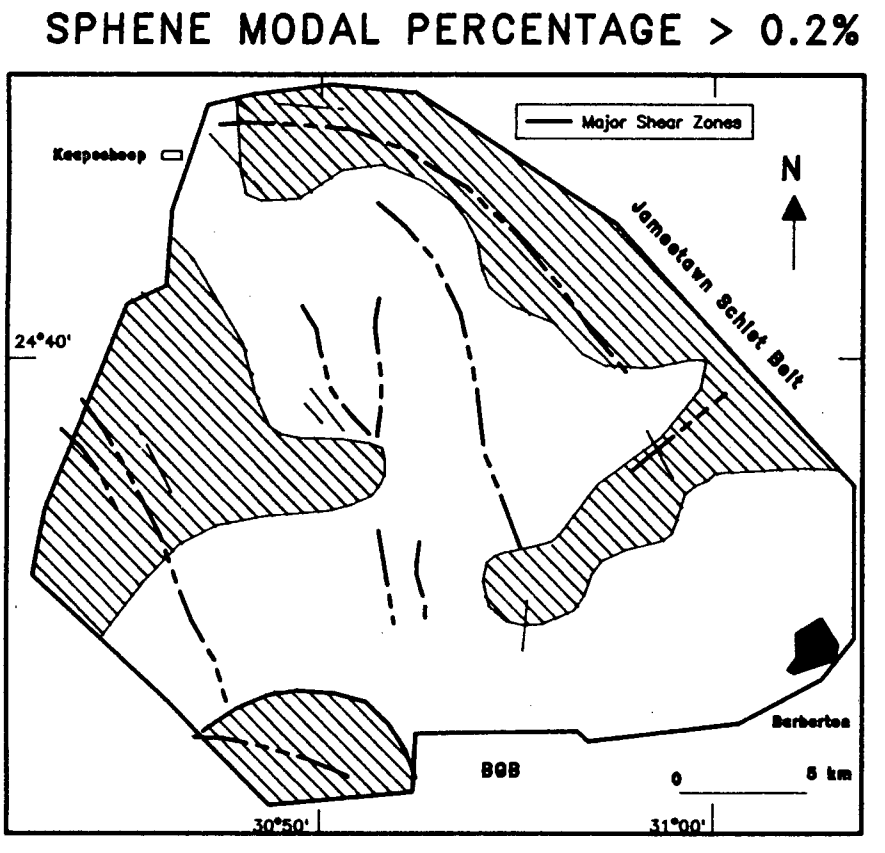

Figure 4.14 Continued.....

KVT AREA WHICH HAS A HIGH PROPORTION OF HYDROUS MINERALS AND ALTERED PRIMARY MINERALS

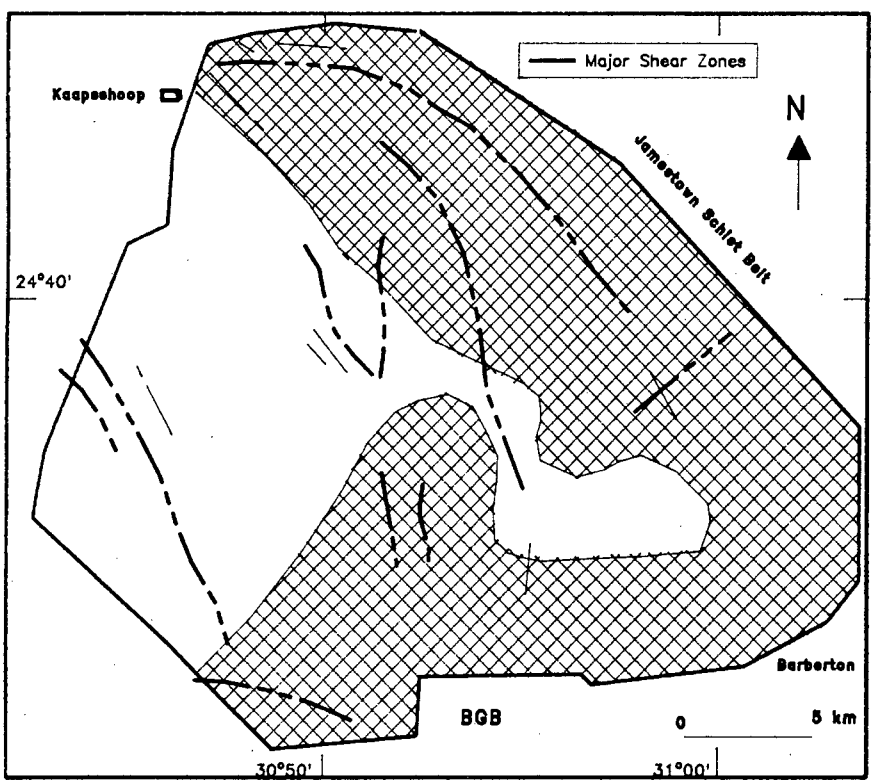

Figure 4.15 The hatched area in this diagram incorporates overlapping areas of increased mineral alteration, as delineated in Figure 4.14.

The KVT, from petrographic studies, appears to have been originally a homogenous rock in terms of its mineral abundances. It follows that one should then be able to map out alteration assemblages precipitating from a fluid. In this case however, it might not be so simple because the KVT has been exposed to a 3,2 Ga history and may have been subject to multiple alteration events. The petrographic evidence and mineral distribution patterns of the KVT do highlight trends for which there must be some explanations:

1. The KVT was originally a hornblende (15-20%) plus biotite (5-10%) tonalite which was generally homogenous with respect to its mineral abundances.

2. The KVT had been infiltrated by fluids and has undergone wide-scale alteration. The alteration minerals chlorite, epidote, sericite, carbonate and (very) locally quartz are assemblages associated with propylitic, sericitic (potassic) and carbonate alteration, (Meyer and Hemley, 1976). Chlorites have crystallisation temperatures averaging 250°C based on the Cathelineau and Nieva (1986) solid solution geothermometer. Low temperature chlorites (~140°C) from veins and higher temperature chlorites (up to 290°C) after biotite and chlorite are also present. No petrographic evidence was observed to suggest that more than one age/phase of alteration fluid was present within the KVT.

3. The order of increasing susceptibility to mineralogical alteration during hydrothermal alteration and recrystallisation of the tonalite is quartz < amphibole < biotite < plagioclase. This is important for interpreting oxygen stable isotope data as this indicates the increased susceptibility for isotopic re-equilibration.

4. The propylitic and sericitic alteration is present across the whole pluton but this alteration is generally not accompanied by penetrative deformation.

5. Zones of intense propylitic and sericitic alteration accompanied by carbonate alteration and locally quartz re-crystallisation have

been delineated within the KVT. These broadly overlap along trends following the KVT/Jamestown Schist Belt, the southern KVT/BGB contact and two north south trends in the southern part of the KVT. These zones overlap with some of the major shear zones within the KVT and the KVT/BGB contact. The shear zones could have been conduits along which alteration fluids were channelled to cause the intense propylitic, sericitic and carbonate alteration. In some cases penetrative deformation resulted in the recrystallisation of quartz which is generally sluggish to be reprecipitated by alteration fluids.

6. A regional alteration pattern could potentially be used in delineating possible targets for localised mineralisation from petrographic studies as a relatively cheap exploration tool.

5. OXYGEN ISOTOPES in KVT SILICATES

5.1 INTRODUCTION

In this chapter oxygen isotope data is presented for selected minerals and whole rocks, to possibly identify the source of fluids that have been responsible for the alteration/mineralisation processes described in the previous chapter and to consider possible sources for the KVT magma. A brief review of the theoretical and experimental aspects of stable isotope geochemistry are described in detail in Appendix 1 and Chapter 3 respectively.

The $\delta^{18}O$ values of igneous rocks and their minerals are controlled by several factors such as:

1. the $\delta^{18}O$ of the magma
2. the temperature of crystallisation
3. effects of fractional crystallisation
4. retrograde effects resulting from re-equilibration at subsolidus temperatures and
5. interaction with aqueous solutions.

These aspects will be considered when interpreting the $\delta^{18}O$ data obtained in this study.

In addition to temperatures of formation of minerals, it may be possible to estimate the $\delta^{18}O$ ratio of fluid that was in equilibrium with the particular minerals, ascertain the degree of equilibrium attained during crystallisation and the amount of interaction with country rock and/or extraneous fluids (Taylor, 1968).

5.2 PREVIOUS O-ISOTOPE STUDIES of BARBERTON MOUNTAIN LAND GRANITOIDS

Taylor and Magaritz (1975) determined $\delta^{18}O$ and δD ratios of some TTG in a regional study of the Barberton Mountain Land. Taylor (1977)

compared these results with the field of "normal" igneous rock values which is principally based on studies of Phanerozoic granitoids (Fig. 5.1). The chloritisation of the Transvaal tonalite domes (3 KVT samples) was attributed to meteoric-hydrothermal alteration processes (Taylor, 1977). Such effects were considered to decrease with increasing depth, with deeply eroded Swaziland gneisses being extremely fresh and unaltered. Apparently no unchloritised TTG samples were analysed.

5.3 O-Isotopic Compositions of the KVT

5.3.1 $\delta^{18}O$ *Data for the KVT*

The $\delta^{18}O$ values obtained from the KVT mineral separates and whole-rocks are presented in Table 5.1. Whole-rock $\delta^{18}O$ values were also calculated using mineral $\delta^{18}O$ values and their weight percent abundances.

It is clear from Table 5.1 that the $\delta^{18}O$ of the quartz separated from the KVT samples is very constant. The (arithmetic) mean and standard deviation for the $\delta^{18}O$ quartz values are +9.7 ±0.3 ‰. The only sample which falls significantly out of this range (analytical error taken into consideration) is KF36 in which the $\delta^{18}O$ of quartz is ~ 1 ‰ lighter.

KVT plagioclases analysed have a mean $\delta^{18}O$ of +7.2 ±0.6. Values are more variable than the quartz data, especially those of samples KF36 and KF77 (Table 5.1). The KVT, which is composed of approximately 65 % plagioclase, has $\delta^{18}O_{WR}$ values that are approximately equal to that of the $\delta^{18}O$ plagioclase values.

Hornblende $\delta^{18}O$ values do not show any significant deviation from the mean value of +5.4 ±0.3 ‰. Five biotite samples analysed have a mean $\delta^{18}O$ value of +3.1 ±0.3 ‰. It is worth noting, that in samples KF36 and KF77, no primary hornblende or biotite is left since both minerals have been completely altered.

It has been shown in Chapter 4 that chlorite is a secondary mineral replacing primary biotite in the KVT. The $\delta^{18}O$ data of the chlorite is important because it allows for some predictions regarding the

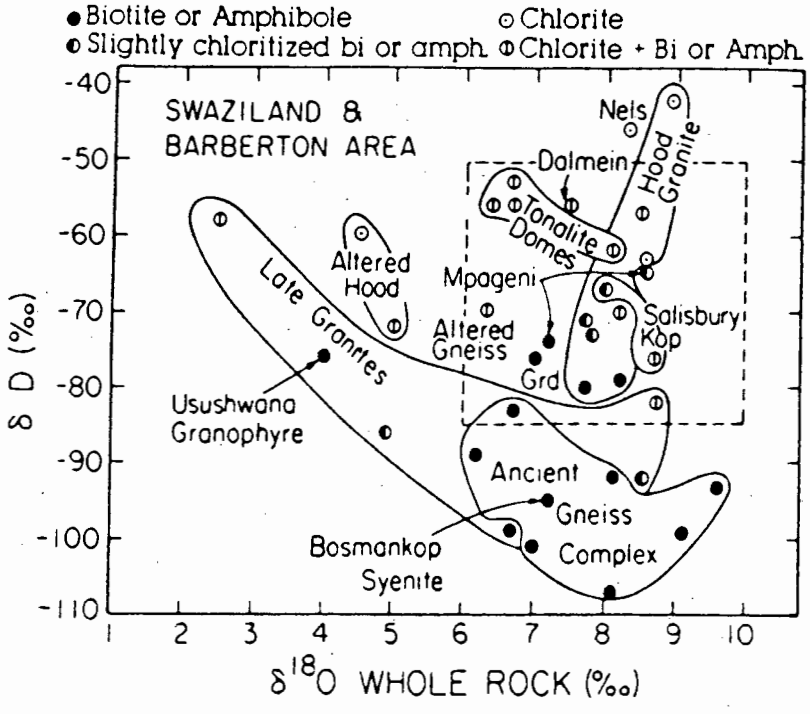

Figure 5.1 δD vs $\delta^{18}O$ for Archaean granitoids and gneisses from the Barberton and Swaziland regions of southern Africa. The "box", outlined with a broken line , represents the "normal" range of δD and $\delta^{18}O$ values based on studies of Phanerozoic granitoids. The tonalite domes (of which 3 samples are from the KVT) plot within this range. After Taylor and Magaritz (1975), in Taylor, (1977).

Table 5.1: Oxygen Isotope Data For Silicate Minerals and whole-rocks from the Kaap Valley Tonalite. All analyses were done in duplicate and reported in per mil (‰) relative V-SMOW. The difference between duplicates of each analysis is better than 0.1 ‰ except for values with * which have differences between 0.1 and 0.2 ‰.

	QTZ	PLG	HBL	BIO	CHL	EPI	WR	CWR
KF2	9.2	6.5	4.9	-	2.6	2.7*	6.6	6.4
KF11	9.8	7.4	5.6	3.5	-	-	7.6	7.4
KF19	9.8	7.3	5.6	3.2	-	-	7.3*	6.8
KF29	9.9	7.5	4.9	-	2.9	-	-	7.2
KF33	9.8	7.4	-	-	-	-	-	7.3
KF36	9.0	5.3	-	-	1.0	2.4*	6.0	5.6
KF39	9.7	7.1	5.8	2.8	-	-	8.2	7.3
KF42	9.9	7.4	5.7	-	3.8	-	-	7.7
KF43	-	-	-	-	-	-	8.3	-
KF52	9.6*	6.6	5.6	-	2.7	-	7.5	-
KF60	10.2	7.3	5.5	-	-	-	-	7.8
KF65	9.6	7.5	5.5	3.3	-	-	7.2*	6.8
KF68	9.9	7.5	5.7	-	3.1	-	8.2	7.5
KF71	-	-	-	-	-	-	7.2	-
KF72	-	-	-	-	-	-	7.0	-
KF73	-	-	-	-	-	-	7.2	-
KF75	9.6	6.7	5.2	-	2.5	-	-	6.8
KF77	9.5	8.6	-	-	-	-	8.5	8.3
KF88	9.9	8.0	-	-	-	-	-	-
KF91	9.7	7.5	5.1	-	2.3	-	-	7.4

Table 5.1: continued.....

Table 5.1: continued.....

	QTZ	PLG	HBL	BIO	CHL	EPI	WR	CWR
KF96	9.8	7.3	5.6	-	2.5	-	-	6.9
KF102	9.9	7.4	-	-	3.5	-	8.0	7.5
KF108	10.0	7.4	5.4	-	-	-	-	7.0
KF114	9.3	7.4	5.6	2.8	3.1	-	7.61	7.48
KF118	9.5	6.9	4.8*	-	1.9	-	-	6.5
KF121	9.5	6.7	5.1	-	2.6	-	-	6.5
mean	9.7	7.2	5.4	3.1	2.6	2.6	7.5	7.1
1 std dev.	0.3	0.6	0.3	0.3	0.7	0.2	0.7	0.6

Abbreviations:
QTZ-quartz; PLG-plagioclase; HBL-hornblende; BIO-biotite; CHL-chlorite; EPI- epidote; WR-whole rock; CWR-calculated WR; Δ-difference between duplicate $\delta^{18}O$ value

alteration fluid. Notably KF36 has the lowest chlorite $\delta^{18}O$ value. It was not possible to separate any pure chlorite from KF77 as this mineral was too small and contained abundant inclusions.

Low oxygen yields were obtained from the epidote samples (Chapter 3) and the average difference in duplication was 0.2 ‰. Only two epidote samples were analysed because of the difficulty in separating pure epidote and also because of their small sizes. The $\delta^{18}O$ values for epidote minerals may therefore not be representative of the KVT epidotes and could be unreliable.

Vein-quartz samples from the KVT have been analysed for their $\delta^{18}O$ values (Table 5.2). The mean $\delta^{18}O$ value of the vein-quartz is +10.8 ±1.2 ‰ which does not include the KF37 value (+3.9 ‰), as it is an obvious outlier.

5.3.2 *Discussion*

The tendency of silicate minerals to concentrate ^{18}O is related to their chemical compositions. For minerals that are in equilibrium with each other, the minerals with the most Si-O-Si bonds will have the highest $\delta^{18}O$, while those containing Si-O-Mg and Si-O-Fe bonds have $\delta^{18}O$ values 2-4 ‰ lower (Taylor and Epstein, 1962). In theory, therefore, the following sequence of increasing ^{18}O enrichment is predicted, quartz, plagioclase, hornblende, biotite and chlorite for the minerals in this study, provided they are in isotopic equilibrium. The $\delta^{18}O$ enrichment sequence of the KVT minerals is as predicted from theory (Taylor and Epstein, 1962) and no isotopic reversals are observed.

Two methods of establishing whether isotopic equilibrium is present in co-existing minerals are: (1) by means of δ-δ plots (Gregory and Criss, 1986; Gregory et al., 1989) and (2) using the mineral "isotherm method" (Javoy et al., 1970). The δ-δ diagrams are useful in evaluating open versus closed system behaviour. This is especially the case if minerals with different isotopic exchange rates are used. In general terms, a closed system consists of an assemblage of minerals, occurring in fixed modal proportions, in which the minerals are

Table 5.2: The $\delta^{18}O$ results of the KVT vein-quartz analyses. The difference between duplicate analyses are better than 0.1 ‰ unless an * appears next to a value. The $\delta^{18}O$ value of KF37 is considered to be an outlier and is not included in the mean $\delta^{18}O$ of the vein-quartz.

	$\delta^{18}O$ Vein-Quartz
KF16	11.1
KF37	3.9
KF46	9.5
KF53	9.5
KF78	10.5
KF81	11.4*
KF85	10.3
KF106	13.2
KF136	10.6*
mean	10.8
1 std dev.	1.2

constrained to exchange only with each other, while the bulk oxygen isotopic composition remains constant. In an open system, the bulk composition of a rock is influenced by interactions with externally derived oxygen reservoirs such as fluid, for example H_2O (Gregory and Criss, 1986). If closed system conditions prevailed, the data should fall on a straight line in a δ-δ plot, with slope of 45°. For any 45° line, δ_a-δ_b = Δ_{a-b} is constant and therefore temperature is constant, and these lines are isotherms. Open system behaviour may be apparent on δ-δ plots as the trends formed will not lie on a 45° line (i.e. exchange with an external fluid). If the mineral with the faster exchange rate is on the y-axis the open system array will be steeper than the 45° isotherms (Gregory and Criss, 1986).

The "isotherm method" was used by Javoy et al. (1970) to test for the presence of disequilibrium isotopic relations. The "isotherm method" differs from the δ-δ plots in that temperature relations can also be compared. It is based on the following equation:

$$\delta_1-\delta_2 = \Delta_{1,2} = A/T^2 + B \qquad \text{eqn. 5.1}$$

where A and B are constants, 1 and 2 are minerals and T is the temperature in K. Equation 5.1 rearranged reads:

$$\Delta_{1,2} - B = A/T^2 \qquad \text{eqn. 5.2}$$

Normally two minerals are chosen with differing susceptibility for exchange, one of which is usually quartz. Plotting ($\Delta_{1,2}$ - B) versus A should yield a straight line through the origin if the minerals are in isotopic equilibrium. The X-axis is fixed by the constant A (from calibration curves) and does not vary. The Y-axis values will vary dependent on the $\Delta_{1,2}$ value. The temperature is calculated from the slope of the line. Disequilibrium is indicated when the points are not co-linear or, if they are co-linear, where the line does not go through the origin.

The narrow range of quartz $\delta^{18}O$ values suggest that the oxygen in the quartz did not re-equilibrate after closure during magmatic cooling,

except perhaps for sample KF36 (Table 5.1). Small quartz neoblasts present in KF36 support the idea that KF36 quartz has been dissolved and re-precipitated at a different temperature. In Chapter 4 it was established from petrographic evidence (of a larger sample population) that silica was only locally introduced to the system.

The KVT plagioclase data is distinctly more varied than the quartz data (Table 5.1). The $\Delta_{qtz-plg}$ of the KVT is ~3 ‰ which is high compared to some other tonalites, for example the Bonsal and San Jose tonalites in California have $\Delta_{qtz-plg}$ of 1.8 and 1.7‰ respectively (Taylor and Epstein, 1962). The quartz-plagioclase δ-δ has an array which is not parallel to isotherms (Fig. 5.2) and the "isotherm" diagram (Fig. 5.3) also suggests open system behaviour. The plagioclase data therefore indicates that it has exchanged oxygen. On a δ-δ diagram KF36 and KF77 plot on the opposite ends of a steep trajectory (Fig. 5.2) and on a "isotherm" diagram, at both the highest and lowest quartz-plagioclase temperatures (Fig. 5.3). If the $\delta^{18}O$ of the plagioclases are compared to the intensity of their alteration (turbidity/sericitisation) it is apparent that relatively unaltered plagioclases have constant $\delta^{18}O$ of +7.4 ‰ and highly altered plagioclases have a larger range of $\delta^{18}O$ values from +5.3 to +8.6 ‰ (Fig. 5.4). This may indicate that more than one type of alteration fluid was present within the KVT or alternatively that one fluid altered the rock over a range in temperatures. As stated above, the effects of alteration on the $\delta^{18}O$ of the plagioclases are mirrored by those of $\delta^{18}O_{WR}$ values (Fig. 5.4).

The hornblende $\delta^{18}O$ data, although nearly paralleling isothermal lines in a δ-δ plot relative to quartz (Fig. 5.2) do not, however, lie on straight lines through the origin in the "isothermal" diagram (Fig. 5.3). The effects of the alteration fluids on the hornblende and biotite are probably not well illustrated by Figures 5.2 and 5.2 because only "fresh" hornblende and biotite were analysed. The altered biotite and hornblende are now secondary chlorite and epidote. The temperature indicated for the quartz-chlorite in Figure 5.3 is not considered significant because these two minerals did not crystallise in

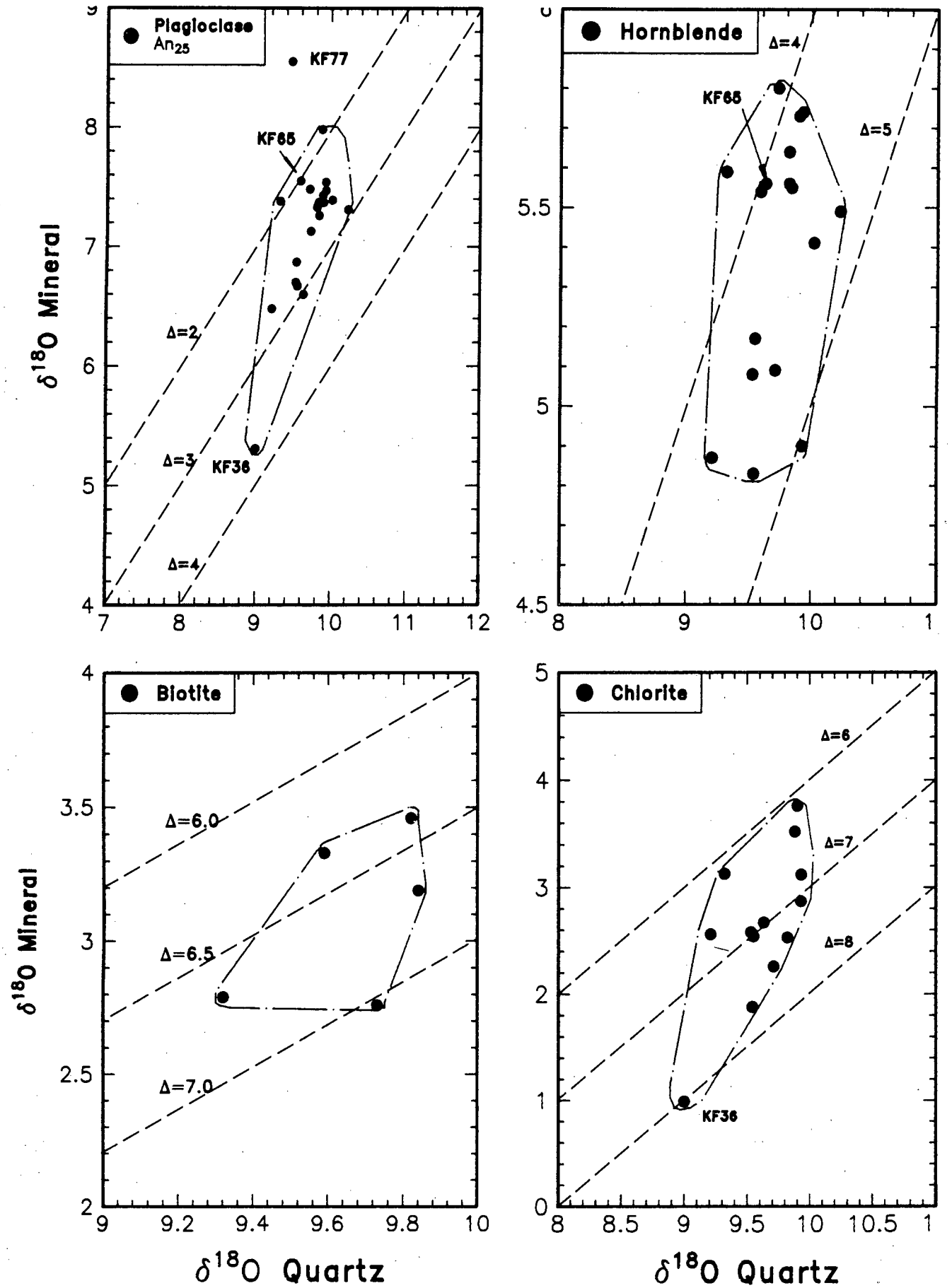
Plagioclase
An25
KF77
KF65
KF36
Δ=2
Δ=3
Δ=4
Hornblende
Δ=4
Δ=5
Biotite
Δ=6.0
Δ=6.5
Δ=7.0
Chlorite
Δ=6
Δ=7
Δ=8
δ18O Mineral
δ18O Quartz

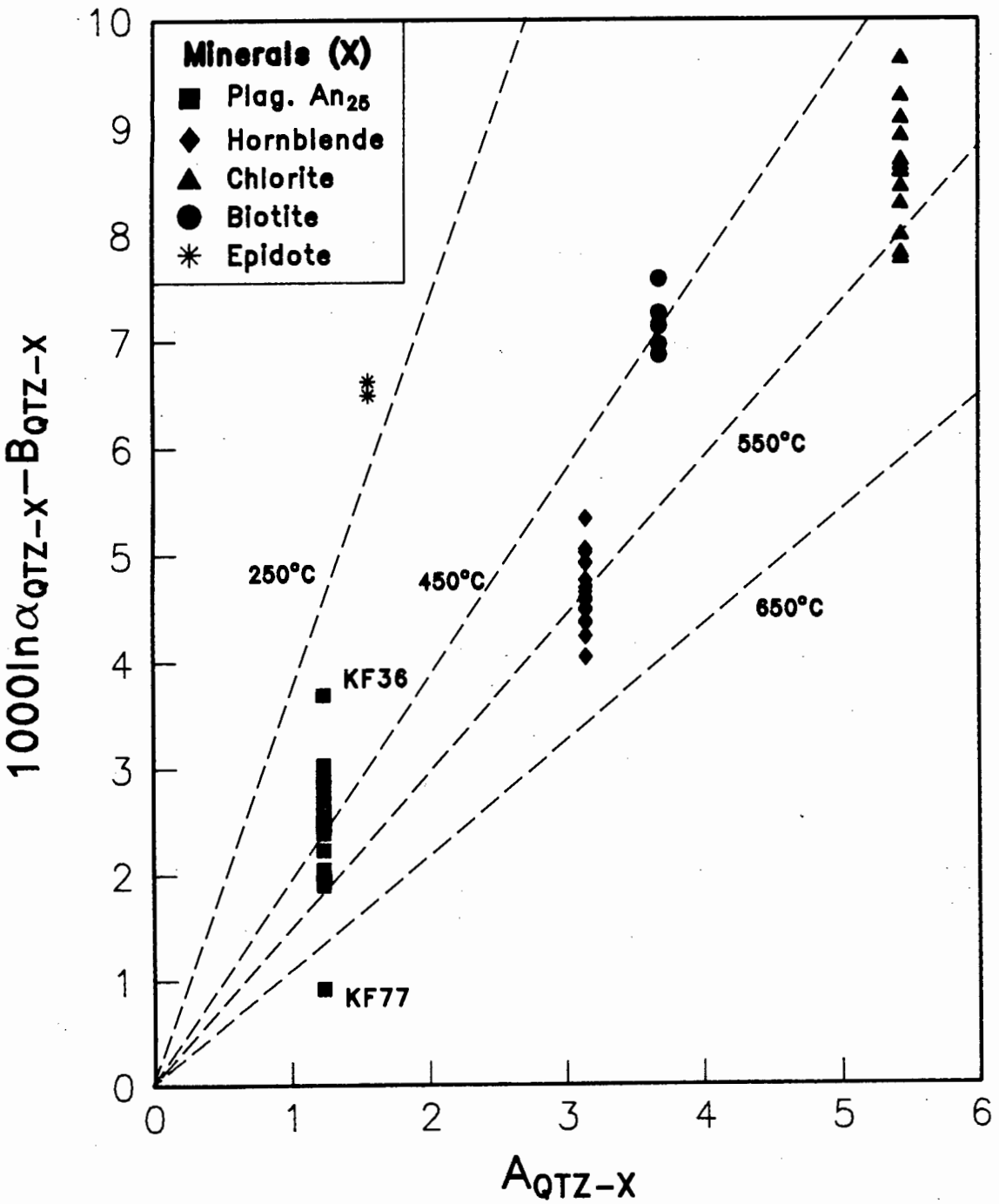

Figure 5.3 An "isotherm" plot for the KVT mineral separates. This diagram indicates both temperature of equilibration and the presence of isotopic disequilibrium. It is based on equations relating temperature and fractionation factors between quartz and other minerals from the KVT. Factors A and B are constants derived from $\alpha_{Min-Min}$ and temperature calibrations (see Appendix 1 for calibration equations). The X-axis is fixed by the constant A in equation 5.2 and does not vary. The Y-axis values will vary dependent on the $\Delta_{QTZ-Mineral}$ value. If the points plotted do not yield a straight line, that passes through the origin, disequilibrium is indicated. The KVT data plotted on the "isotherm" diagram of Javoy (1970), indicates mineral disequilibria and suggests open system conditions.

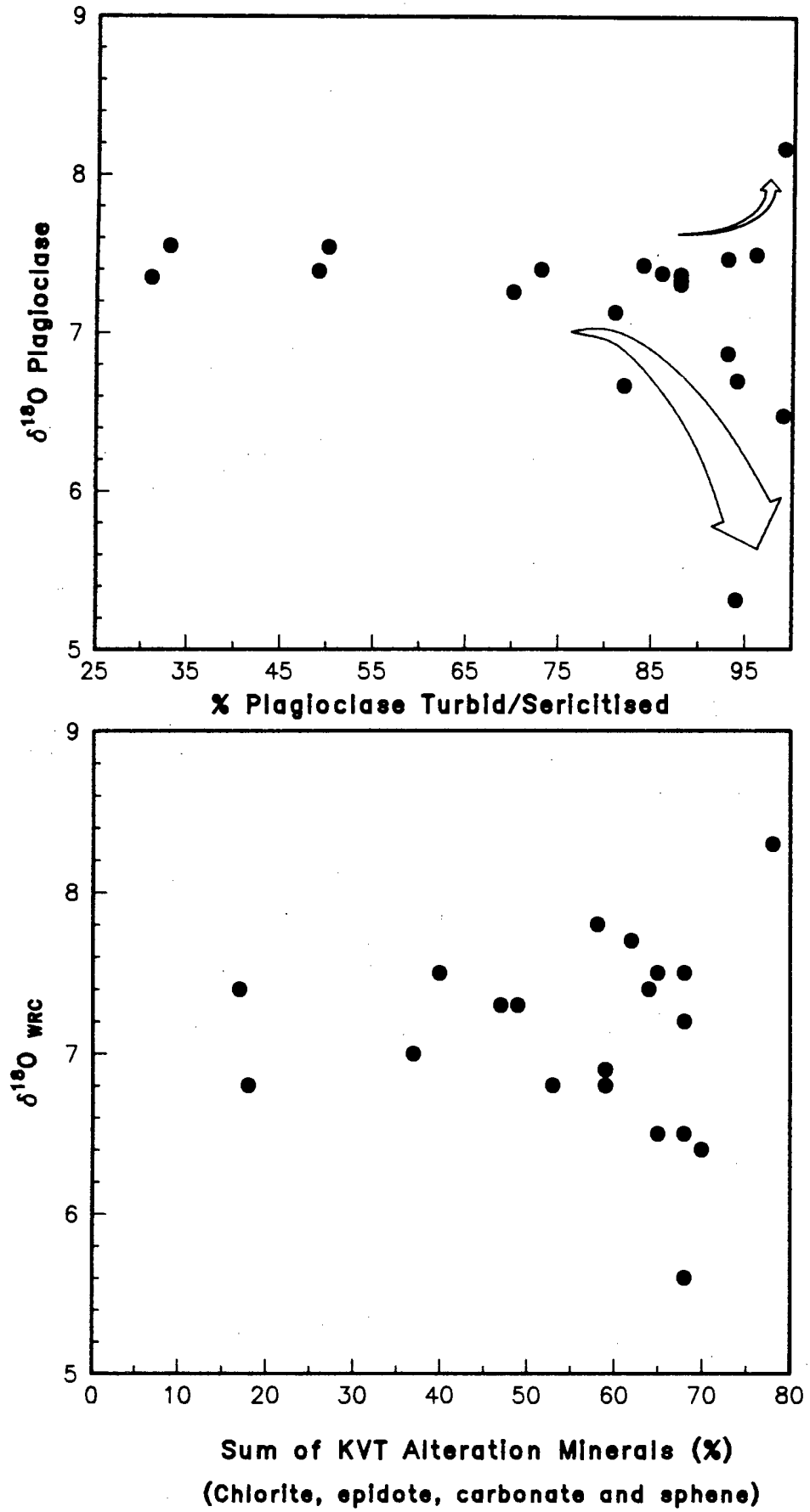
9
8
7
6
5
δ18O Plagioclase
25
35
45
55
65
75
85
95
% Plagioclase Turbid/Sericitised
9
8
7
6
5
δ18O WRC
0
10
20
30
40
50
60
70
80
Sum of KVT Alteration Minerals (%)
(Chlorite, epidote, carbonate and sphene)

equilibrium with each other. The temperatures suggested are also much higher than the 252 ±22 °C calculated for chlorite using the Cathelineau and Nieva (1986) geothermometer (Chapter 4).

The $\delta^{18}O$ data is most consistent with oxygen exchange with an external fluid and therefore open system conditions (Table 5.1, Figs 5.2, 5.3 and 5.4). Both oxygen and petrographic data supports open system conditions. Lack of oxygen isotope reversals and the absence of significant disequilibrium trends on δ-δ diagrams suggest that exchange with fluid was limited and that water/rock (W/R) ratio was therefore small.

5.4 KVT O-ISOTOPE DISTRIBUTION

The variation in oxygen isotopic composition of the various minerals across the KVT pluton is illustrated by means of contour diagrams in Appendix 4 and summarised in Figure 5.5. The areas where plagioclase, quartz, hornblende and chlorite $\delta^{18}O$ values are less than their arithmetic mean, generally overlap one another (Fig. 5.5). This is especially true for the plagioclase, hornblende and chlorite. The zone delineated by decreasing $\delta^{18}O$ values for plagioclase, hornblende and chlorite, covers the eastern and south-eastern portion, up to the KVT/BGB contacts, of the KVT (Fig. 5.6). This part of the intrusion is therefore where fluid interaction has been greatest (Fig. 5.6).

5.5 O-ISOTOPE THERMOMETRY

Isotope analysis of high-temperature rocks and minerals (Taylor and Epstein, 1962; O'Neil, 1968): have shown that:

1. isotopic fractionations decrease with increasing temperature and are independent of pressure changes

2. isotopic fractionations among co-existing minerals at high temperatures are still large compared to the analytical error.

The rationale for the temperature dependence on the isotopic fraction between minerals is described in Appendix 1.

Oxygen isotope thermometry has been reviewed and debated extensively in

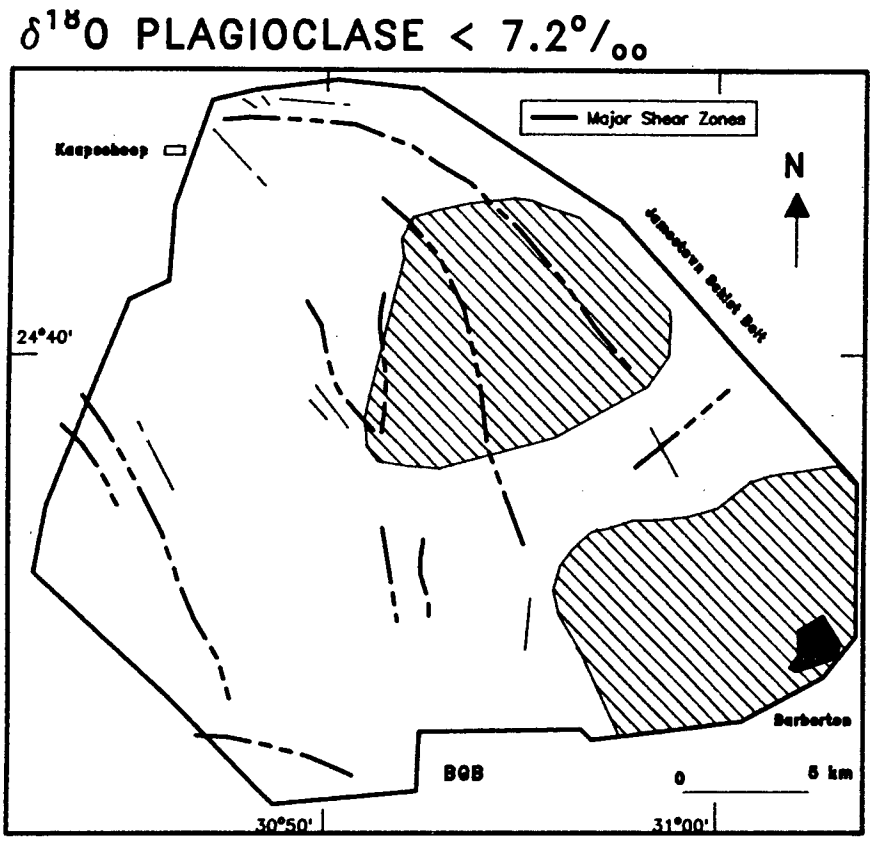

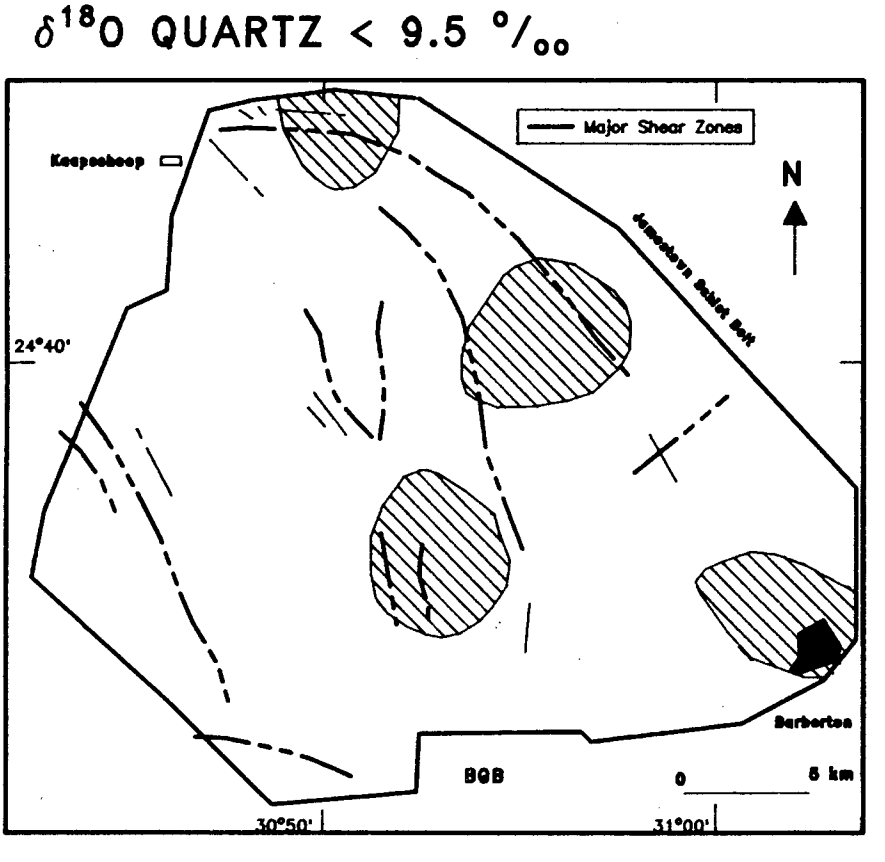

Figure 5.5 These diagrams illustrate the $\delta^{18}O$ variations of the KVT minerals analysed for their oxygen isotope compositions. They are constructed from the $\delta^{18}O$ mineral contour plots in Appendix 4. The cut-off values, indicated above each diagram, are values less than the mean $\delta^{18}O$ value established for each mineral analysed from the KVT (Table 5.1). See text for discussion. Continued.....

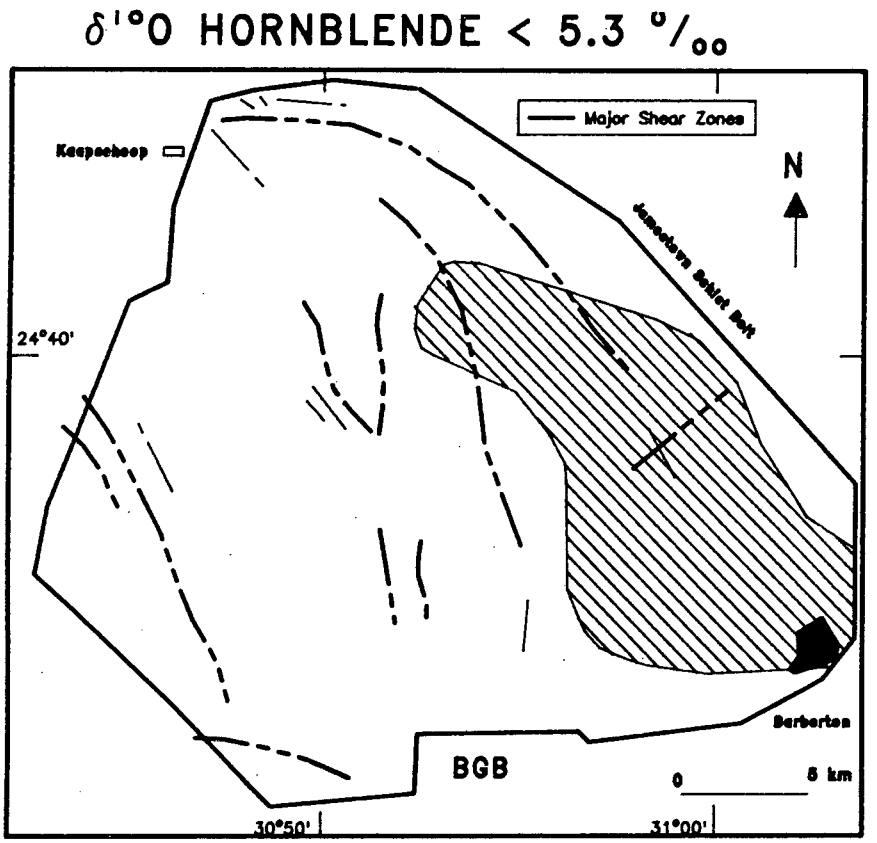

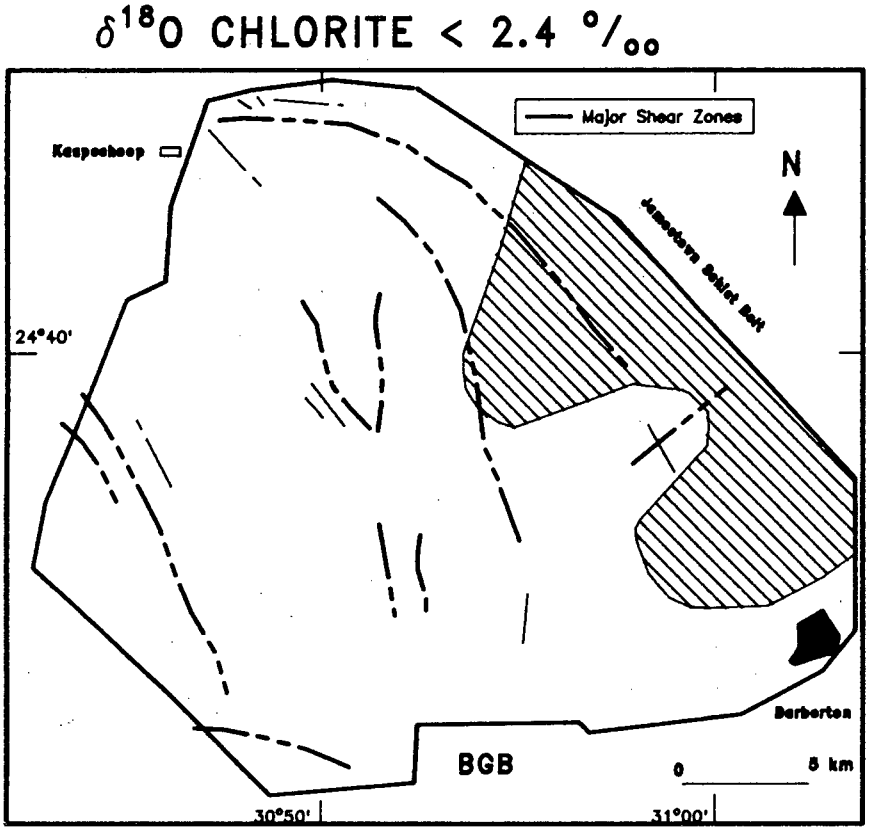

Figure 5.5 Continued.....

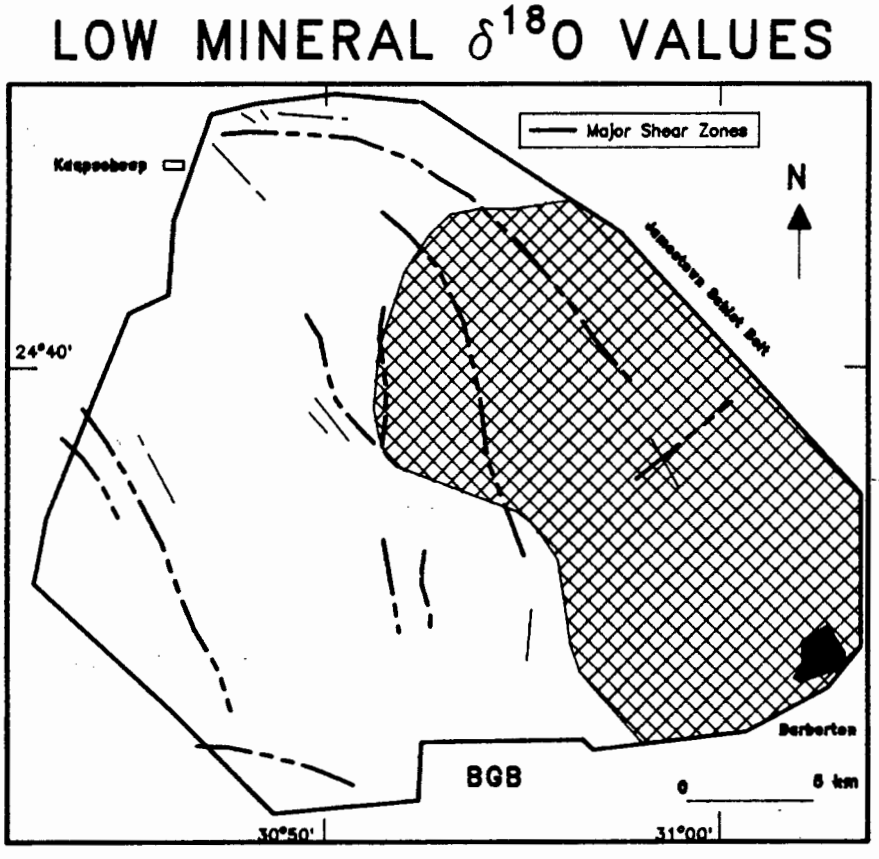

Figure 5.6 This is a compilation diagram of overlapping areas that have decreasing mineral $\delta^{18}O$ values, constructed from Figure 5.5 diagrams. This zone is probably indicative of higher W/R ratios.

the literature, partly because of disagreements between the calibration of fractionation factors relative to temperatures, determined by different techniques and in different laboratories (Bottinga and Javoy, 1973, 1975; 1988; Matsuhisa et al., 1978,1979; Matthews 1983a, b; Clayton et al., 1989). Clayton et al. (1989) have recently made measurements of oxygen fractionation between some silicates and calcite at temperatures of 600 °C and above. There are significant discrepancies with some of the earlier calibrations performed in hydrothermal experiments. The reasons for this are not known (Clayton et al., 1989). Generally, however, good agreement was obtained between mineral-pair fractionation factors presented by Bottinga and Javoy (1973), Clayton et al. (1989) and calculations derived by Kieffer (1982).

5.5.1 *O-Isotope Thermometry of the KVT*

It has already been demonstrated that quartz is the only mineral that has its "original" $\delta^{18}O$ value. It appears that none of the phases are in oxygen isotopic equilibrium except perhaps quartz-hornblende and any temperatures calculated from them will not indicate the true temperature of crystallisation. Bottinga and Javoy (1973, 1975), whose calibrations are in good agreement with those of Clayton et al. (1989) and calculations by Kieffer (1982), give equations for all the minerals analysed in this study and therefore for internal consistency only temperature estimates using those calibrations are presented in Table 5.3.

The following decreasing mean mineral-mineral temperature sequence from 970 °C to 430 °C is observed: plagioclase-hornblende, hornblende-biotite, quartz-hornblende, quartz-biotite ~ plagioclase-biotite, quartz-plagioclase. The different mineral-mineral temperatures observed are not crystallisation temperatures but rather temperatures representing oxygen isotopic fractionations at the time of closure of the different mineral pairs to oxygen exchange and also of exchange rates. Oxygen diffusion data indicate that rapid diffusion down to low temperatures can take place in some minerals, especially plagioclase (Gilletti, 1986). The mineral disequilibrium and open system conditions

Table 5.3: Oxygen Isotope-thermometry of KVT Silicate Minerals. The mineral-mineral closing temperatures are estimated from calibrations of Bottinga and Javoy (1973, 1975).

	Mineral-Mineral Temperatures °C					
	QTZ-PLG	QTZ-HBL	QTZ-BIO	PLG-HBL	PLG-BIO	HBL-BIO
KF 2	398	551	-	1011	-	-
KF11	433	566	455	979	467	668
KF19	418	555	440	979	452	639
KF2	434	496	-	775	-	-
KF33	436	-	-	-	-	-
KF36	304	-	-	-	-	-
KF39	415	590	425	1117	431	549
KF42	424	567	-	1001	-	-
KF52	364	576	-	1260	-	-
KF60	376	518	-	946	-	-
KF65	502	578	460	897	442	663
KF68	444	565	-	952	-	-
KF75	381	547	-	1050	-	-
KF77	883	-	-	-	-	-
KF88	532	-	-	-	-	-
KF91	470	527	-	809	-	-
KF96	430	558	-	961	-	-
KF102	436	-	-	-	-	-
KF108	410	-	-	-	-	-
KF114	523	611	446	955	416	578
KF118	406	520	-	887	-	-
KF121	386	541	-	1008	-	-

Table 5.3 continued....

Table 5.3: continued....

	Mineral-Mineral Temperatures °C					
	QTZ-PLG	QTZ-HBL	QTZ-BIO	PLG-HBL	PLG-BIO	HBL-BIO
Mean	445	554	445	974	442	620
1 std dev.	110	29	14	114	20	53

for the KVT are thus confirmed. The quartz-hornblende should be the most reliable, given the constraints of Figure 5.2. The mean temperature obtained from quartz-hornblende pairs is 554 °C (range 496 to 611 °C) which is too low for a crystallisation temperature.

5.6 The $\delta^{18}O$ of KVT ALTERATION FLUIDS

The $\delta^{18}O$ of magmatic water, "water that has equilibrated with a magma" (Sheppard, 1986, page 166), has values between +6 and +12 ‰ for fresh I- and S-type granitoids (Ohmoto, 1986). On the other hand metamorphic waters have a wide range of $\delta^{18}O$ from +5 to +25 ‰ (Taylor, 1974). It is therefore not always possible to distinguish between either magmatic or metamorphic waters by using oxygen isotope data alone.

It is possible to estimate the $\delta^{18}O_{H2O}$ of a fluid, in equilibrium with a mineral, from $\Delta_{mineral-H2O}$ versus temperature calibrations. $\Delta_{mineral-H2O}$ is temperature dependent and temperature has to be assumed or established via other approaches or techniques. The only mineral phase for which it is possible to establish the $\delta^{18}O_{H2O}$ of the fluid with which it equilibrated is chlorite because it is entirely secondary and its temperature of formation (~ 250 °C) has been established in Chapter 4 using the Cathelineau and Nieva (1986) geothermometer.

Two chlorite-H_2O versus temperature calibrations are available (Javoy, 1977; Wenner and Taylor, 1971). Table 5.4 gives the $\delta^{18}O$ values of water in equilibrium with the chlorite at 250 °C using these calibration curves. The Javoy (1977) chlorite-H_2O calibration gives a mean $\delta^{18}O_{H2O}$ estimate of +9.7 ±0.7 ‰ and the Wenner and Taylor (1971) calibration a mean value of + 1.7 ±0.7‰. According to the Javoy (1977) calibration equation all the factors are negative and the $\delta^{18}O_{H2O}$ will always be greater than the $\delta^{18}O$ of the chlorite at any temperature (Appendix 1). The $\delta^{18}O_{H2O}$ in equilibrium with the epidote analysed from two samples are significantly lower (~ -3 ‰) than those calculated for the chlorite (Tables 5.4, 5.5). In light of the low oxygen yields of the epidote and the small sample population, little

Table 5.4: $\delta^{18}O_{H2O}$ of the alteration fluid using the chlorite-H_2O calibration of Javoy (1977) and Wenner and Taylor (1971). The mean temperature of chlorite formation is 250 °C which was calculated using the Cathelineau and Nieva (1986) geothermometer (Chapter 4).

		$\delta^{18}O$ H_2O	
		Javoy(1977)	Wenner and Taylor(1971)
	$\delta^{18}O_{chl}$	250°C	250°C
KF 2	2.6	9.5	1.6
KF29	2.9	9.8	1.9
KF36	1.0	8.0	0.0
KF42	3.8	10.7	2.8
KF52	2.7	9.6	1.7
KF68	3.1	10.1	2.1
KF75	2.5	9.5	1.5
KF91	2.3	9.2	1.3
KF96	2.5	9.5	1.5
KF102	3.5	9.5	2.5
KF114	3.1	10.5	2.1
KF118	1.9	10.1	0.9
KF121	2.6	8.9	1.6
mean		9.7	1.7
1 std dev.		0.7	0.7

Table 5.5: $\delta^{18}O_{H2O}$ of the alteration fluid using the epidote-H_2O fractionation of Javoy (1975).

	$\delta^{18}O\ H_2O$	
	$\delta^{18}O_{epi}$	250°C
KF2	2.7	-2.9
KF36	2.4	-3.2

confidence is placed in the epidote calculations.

According to the Javoy (1977) calibration the KVT alteration fluids in equilibrium with the chlorite generally had magmatic and/or metamorphic oxygen isotopic signatures. It has been shown, however, that for intensely altered plagioclase (plagioclase has high exchange rates for oxygen, Gilletti 1986) the $\delta^{18}O$ values generally decrease or stay the same and less frequently increase relative to "unaltered" plagioclase (Table 5.3). This suggests that $\Delta_{plag-H2O}$ and $\delta^{18}O_{H2O}$ were such that little change in the $\delta^{18}O$ plagioclase occurred. $\Delta_{plag-H2O}$ at 250 °C is 6.8 which is consistent with $\delta^{18}O$ value for coexisting water of +0.6 ‰. It therefore seems more likely that the average $\delta^{18}O_{H2O}$ of + 1.7 ‰ at 250 °C estimated by the Wenner and Taylor (1971) calibration is the correct one. The $\delta^{18}O$ of water in equilibrium with the intensely altered plagioclase, which has $\delta^{18}O$ values similar to "unaltered" plagioclase (+7.4 ‰), is ~ +0.6 ‰ at 250 °C. This is a similar value obtained from the chlorite-water calibration (+ 1.7 ‰) at the same temperature. The higher $\delta^{18}O$ plagioclase values of KF77, may be due to local variations in the $\delta^{18}O$ or temperature of the fluid.

If it is assumed that the alteration fluid had a $\delta^{18}O_{H2O}$ of ~ +9 ‰ as indicated by the $\Delta_{chl-H2O}$ calibration of Javoy (1977) then the temperature of formation of vein-quartz ($\delta^{18}O$ ~ +10.5 ‰) is 660 °C. Assuming the vein-quartz is epigenetic then this estimation is ~ 400 °C too high. If the Wenner and Taylor (1971) calibration is assumed correct and the $\delta^{18}O_{H2O}$ is +1.7 ‰ then formation temperatures of vein quartz of ~ 250 °C are indicated. This temperature is similar to that estimated for chlorite formation (252 ±22 °C) using the Cathelineau and Nieva (1986) geothermometer. Solid-solution geothermometry and $\delta^{18}O$ of chlorite and $\delta^{18}O$ data from plagioclases which are highly altered and vein-quartz argue for an alteration fluid with a $\delta^{18}O$ of approximately 0 to +2 ‰ and a temperature of 250 °C.

Possible sources for a fluid with a $\delta^{18}O$ of 0 to +2 ‰ are magmatic fluids which exchange oxygen with KVT wall rocks during cooling of the

pluton to temperatures of 300 °C (Ohmoto, 1986) and where W/R was low; meteoric fluids at low W/R ratios ($d^{18}O$ -10 to 0 ‰, Sheppard, 1986) which were buffered by the oxygen of the KVT; and a mixture of meteoric and magmatic water. It is not possible to distinguish between these fluids on the basis of oxygen isotope data alone.

5.7 O-ISOTOPE CONSTRAINTS on the KVT SOURCE

5.7.1 *Introduction*

Oxygen isotope analyses of granitic rocks are useful in differentiating the type of source (Taylor, 1968; O'Neil and Chappell, 1977). The main reason for this is that mantle $d^{18}O$ is generally lighter than crustal $d^{18}O$ and therefore the two sources can be distinguished. Reasonable amounts of crystal fractionation (< 80 %) cannot change the $^{18}O/^{16}O$ by more than 1‰ (Sheppard and Harris, 1985; Taylor, 1986).

White and Chappell (1977) suggested that granitic plutons can be divided into I- and S-types which are presumed to reflect mantle and metasedimentary sources respectively. I-type granites usually have hornblende present and sphene as an accessory mineral and no aluminosilicate minerals such as cordierite and garnet. S-type granites contain no amphibole and instead biotite and muscovite may be abundant and they may also contain aluminosilicates such as cordierite and garnet. The S-type granites have molecular $Al_2O_3/(Na_2O+K_2O+CaO) > 1.1$ and I-type granites < 1.1. O'Neil et al. (1977) and O'Neil and Chappell (1977) found that the S-type granitic rocks in Australia have $d^{18}O$ values of +9.9 to +12.5 ‰ while I-type granites have $d^{18}O$ values of +7.9 to +9.4 ‰. Taylor (1988) considers that granitic plutons of western North America with $d^{18}O$ of ca +7 to +9 ‰ are derived from the lower continental crust. Classification of granites into I- and S-type have largely been done on Proterozoic granites and it is questionable whether this classification scheme can be applied to granitoids formed during the Archaean.

5.7.2 *Possible Sources for the KVT*

The predominant mafic minerals of the KVT are hornblende and biotite.

Hornblende and biotite is characteristic of I-type granitoids. No muscovite (except sericite after plagioclase), cordierite or garnet was observed. It has been shown previously (Chapter 4) that there is some overlap between hornblendes of the BGB xenoliths and the KVT and there also is evidence for possible disequilibrium between hornblende-biotite pairs of different KVT samples. The molecular $Al_2O_3/(Na_2O+K_2O+CaO)$ of the KVT has a mean of 1.4 (Robb et al., 1986) which satisfies S-type granitoid criteria.

If the effect of alteration processes can be eliminated, then the only other control on the isotopic signature of igneous rocks is the source of the magma and its interaction with rocks enroute to the surface, e.g. mixing. All of the KVT minerals with the exception of quartz appear to have undergone oxygen isotope re-equilibration, subsequent to crystallisation. The only reliable guide to magma $\delta^{18}O$ for the KVT is therefore the $\delta^{18}O$ of the quartz. One of the best examples of a mantle derived granite are alkali-granite xenoliths from Ascension Island (Harris, 1983). This granite is from an oceanic island and has therefore not been affected by crustal contamination. Quartz from these granite xenoliths have $\delta^{18}O$ values of ~ +7 ‰ (Sheppard and Harris, 1985). These rocks are demonstrably fresh and unaltered by fluids. Quartz crystallising in a mantle derived granite should therefore have $\delta^{18}O$ values of about +7 ‰. The $\delta^{18}O$ mean of KVT quartz is +9.7 ±0.3 ‰. This is approximately +2.7 ‰ higher than the quartz from the Ascension granites, which suggests that the the KVT magma $\delta^{18}O$ value was ~ +2.7 ‰ heavier than would be expected if it were entirely mantle derived. Possible reasons for this are;

1. assimilation of crust and
2. the melting of rocks with higher $\delta^{18}O$ than assumed for mantle melts.

The possible extent of crustal assimilation can be estimated from equation 6 in Taylor and Sheppard (1986). For a constant ratio of cumulates to assimilated rock (R) of 2 it would take 30% assimilation of a country rock with $\delta^{18}O$ of ~ +15 ‰, to raise the $\delta^{18}O$ of +6 ‰

by 2.7 ‰. As for the second mechanism (above), it has been pointed out by Sheppard (1986) that very early Archaean sediments could contain a major portion of mantle derived material, and the time interval between sedimentation and magma genesis could have been short. The KVT may therefore be a S-type granite because the $\delta^{18}O$ value of Archaean sediments would be expected to be lower than present day sediments.

5.8 SUMMARY

The $\delta^{18}O$ data from the KVT minerals, with the exception of quartz, indicate that they have undergone oxygen isotope exchange at subsolidus temperatures. The presence of abundant hydrous alteration minerals such as chlorite, epidote, sericite and carbonate, especially along shear and the KVT/BGB contact zones, are also considered to indicate open-system conditions, although with W/R ratios which are comparatively small. The chlorite composition suggests a temperature of alteration (i.e. chlorite formation) of 250 °C. At this temperature the Wenner and Taylor chlorite-H_2O calibration curve indicates a $\delta^{18}O_{H2O}$ value for the alteration fluid of ~ +1 ‰, which is supported by the $\delta^{18}O$ data from vein-quartz. The $\delta^{18}O_{H2O}$ value is consistent with meteoric water which has exchanged with country rock at low W/R or a mixture of meteoric and magmatic water. This alteration temperature and $\delta^{18}O$ of the alteration fluid are consistent with a buffering of plagioclase $\delta^{18}O$ values during alteration.

From the mineralogy and mineral chemistry it is not clear whether the KVT belongs to the I- or S-type granitoids, however, the molecular $Al_2O_3/(Na_2O+K_2O+CaO)$ of the KVT is ~1.4 (Robb et al., 1986) which suggests that it is a S-type granitoid. The quartz $\delta^{18}O$ values suggest that the KVT magmas had a $\delta^{18}O$ value ~ +2 ‰ heavier than would be expected if it was entirely mantle derived. Possible mechanisms for increasing the $\delta^{18}O$ are assimilation of crust by a mantle derived magma, melting of primordial mafic crust including some Archaean sediments. It is not possible on the basis of oxygen isotope data alone to distinguish between these possibilities.

6. STABLE ISOTOPES in KVT CARBONATES

6.1 INTRODUCTION

Carbon occurs in the reduced form in organic compounds and in coal. It also occurs in the oxidized state primarily as carbon dioxide, carbonate ions in solution, and as carbonate minerals. In addition, it is found as a native element in the form of graphite and diamond. The two most important carbon reservoirs on Earth are:

1. the biogenically reduced carbon compounds which are isotopically light with a mean $\delta^{13}C$ value around -25‰ (PDB) and

2. oxidized carbonates which are isotopically heavy with a mean $\delta^{13}C$ value around 0 ‰ (Hoefs, 1987).

The isotopic composition of carbonate precipitated from aqueous solutions is controlled by several factors, including the total $\delta^{13}C$ in the circulating fluid but also on the fugacity of the oxygen, the pH, the temperature of isotopic equilibrium, the ionic strength of the fluid and on the total concentration of carbon (Ohmoto and Rye, 1979). The principal carbon species that may become important in hydrothermal fluids below 600°C are; $CO_2(aq)$, H_2CO_3, HCO_3^-, CO_3^{2-} and $CH_4(aq)$. The carbon isotope fractionations among these different species are summarised by Friedman and O'Neil (1977) and Hoefs (1987).

It has been shown previously (Chapter 4) that the KVT has been altered by a carbon-bearing fluid which has resulted in the precipitation of calcite, ankerite and siderite in veins and veinlets and to a lesser extent disseminated within hornblende. The carbonated KVT broadly overlaps with other zones which have been intensely altered (Chapter 4). Petrographic evidence suggests that the fluid responsible for the intense propylitic and sericitic alteration was also responsible for the precipitation of the carbonate. It will be assumed that this alteration fluid was water containing either CO_2 or HCO_3^- ions in solution. The $\delta^{18}O$ and $\delta^{13}C$ values presented here are therefore only of the CO_2 from the calcite in the carbonate KVT that has been liberated

during the extraction processes.

The primary carbon content of granitoids is substantially lower than that of the KVT. The $\delta^{13}C$ data are therefore more readily interpreted than the oxygen data as it can be assumed that all the carbon within the carbonate minerals was introduced during the alteration processes. The oxygen isotope values of the carbonate minerals, however, may not only reflect the fluid source composition but also the temperature of carbonate precipitation and the exchange of oxygen between fluid and the other silicate minerals within the host rock.

The theoretical and experimental aspects of stable isotopes in carbonates are presented in Appendix 1 and Chapter 3.

6.2 $\delta^{13}C$ and $\delta^{18}O$ DATA for the KVT CARBONATES

The $\delta^{13}C$ and $\delta^{18}O$ values obtained during this study on the KVT samples are presented in Table 6.1 and Figure 6.1. The $\delta^{13}C$ values of the KVT carbonates form a more or less continuous range between -6 and 0 ‰.

The $\delta^{18}O$ values of the KVT carbonates differ from their $\delta^{13}C$ values in that the $\delta^{18}O$ forms two distinct groups. A tight cluster between +6.5 and +9.5 ‰ (group **A**) and a more dispersed linear group ranging between $\delta^{18}O$ +12 and +25 ‰ (group **B**). Group A has $\delta^{13}C$ values between -5.8 and -1.2 ‰ and group B $\delta^{13}C$ values between -3.1 and 0.1 ‰. The $\delta^{13}C$ values of group B are therefore slightly heavier than those of group A. The distribution of the two $\delta^{18}O$ groups across the KVT are not systematic (Fig. 6.2).

6.2.1 *Discussion*

The salient points of Figure 6.1 are that the carbonate isotope data can be subdivided into two groups, **A** and **B**, mainly on the basis of the $\delta^{18}O$ data. Group B is distinct from A in that it has higher $\delta^{18}O$ values which show a greater range ($\delta^{18}O$ mean group A = +7.9 ±0.9 ‰ and group B = +18.4 ±4.4 ‰). The $\delta^{13}C$ values of group A and B

Table 6.1: Carbon and oxygen stable isotopes of carbonates from KVT whole-rocks. The difference in duplicates are all better than 0.1 ‰. Group A carbonates have $\delta^{18}O$ values between +6.5 and +9.5 ‰ and group B values beteen +11.9 and +24.4 ‰. See text for discussion.

	Group A			Group B	
	$\delta^{18}O$	$\delta^{13}C$		$\delta^{18}O$	$\delta^{13}C$
KF 2	8.7	-5.8	KF 5	19.1	-2.2
KF 7	7.6	-4.0	KF 10	12.7	-3.1
KF14	8.6	-1.2	KF 15	15.2	-1.1
KF36	6.5	-2.7	KF 18	17.5	-1.1
KF43	7.7	-1.2	KF 31	11.9	-2.9
KF44	9.5	-3.7	KF 45	15.8	-1.5
KF47	7.4	-5.0	KF 49	23.7	-0.4
KF48	7.3	-4.7	KF 62	24.4	-0.6
KF52	7.2	-2.5	KF 75	21.3	-0.1
KF67	7.5	-4.1	KF 84	23.6	-0.4
KF97	6.7	-3.9	KF 125	17.5	-0.3
KF107	9.0	-2.5			
KF118	7.4	-3.1			
KF135	8.7	-2.9			
KF142	7.9	-3.2			
KF144	9.1	-5.3			
mean	7.9	-3.5		18.4	-1.2
1 std dev.	0.9	1.3		4.4	1.1

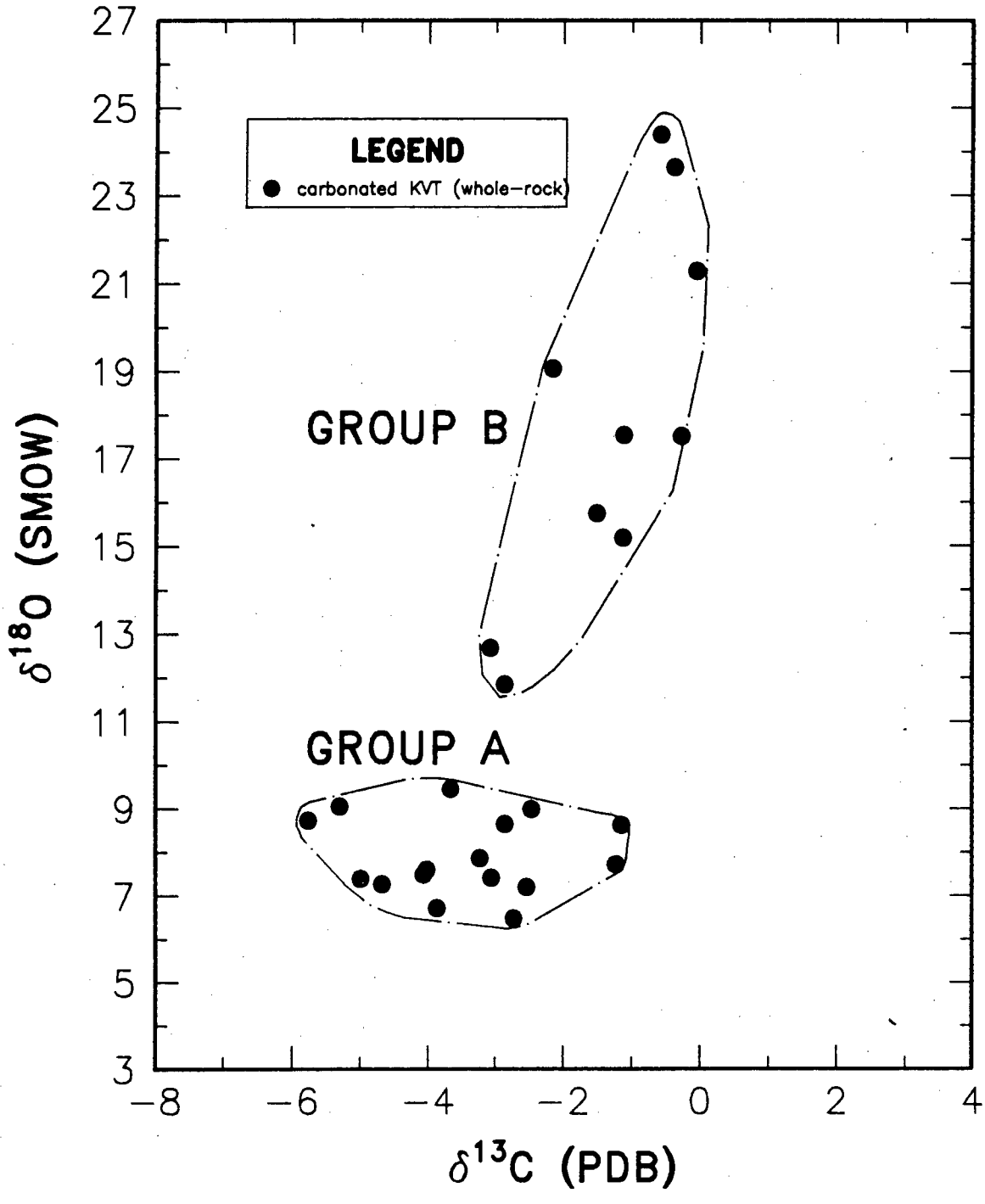

Figure 6.1 This is a $\delta^{18}O$ vs $\delta^{13}C$ plot of carbonates from carbonated KVT. The $\delta^{18}O$ is only of the carbonate material, not the whole-rock. The data can be sub-divided into two groups (A and B), based on the $\delta^{18}O$ values. The data cannot be strictly distinguished from their $\delta^{13}C$ values but the group A carbonates tend to be lighter in $\delta^{13}C$ than group B carbonates.

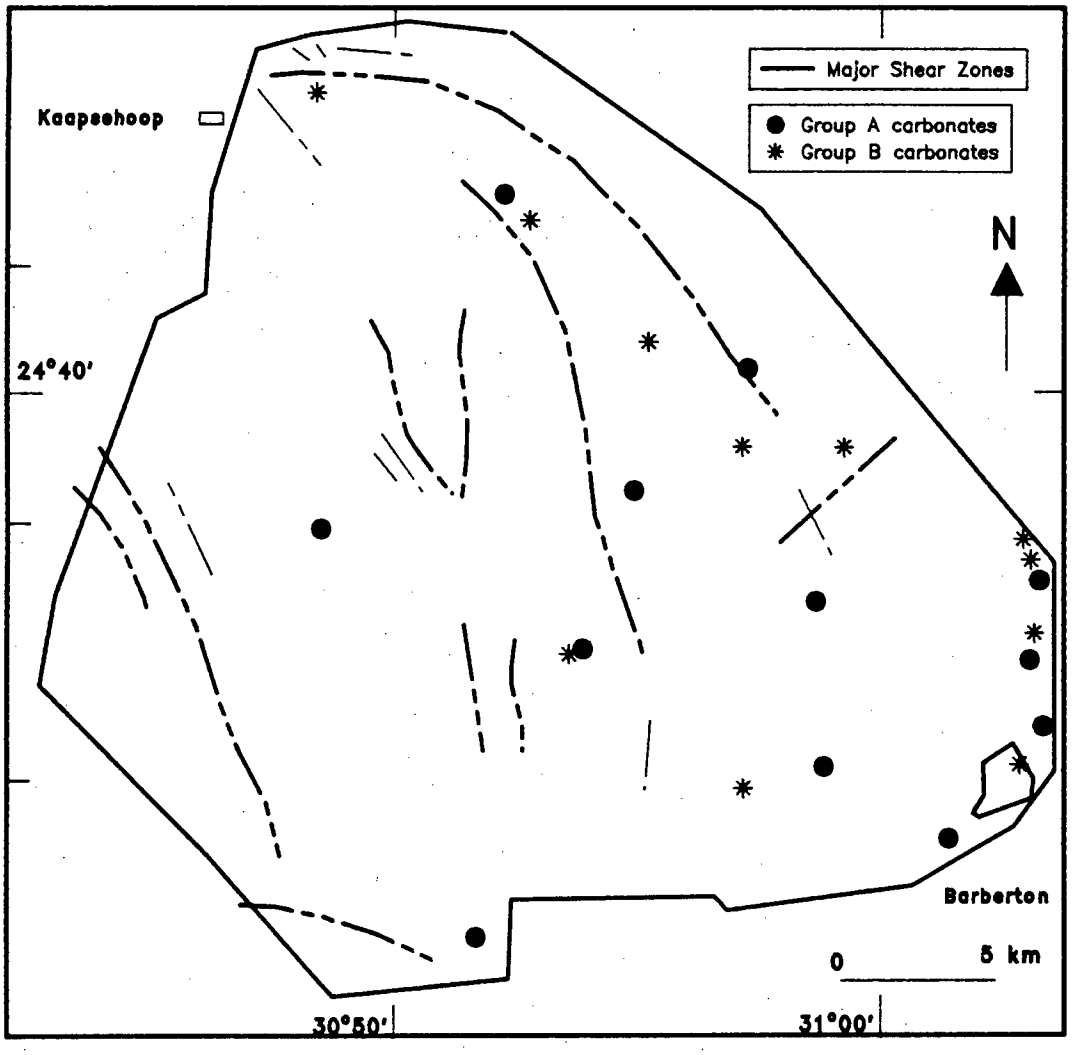

Figure 6.2 The distribution of group A and B carbonates from the KVT. No systematic distribution of the two groups is evident.

overlap but group B values tend to be more positive than those of group A ($\delta^{13}C$ mean group A = -3.5 ±1.3 ‰ and group B = -1.2 ±1.1 ‰).

In considering the $\delta^{18}O$ values of the carbonates it is possible that a fluid with low W/R ratio, at reasonably high temperatures (~250 °C) could have its $\delta^{18}O$ buffered by the KVT ($\delta^{18}O_{WR}$ +6 to +8 ‰). It has been previously estimated that the most likely alteration fluid circulating through the KVT had an approximate $\delta^{18}O_{H2O}$ of +1 ‰ at a mean temperature of 250 °C (Section 5.6). The $\Delta_{calcite-H2O}$ at 250 °C is ~ 7 and if the $\delta^{18}O_{H2O}$ is ~ +1 ‰, then the calcite precipitating from this fluid will have $\delta^{18}O$ values of ~ +8 ‰ which is close to group A $\delta^{18}O$ values (mean group A = +7.9 ‰). If the same fluid remains in the KVT during cooling, lower temperatures will give progressively higher $\delta^{18}O$ values of calcite.

The relationship between the $\delta^{13}C$ of the calcite and that of the fluid from which it precipitates depends on the carbon species in the fluid. The $\Delta_{HCO3^- - calcite}$ ranges from 0 to -4 ‰ for temperatures less than 500°C, the values remaining fairly constant (-4 to -2) at temperatures below 400°C. The mean $\delta^{13}C$ value for group A carbonates is -3.5 ‰. If the calcite was precipitated from HCO_3^- bearing fluids then the $\delta^{13}C$ of that fluid was -6.5 ‰. During cooling from 250°C the $\delta^{13}C$ of the precipitating calcite will only get slightly heavier. Figure 6.3 shows the effect of cooling on calcite precipitation from a hypothetical HCO_3^--bearing fluid. The initial calcite formed is constrained to be that of average group A, the curve represents the locus of $\delta^{18}O$ and $\delta^{13}C$ values of calcites precipitating from the same fluid at lower temperatures. The trend produced is slightly negative whereas that of group B is positive suggesting that precipitation from cooling HCO_3^--bearing fluids could not cause the group B trend.

The $\delta^{13}C$ value of calcite precipitated from H_2CO_3 in solution, shows more variation with change in temperature (Hoefs 1987, page 35). The $\Delta_{H2CO3 - calcite}$ has a crossover point from positive to negative at ~200°C. For temperatures greater than 200 °C the calcite will have a $\delta^{13}C$ lighter than the fluid and for temperatures less than

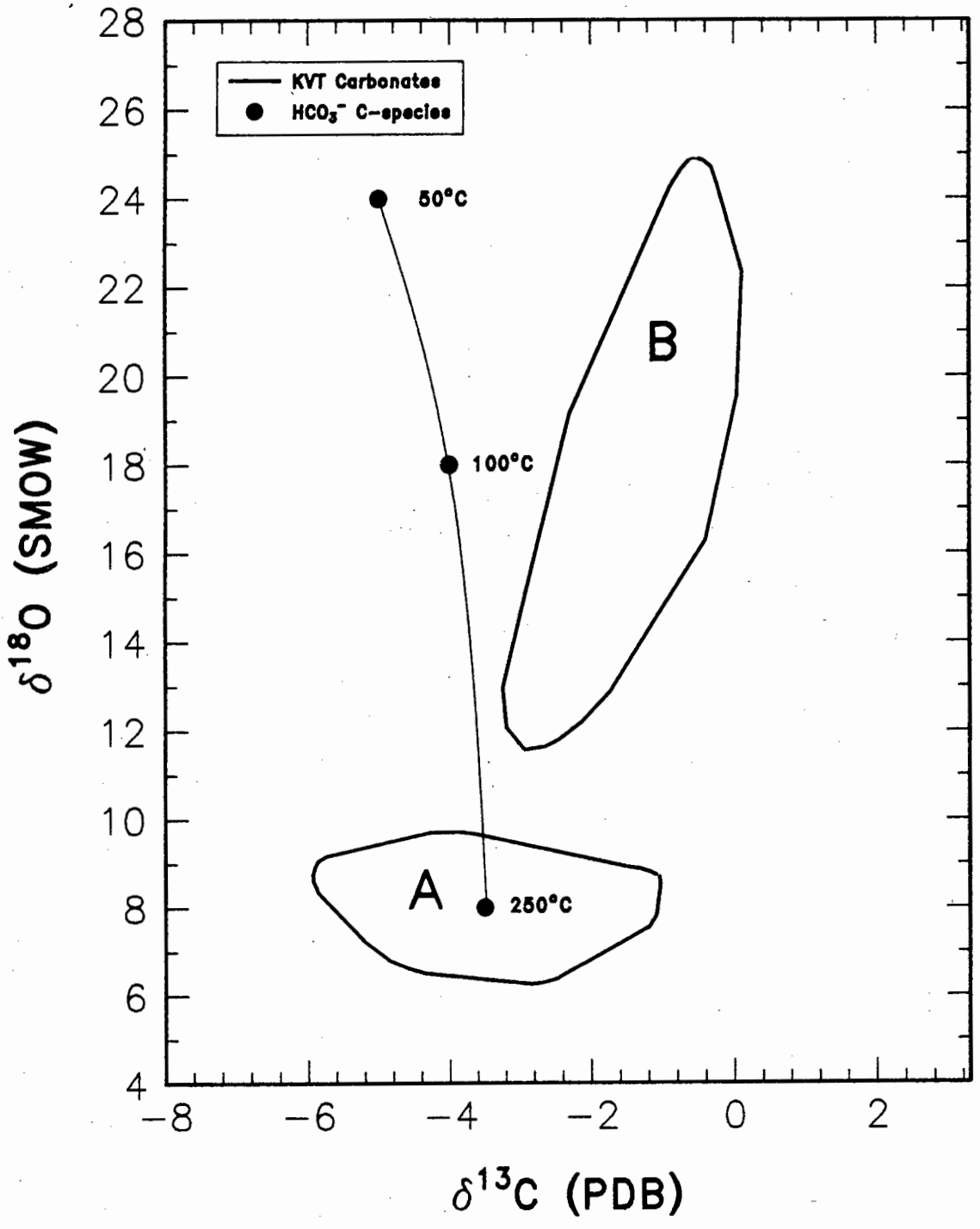
KVT Carbonates
HCO_3^- C-species
50°C
100°C
250°C
A
B
28
26
24
22
20
18
16
14
12
10
8
6
4
−8
−6
−4
−2
0
2
$\delta^{18}O$ (SMOW)
$\delta^{13}C$ (PDB)

200 °C the calcite values will be from 0 up to 8 ‰ heavier. If the calcite (group A mean = -3.5 ‰) was precipitated from H_2CO_3 then the $\delta^{13}C$ of the fluid in equilibrium with the calcite at ~250 °C is -2.5‰. Cooling of this fluid from 250 °C from a H_2CO_3-bearing fluid produces a positively sloped trend similar to that of group B (Fig. 6.4). The slope of the cooling trend in this model suggests that the carbon species precipitating the calcite, to produce group A and B, is more likely to have been H_2CO_3 rather than HCO_3^-.

Another possible explanation of the carbonate data could be that two generations of calcite exist. In this model, group A carbonates form in the same way as in the previous model, i.e. at temperatures of 250 °C during the formation of chlorite. It does not matter for this model whether the calcite precipitates from a H_2CO_3- or a HCO_3^--bearing fluid. Average group A calcite ($\delta^{13}C$ = -3.5 ‰ and $\delta^{18}O$ = +7.9 ‰) forming at 250 °C from a H_2CO_3-bearing fluid requires that the fluid had a $\delta^{18}O$ value of ~ +1 ‰ and $\delta^{13}C$ of ~ -2.5 ‰. If the group A calcites (mean -3.5 ‰) precipitated from HCO_3^--bearing fluids at ~ 250 °C, the fluids would have had $\delta^{18}O$ values of ~ +1 ‰ and $\delta^{13}C$ values of ~ -7 ‰. The $\delta^{13}C$ values of calcites precipitating from H_2CO_3- or HCO_3^--bearing fluids (-2.5 and -7 ‰) are within the range for a source being geothermal waters and/or deep seated carbon, suggesting a possible magmatic origin (Hoefs, 1987, page 101). Group B calcite, in this model, is a series of mixtures of another generation calcite and group A calcite. If the second generation calcite has a $\delta^{18}O$ value of ~ +25 ‰ and $\delta^{13}C$ of ~ 0 ‰, group B calcite is therefore a series of mixtures of different proportions of these two generations of calcite generated during dissolution of the total calcite in these samples.

A possible end-member, for mixing with group A to produce group B calcites, having $\delta^{18}O$ value of ~ +25 ‰ implies low temperatures of deposition, which in turn suggests a meteoric and/or sea water origin. Water having a $\delta^{18}O$ of ~ 0 ‰ would precipitate calcite of ~ +25 ‰ at temperatures of ~ 50 °C and water of ~ -5 ‰ would precipitate similar calcite at ~ 20 °C. Figure 6.5 shows the effect of mixing

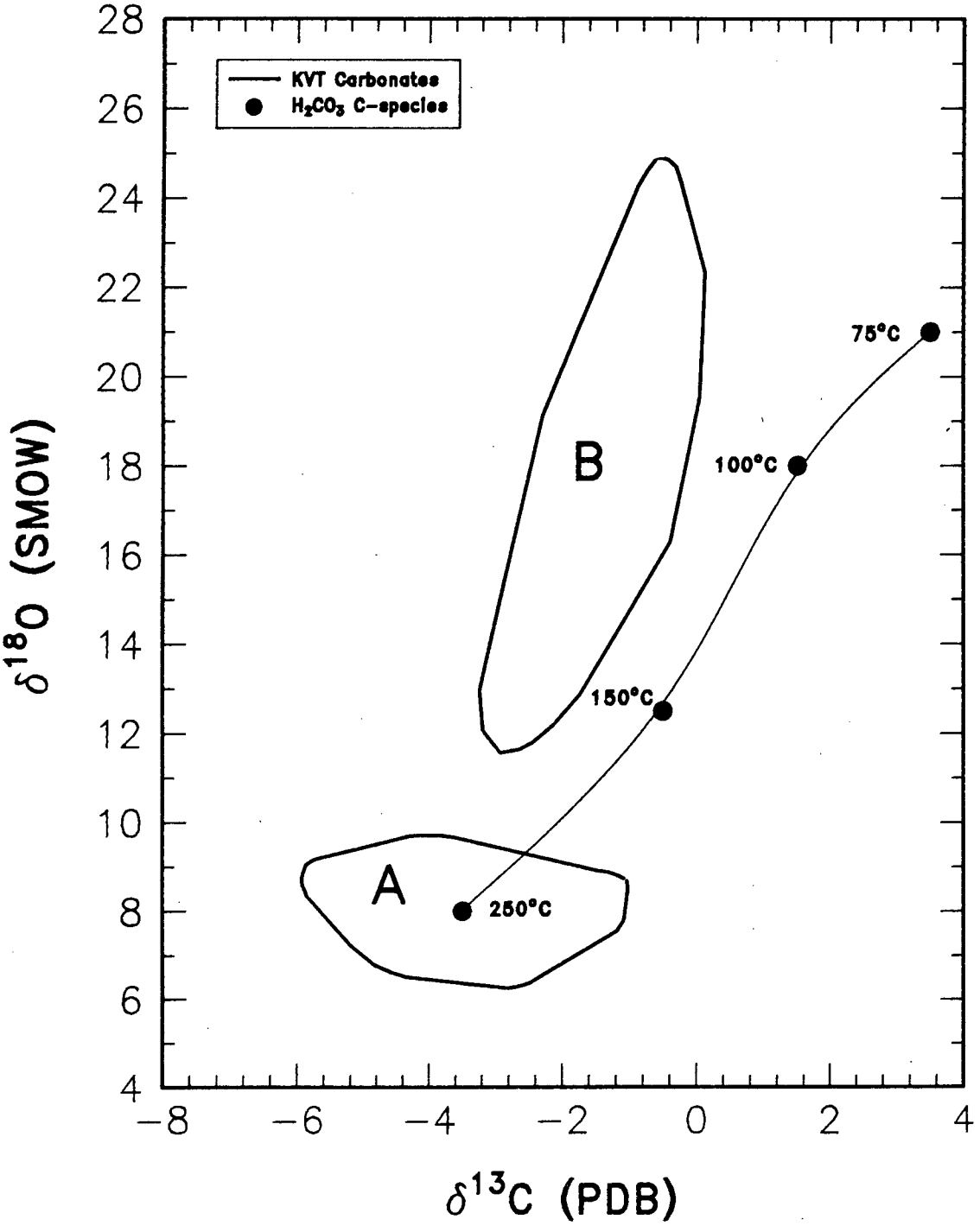

Figure 6.4 In the case of H_2CO_3-bearing fluids from the same source, precipitating calcite with $\delta^{13}C$ = -3.5 ‰ (mean of group A), will have a $\delta^{13}C_{H2O}$ of -2.5 ‰ (at ~ 250 °C. Cooling of this fluid will precipitate calcite along a curve which is similar to group B carbonates, but with a slightly more positive slope. The carbon species precipitating calcite, to produce group A and B, is more likely to have been H_2CO_3 rather than HCO_3^-.

Figure 6.5 Another possible explanation of the carbonate data could be that **two** generations of calcite exist. In this model, group A carbonates form in the same way as in the previous model, i.e. at temperatures of 250 °C during the formation of chlorite (Fig.6.3). It does not matter for this model whether the calcite precipitates from a H_2CO_3- or a HCO_3^--bearing fluid (see text). Group B calcite, in this model, is a series of mixtures of another generation calcite (LC) and group A calcite (EC). If the second generation calcite has a $\delta^{18}O$ value of ~ +25 ‰ and $\delta^{13}C$ Of ~ 0 ‰, group B calcite is therefore a series of mixtures of different proportions of these two generations of calcite, generated during dissolution of the total calcite in these samples. A possible end-member, for mixing with group A to produce group B calcites, having $\delta^{18}O$ value of ~ +25 ‰ implies low temperatures of deposition, which in turn suggests a meteoric and/or sea water origin.

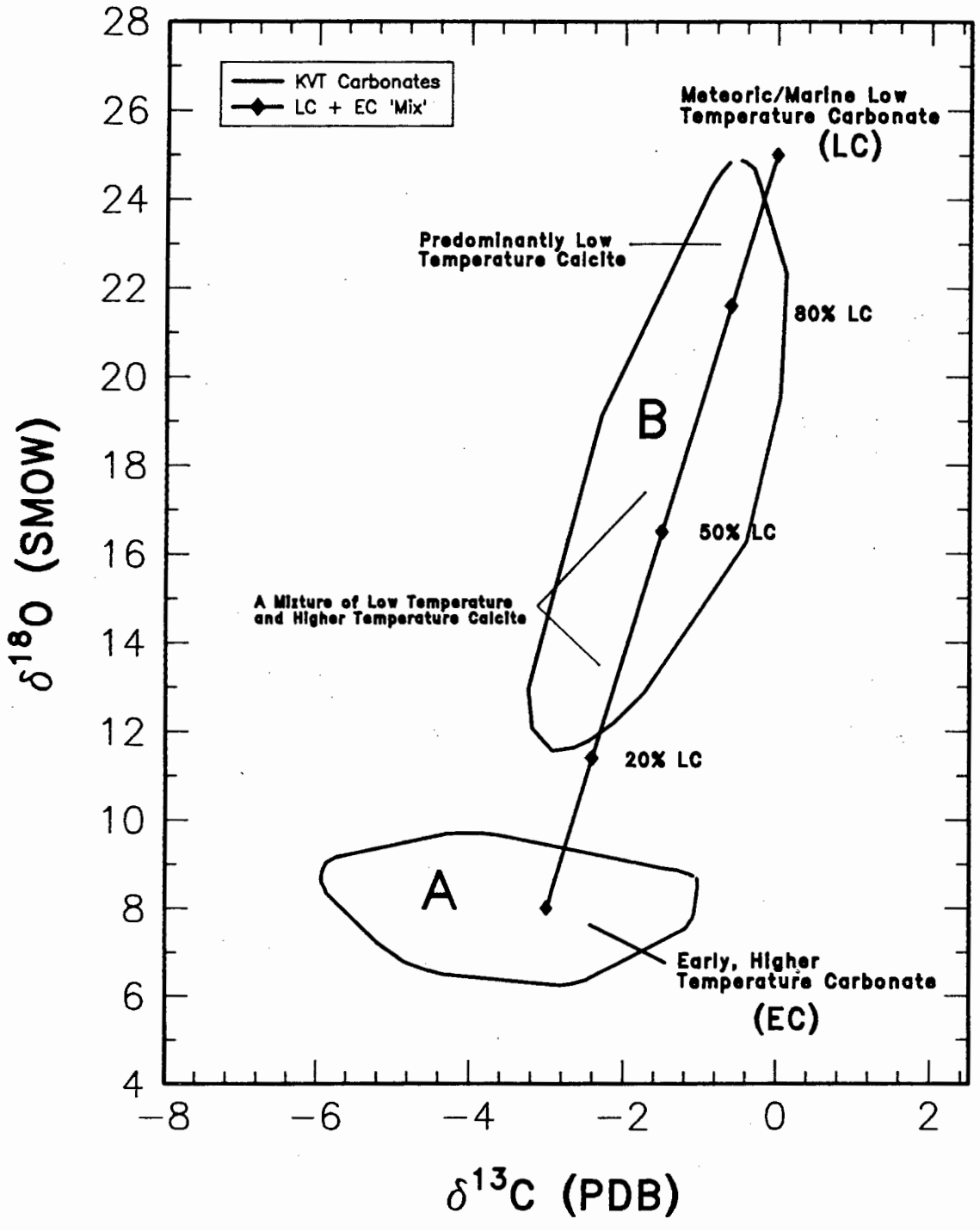
KVT Carbonates
LC + EC 'Mix'
Meteoric/Marine Low Temperature Carbonate (LC)
Predominantly Low Temperature Calcite
80% LC
B
50% LC
A Mixture of Low Temperature and Higher Temperature Calcite
20% LC
A
Early, Higher Temperature Carbonate (EC)
28
26
24
22
20
18
16
14
12
10
8
6
4
−8
−6
−4
−2
0
2
δ18O (SMOW)
δ13C (PDB)

group A calcite with low temperature calcite (LC). The group B trend is more closely reproduced using this model than with a model involving calcite precipitated over a range of temperatures, either from a H_2CO_3 or a HCO_3^- fluid.

Convincing petrographic evidence for a two source model is lacking. Group A calcites, however, are generally associated with chlorite and muscovite veinlets and group B calcites are predominantly small disseminated grains within the carbonated KVT. Figure 6.6 is a plot of the amount of CO_2 extracted from carbonated KVT (per gram) versus its $\delta^{18}O$ value. Calcites which have $\delta^{18}O$ values in group A, are generally more abundant in the whole rock than calcites which have $\delta^{18}O$ values in group B. This is consistent with the observation that group B calcites are small disseminated calcite grains whereas group A calcite is more locally abundant vein calcite. It has unfortunately been impossible to isolate the two calcite types before stable isotope analysis.

Possible source reservoirs of carbon for the carbonates are magmatic carbon from the KVT, deep seated metamorphic fluids, carbonate metasediments from the mafic-felsic units of the Onverwacht Group of the lower Barberton Sequence (S.A.C.S, 1980) and sea water. Organic reduced carbon ($\delta^{13}C$ ~ -25 ‰) is not considered a possible source because the KVT $\delta^{13}C$ values are much heavier. The dominant carbon-bearing species in ocean water is HCO_3^- (Hoefs, 1987, page 133). The $\delta^{13}C$ values of sea water are between -4 and +2 ‰, and at 250 °C the $\Delta_{cc-HCO3^-}$ is +3.5 (Hoefs, 1987). So calcite precipitating would have a $\delta^{13}C$ of -0.5 to +5.5 ‰. Sea water precipitating calcite at temperatures of 250 °C therefore seems an unlikely source.

Figure 6.7 shows the range of the $\delta^{13}C$ values from regionally altered Barberton greenstones (Smith, 1986) and carbonates from lode gold deposits in the Barberton greenstones surrounding the KVT (de Ronde et al., 1988). The three fields of carbonates in Figure 6.7 have remarkably good overlap of $\delta^{13}C$ values that could indicate a cogenetic source but different temperatures of precipitation, could account for the slightly different $\delta^{18}O$ values. The relative ages of the three groups

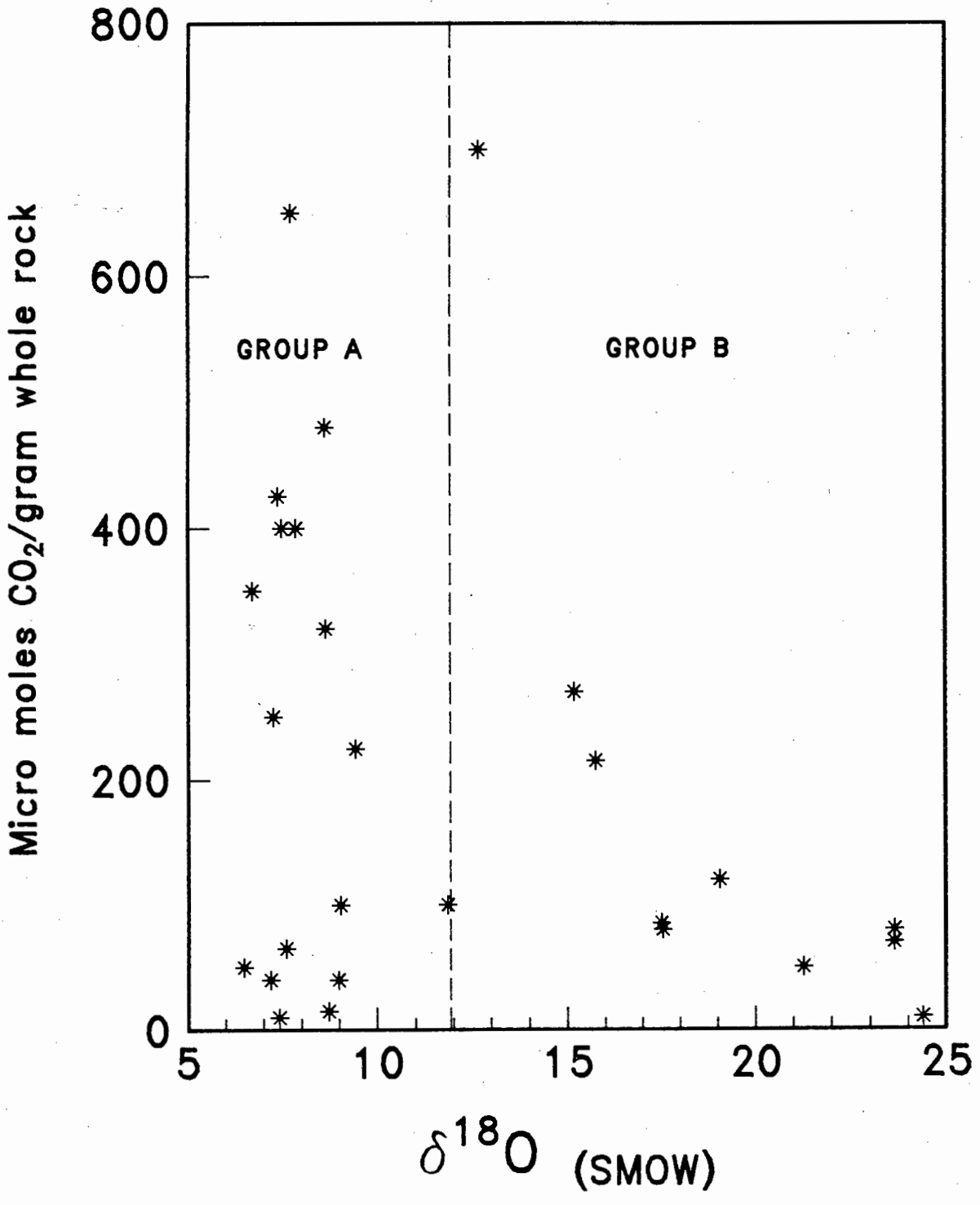

Figure 6.6 The amount of CO_2 (micro moles/gram whole rock) extracted during analysis of the carbonated KVT samples are compared to their $\delta^{18}O$ values. KVT samples with calcite in group A contain more calcite than KVT samples with calcite in group B. This is consistent with the observation that group B calcites are small disseminated calcite grains whereas group A calcite is more locally abundant vein calcite.

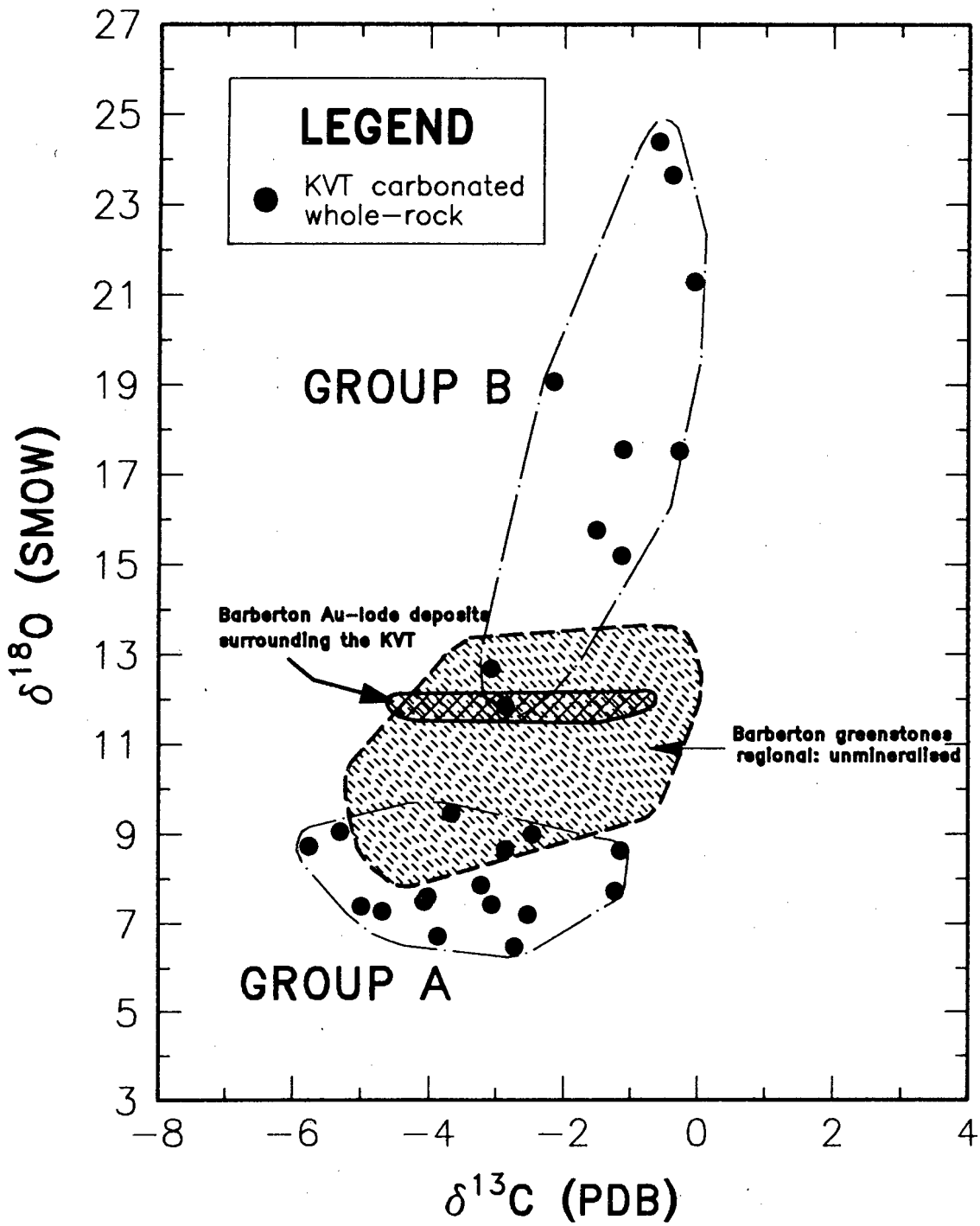

Figure 6.7 The $\delta^{18}O$ and $\delta^{13}C$ fields of regionally altered Barberton greenstones (Smith, 1986) and carbonates from lode gold deposits in the Barberton greenstones, surrounding the KVT (de Ronde et al., 1988) are plotted with values obtained from the carbonated KVT. The fields show good overlap of δ^{13C} values which could indicate a cogenetic source for the carbon. The $\delta^{18}O$ values of the different fields probably reflect different temperatures of precipitation and/or buffering of oxygen with their different host rocks.

of carbonates are not known.

6.3 SUMMARY

It is assumed reasonable that the chlorites and at least some of the calcite were formed in equilibrium from the same fluid. Mineralogical data suggest that the chlorites were formed at a mean temperature of 250 °C, and this is consistent with a fluid $\delta^{18}O_{H2O}$ value of ~ +1.5 ‰. The carbon and oxygen isotope data of the carbonated KVT forms two groups, A and B. The formation of these two groups may be explained by two models:

1. Group A calcite precipitated from the same fluid which resulted in the chlorite alteration at the same time (~ 250 °C). Group B carbonates precipitated at lower temperatures. A gradual cooling of the fluid would result in progressively heavier $\delta^{18}O$ values for the precipitated calcite. Precipitation from HCO_3^--bearing fluids cannot account for the group B trend, as the lower temperature calcites would have more negative $\delta^{13}C$ values. Precipitation from H_2CO_3-bearing fluids would result in the observed positive correlation between $\delta^{18}O$ and $\delta^{13}C$ seen in group B, but would produce greater than observed changes in $\delta^{13}C$ (Fig. 6.3).

2. An alternative model is that there are two generations of calcite which were deposited at different temperatures and from different fluids. Group A calcites were deposited at the same time as the chlorite alteration. A second generation of calcite was precipitated at low temperatures and mixtures of these two types produced during extraction resulted in the group B trend.

   a. a probably early magmatic (external and/or internal to the KVT)/metamorphic fluid source which had a $\delta^{13}C$ between -6 and -2 ‰ and $\delta^{18}O$ with values similar to those estimated from the chlorites (+1 to+2 ‰) and precipitated at temperatures of ~ 250 °C and formed group A carbonates

   b. a probably later meteoric/sea water ($\delta^{18}O$ -5 to 0 ‰) fluid which had dissolved BGB carbonate metasediments at very low

temperatures and had mean Archaean sedimentary carbonate $\delta^{13}C$ values of ~0 ‰ ($\delta^{18}O$ same as fluid) and precipitated the calcite at < 50 °C. The two generations of carbonate had their $\delta^{18}O$ and $\delta^{13}C$ values "mixed" during extraction and therefore plotted along a mixing line between the two groups.

It appears that group A calcites are associated with veins (plus chlorite and muscovite) and group B calcites are predominantly small disseminations. The "two source" model is preferred to the "same source" model because the group B trend is more closely reproduced in the former (Fig.5.6).

7. CONCLUSIONS

7.1 GEOLOGY AND PETROGRAPHY

The previous interpretation that the KVT is a two phase tonalite, with a hornblende phase and a hornblende + biotite phase, is not substantiated by this study. The petrographic evidence presented indicates that the KVT crystallised as a homogenous hornblende (15-20%) + biotite (5-10%) tonalite. Fine- to medium-grained tonalite dykelets intruded the KVT while it was probably still in a semi-solid state. The KVT has been subjected to an overall propylitic and potassic alteration but no aplites, pegmatites or evidence of greisenisation was observed to indicate that the KVT contained more H_2O than would be expected from an average granitoid magma. If the tonalite magma contained an average amount of residual fluids then an additional source for fluids must be evoked to account for the alteration that has been delineated from KVT samples which have high proportions of hydrous secondary minerals (e.g. chlorite and carbonates). The Cathelineau and Nieva (1986) solid-solution geothermometer indicates that the KVT chlorites were formed at temperatures ranging from 300 to 150 °C (mean ~ 250 °C). The areas of intense alteration encompass the zones along the northern, eastern and southern portions of the pluton. This zone coincides also with two structural features:

1. the contact zone between the KVT and the BGB and
2. major shear zones along the KVT/Jamestown Schist Belt contact and north-south shears in the southern portion of the pluton.

The KVT was intruded by doleritic dykes of several ages. Major shear zones which parallel the north-westerly strike of early Proterozoic doleritic dykes, can persist for distances up to 45 km and 0.5 km wide. KVT areas which have high proportions of hydrous alteration minerals coincide with some of these shear zones.

7.2 STABLE ISOTOPES

The $^{18}O/^{16}O$ values of the silicate minerals of the KVT show that exchange of oxygen isotopes in an open system occurred. The temperatures estimated from mineral pairs do not indicate crystallisation temperatures. The δ-δ plots show some evidence for disequilibrium trends, especially for $\delta^{18}O_{PLAG}$ versus $\delta^{18}O_{QTZ}$. The plots, however, are not consistent with high W/R ratios.

The $\delta^{18}O$ values of the alteration fluid was estimated from chlorites which are present over the entire pluton and are the secondary minerals mainly after the original KVT biotites. The $\delta^{18}O_{H2O}$ estimated from the chlorites at 250 °C is ~ +1 ‰ using the Wenner and Taylor (1971) calibration curve. $\delta^{18}O$ data from vein-quartz indicate that they were also in equilibrium with a fluid of ~ +1 ‰. This $\delta^{18}O_{H2O}$ is consistent with a meteoric/sea water origin, with some exchange with country rock at low W/R or mixing with magmatic/metamorphic fluids.

The $\delta^{18}O$ and $\delta^{13}C$ values of the carbonates from the carbonated KVT can be separated into two groups:

- **A**: which has $\delta^{13}C$ between -6 and -2 ‰ and $\delta^{18}O$ between +6 and +9 ‰ and
- **B**: $\delta^{13}C$ between -3 and 0 ‰ and $\delta^{18}O$ between +11 and +25 ‰.

The two groups can be explained by two models. The first model requires only one fluid which is CO_2-bearing. Calcite precipitated at different temperatures and resulted in the formation of two groups of carbonate. Group A which precipitated at higher temperatures (~ 250 °C) and group B which precipitated at lower temperatures resulting in significantly heavier $\delta^{18}O$ values and slightly heavier $\delta^{13}C$ values. The carbon-bearing species in the fluid cannot have been HCO_3^- unless temperatures were significantly higher than 250 °C.
The second model involves two sources of carbonate. The group A carbonates formed in the same way as group A in the first model. Group B carbonates precipitated from entirely different fluids which had a dissolved sedimentary carbon component and most likely post-dated group

A carbonates. This second generation of calcite was precipitated at low temperatures (< 50 °C), resulting in high $\delta^{18}O$ values. The rock therefore contains two types or generations of carbonate. The CO_2 liberated during extraction from the KVT whole-rocks is a mixture of the $\delta^{18}O$ and ^{13}C values of the two types of carbonate and the result is the "mixing" trend seen in the group B carbonates.

7.3 MAGMA SOURCE

The KVT quartz $\delta^{18}O$ values show that the KVT magma was 2.7 ‰ heavier in $\delta^{18}O$ value than a mantle-derived magma. If the KVT is mantle derived its $\delta^{18}O$ value must have been increased by contamination Alternatively the KVT magma was derived by partial melting of Archaean crust. This is in agreement with the conclusions of Robb et al. (1986).

7.4 GOLD MINERALISATION

Gold assays and previous mining and pitting indicate that the north-eastern portion along shear zones and the KVT/Jamestown Schist Belt contact is particularly favourable for mineralisation. The shear zones in the south-central part of the KVT are also promising. The zones favourable for gold mineralisation broadly overlap with zones that have undergone intense mineral decomposition and carbonate alteration. The discussions above would therefore indicate that the gold mineralisation is strongly associated with shears and KVT/BGB contacts which have been infiltrated by carbon-bearing aqueous fluids. The probable source of these fluids was meteoric/marine with the possible mixing with limited magmatic/metamorphic fluids. It is likely therefore that the KVT is only a depositional site for gold- and CO_2-bearing fluids rather than a source of gold.

7.5 FUTURE WORK

This study has shown that alteration processes have taken place within the KVT and that fluids which may have been derived from outside the KVT, passed through permeable zones along the KVT/BGB contact and shear zones. A few suggestions are given for further work to help understand the hydrothermal processes within the KVT and the relationship of the

KVT with the surrounding BGB and its gold mineralisation:

1. The KVT/BGB contact zone must be mapped out in detail.

2. Whole-rock geochemistry must be combined with stable isotope and radiogenic isotope analyses.

3. One of the most common alteration minerals in the KVT is chlorite. D/H analysis of this mineral will give valuable information on δD for the alteration fluid. Using mineral δD, the δD of the fluid which precipitated it can be calculated using mineral-H_2O calibration curves. The δD of the fluid is not affected by exchange with the host rock, unlike $\delta^{18}O$.

4. One of the difficulties interpreting the alteration processes in the KVT and relating them to the surrounding gold deposits in the BGB is that there are no constraints on the timing of the alteration. Dating of the alteration minerals is therefore very important. The temporal and chemical relationship of the fine- to medium-grained tonalite dykelets within the KVT, the porphyries within the BGB surrounding the KVT and the KVT must be established.

5. A stable isotope study similar to this one extended for a few kilometers into the BGB surrounding the KVT, would enhance the understanding of the role that the KVT played in gold mineralisation within the BGB.

ACKNOWLEDGEMENTS

It has been a privilege to study in the geochemistry department of the University of Cape Town. Staff and fellow students have all played some role in this project, for which I am very grateful. Stuart Smith proposed and initially supervised this project. My fellow students in particular Stuart Hill, Ian-Rambo Ransome, Russell Sweeney, Frankie Baars and Ziggy Ziegfried were always available to help and encourage me. Thanks also to Bruce Cairns, Henry Hendricks, Dave Wilson and Rob Oliver for their help with technical aspects and Cathy du Plessis with draughting. Andy Duncan and Dave Hill provided an excellent computer facility and patiently guided an ignoramus. Lynn O'Neill, always friendly, eased any administrative tribulation. Cornel de Ronde from the University of Toronto who openly exchanged ideas, definitely contributed to this study. In particular I want to express my gratitude to Chris Harris, my supervisor, and Torsten Vennemann for maintenance and demonstration in the isotope laboratory and for nursing me through the complexities of stable isotope geochemistry. Thanks Chris and Torsten.

My house-mate and friend Martin Bagley contributed with madness and liquid refreshments. Sue and Bram my parents and Brigette my wife to whom I dedicate this work for all their encouragement and love.

A grant from the Foundation for Research and Developement of the C.S.I.R. provided financial support.

9. REFERENCES

Anderson A. T., Clayton R.N. and Mayeda T.K. (1971). Oxygen isotope thermometry of mafic igneous rocks. J. Geol., **79**, 715-729

Anhaeusser C.R. (1966). Facets of the granitic assemblage on the northwest flank of the Barberton Mountain Land. Inform. Circ. Econ. Geol. Res. Unit, Univ. Witwatersrand , Johannesburg, **32**,27 pp

Anhaeusser C.R. (1969). The stratigraphy, structure and gold mineralisation of the Jamestown and Sheba Hills areas of the Barberton Mountain Land. PhD thesis (unpubl), Univ. Witwatersrand, Johannesburg, 1-332

Anhaeusser C.R. (1976). The nature and distribution of Archaean gold mineralisation in southern Africa. Mins. Sci. Eng.,**8**,no 1, 37 pp

Anhaeusser C.R. (1981). The relationship of mineral deposits to early crustal evolution. Econ. Geol., 75th Anniversary Volume, 42-46

Anhaeusser C.R. (1986). Archaean gold mineralization in the Barberton Mountain Land. In Anhaeusser C.R. and Maske S. (eds) Mineral Dep. S.A. Vols I & II. Geol. Soc. S.A., Johannesburg. 113-154

Anhaeusser C.R. and Robb L.J. (1980). Regional and detailed field and geochemical studies of Archaean trondhjemitic gneisses, migmatites and greenstone xenoliths in the southern part of the Barberton Mountain Land, South Africa. Precambrian Res., **11**, 373-397

Arkani-Hamed J. and Jolly W.T. (1989). Generation of Archaean Tonalites. Geology, **17**, 307-310

Barton J.M. Jr. (1983). Isotopic constraints on possible tectonic models for the crustal evolution in the Barberton Greenstone terrain, South Africa. Spec. Publ. Geol. Soc. S.A., **9**, 73-79

Barton J.M. Robb L.J.,Anhaeusser C.R. and van Nierop D.A. (1983). Geochronologic and Sr-isotopic studies of certain units in the

Barberton granite-greenstone terrain, South Africa. Spec. Publ.Geol.Soc.S.Afr.,**2**,153-188

Bence A.E. and Albee A.L. (1968). Empirical correction factors for the electron microanalysis of silicates and oxides. J. Geol., **76**, 382-403

Borthwick J. and Harmon R.S. (1982). A note regarding ClF_3 as an alternative to BrF_5 for oxygen isotope analysis. Geochim. et Cosmochim. Acta, **46**, 1665-1668

Bottinga Y. and Javoy M. (1973). Comment on oxygen isotope thermometry. Earth Plan. Sci. Lett., **20**, 250-265

Bottinga Y. and Javoy M. (1975). Oxygen isotope partitioning among minerals in igneous and metamorphic rocks. Rev. Geophys. Space Phys., **13**, 401-418

Bottinga Y. and Javoy M. (1988). ^{17}O and ^{18}O exchange between water and quartz. Chem. Geol., **70**, pp 182 (abstract)

Brevart O.B., Dupre B. and Allegre C.J. (1986). Lead-lead age of komatiitic lavas and limitations on the structure and evolution of the Precambrian mantle. Earth Plan. Sci. Lett., **77**, 293-302

Carlson R.W., Hunter M.P. and Barker F. (1983). Sm-Nd age and isotopic systematics of the bimodal suite, Ancient Gneiss Complex, Swaziland. Nature, **305**, 701-704

Cathelineau M. (1988). Chlorite and illite geothermometers. Chem. Geol., **70**, pp 182 (abstract)

Cathelineau M. and Nieva D. (1985). A chlorite solid solution geothermometer. The Los Azufres (Mexico) geothermal system. Contr. Mineral. and Petrol., **91**, 235-244

Clayton R.N, Goldsmith J.R. and Mayeda T.K. (1989). Oxygen isotope fractionation quartz, albite, anorthite and calcite. Geochim. Cosmochim. Acta, **53**, 725-733

Colvine A.C., Fyon J.A., Heather K.B., Marmont S, Smith P.M. and Troop D.G. (1988). Archaean lode gold deposits in Ontario. Ontario Geol. Surv., Misc. Paper **139**

Condie K.C. and Hunter D.R. (1976). Trace element geochemistry of Archaean granitic rocks from the Barberton region, South Africa. Earth Plan. Sci. Lett.,**29**,389-400

de Beer J.H., Stettler E.H., du Plessis J.G. and Blume J. (1988). The deep structure of the Barberton Greenstone Belt: a geophysical study. South Afr. J. Geol., **91**, (2), 184-197

de Ronde C.E.J., de Wit M.J., Spooner E.T.C. (1988). Characteristics of Early Archaean (>3.0 Ga) Au-quartz lode deposits from thrust zones in the mafic ultramafic rocks of the Barberton Greenstone Belt, South Africa. Abstract Gold **88**, Australia

de Wit M.J., Armstrong R., Hart R.J. and Wilson A.J. (1987a). Felsic igneous rocks within the 3.3 to 3.5 Ga Barberton Greenstone Belt: High level equivalents of the surrounding tonalite-trondhjemite terrain, emplaced during thrusting. Tectonics, **6**, (5), 529-549

de Wit M.J., Hart R.A. and Hart R.J. (1987b). The Jamestown Ophiolite Complex, Barberton Mountain Land: a section through 3.5 Ga crust. J. of Afr. Earth Sci., **6**, (5), 681-730

Deer W.A., Howie R.A. and Zussman J. (1979). An introduction to the rock-forming minerals, 1-528, Longman, London

Foster R.P. (1985). Major controls of Archaean gold mineralization in Zimbabwe. In Anhaeusser C.R. and Maske S. (eds) Mineral Dep. S.A. Vols I & II. Geol. Soc. S.A., Johannesburg. 109-133

Friedman I. and O'Neil J.R. (1977). Data of Geochemistry. Sixth Edition. Chapter KK. Compilation of stable isotope fractionation factors of geochemical interest.

Fripp R.E.P., van Nierop D.A., Callow M.J., Lilly P.A. and du Plessis L.U. (1980). Deformation in the Archaean Kaapvaal Craton, South Africa. Precambrian Res., **13**,241-251

Giletti B.J. (1986). Diffusion effects on oxygen isotope temperatures of slowly cooled igneous and metamorphic rocks. Earth and Plan. Sci. Let., **77**, 218-228

Gregory R.T. and Criss R.E. (1986). Isotopic exchange in open and closed systems, 91-128. In: Valley J.W., Taylor H.P Jr. and O'Neil J.R. (eds). Stable Isotopes in High Temperature Geological Processes. Mineral. Soc. of Am., Rev. in Mineral., **16**.

Gregory R.T., Criss R.E and Taylor H.P. Jr. (1989). Oxygen isotope exchange kinetics of mineral pairs in closed and open systems: applications to problems of hydrothermal alteration of igneous rocks and Precambrian iron formations. Chem. Geol., **75**, 1-42

Hall A.L. (1918). The geology of the Barberton gold mining district. Mem. geol. Surv. South Afr., **9**

Hamilton P.J., O'Nions R.K., Bridgewater D. and Nutman A. (1983). Sm-Nd studies of Archaean metasediments and metavolcanics from West Greenland and their implication for the Earth's early history. Earth Plan. Sci. Lett., **62**, 263-372

Harris C. (1983). Petrology of lavas and associated plutonic inclusions of Ascension island. J. Petrol., **24**, 424-470

Henoc J., Heinrich K.F. and Myklebust R.L. (1973). A rigorous correction procedure for quantitative electron probe analysis microanalysis (COR 2). U.S. Bureau of Standards Technical Note **769**. U.S. Govt. printing Office, Washington D.C.

Hey M.H. (1954). A new review of the chlorites. The Mineralogical Magazine, **224**, Vol XXX

Hoefs J. (1987). Stable Isotope Geochemistry. (3rd Edition). Springer-Verlag, New York. 1-208

Hoffman S.E., Wilson M. and Stakes D.S. (1986). An inferred oxygen isotope profile of Archaean crust, Onverwacht Group, South Africa. Nature, **321**, 55-58

Javoy M. (1977). Stable isotopes and geothermometry. J. geol. Soc. London., **133**, 609-636

Javoy M., Fourcade S., Allegre C.J. (1970). Graphical method for examination of $^{18}O/^{16}O$ fractionation in silicate rocks. Earth Plan. Sci. Lett., **10**, 12-16

Kieffer S.W. (1982). Thermodynamics and lattice vibrations of minerals: Applications to phase equilibria, isotopic fractionation, and high-pressure thermodynamic properties. Rev. Geophys. Space Phys., **20**, 827-849

Layer P.W. (1986). Archaean paleomagnetism of South Africa. Ph.D. Stanford Univ. (unpubl.)

Magaritz M. and Taylor H.P. Jr. (1976b). Isotopic evidence for meteoric in the Yakutat Bay and Skagway areas, Alaska. Earth Plan. Sci. Lett., **30**, 179-190

Magaritz, M., and Taylor, H.P. Jr.,(1976a). O^{18}/O^{16} and D/H studies of igneous and sedimentary rocks along a 500 km traverse across the Coast Range batholith into central British Columbia at latitudes 54 °-55°N. Can. J. Earth Sci.,**13**,p. 1514-1536

Matsuhisa Y., Goldsmith J.R. and Clayton R.N. (1979). Oxygen isotopic fractionation in the system quartz-albite-anorthite-water. Geochim. Cosmochim. Acta, **43**, 1131-1140

Matthews A., Goldsmith J.R. and Clayton R.N. (1983a). Oxygen isotope fractionations involving pyroxenes: the calibration of mineral-pair geothermometers. Geochim. Cosmochim. Acta, **47**, 631-644

Matthews A., Goldsmith J.R. and Clayton R.N. (1983b). Oxygen isotope fractionation between zoisite and water. Geochim. Cosmochim. Acta, **47**, 645-654

Matushisa Y. Goldsmith J.R. and Clayton R.N. (1978). Mechanism of hydrothermal crystallisation of quartz at 250 °C and 15 kbar. Geochim. Cosmochim. Acta, **42**, 173-182

McCrea J.M. (1950). On the isotopic chemistry of carbonates and a paleotemperature scale. J. Chem. Physics, **18**, 849-857

Meyer C. and Hemley J.J. (1976). Wall rock alteration, 167-235. In: Barnes H.L. (ed). Geochemistry of Hydrothermal Ore Deposits. Holt, Rhinehart and Winston, Inc., New York.

O'Neil J.R. (1968). Hydrogen and oxygen isotopes in hydrothermal ore deposits. Econ. Geol., **67**, 551-578

O'Neil J.R. (1986). Theoretical and experimental aspects of isotopic fractionation, 1-40. In: Valley J.W., Taylor H.P Jr. and O'Neil J.R. (eds). Stable Isotopes in High Temperature Geological Processes. Mineral. Soc. of Am., Rev. in Mineral., **16**.

O'Neil J.R., Shaw S.E. and Flood R.H. (1977). Oxygen and hydrogen isotopic composition as indicators of granite genesis in the New England Batholith, Australia. Contr. Mineral. Petrol., **62**, 313-328

O'Neil J.R. and Chappell B.W. (1977). Oxygen and hydrogen relations in the Berridale batholith. J. geol. Soc., **133**, 559-571

O'Neil J.R., Silberman, M.L., Fabbi, B.P.and Chesterman, C.W. (1973). Stable isotope and chemical relations during mineralisation in the Bodie mining district, Mono County, California. Econ. Geol.,**68**,p. 765-784

Ohmoto H. (1986). Stable isotope geochemistry of ore deposits. In: Valley J.W., Taylor H.P Jr. and O'Neil J.R. (eds). Stable Isotopes in High Temperature Geological Processes. Mineral. Soc. of Am., Rev. in Mineral., **16**.

Ohmoto H. and Rye R.O. (1979). Isotopes of sulphur and carbon. 509-567. In: Barnes H.L. (ed). Geochemistry of Hydrothermal Ore Deposits, 2nd Edition. J. Wiley and sons, New York.

Oosthuizen E.J. (1970). The geochronology of a suite of rocks from the granite surrounding the Barberton Mountain Land. PhD thesis(unpubl.) Univ. Witwatersrand, Johannesburg, 1-94

Robb L.J. (1981). The geological and geochemical evolution of tonalite-trondhjemitic gneisses and migmatites in the Barberton region, Eastern Transvaal. Ph.D. thesis (unpubl.), Univ. Witwatersrand, Johannesburg, 342pp

Robb L.J. and Anhaeusser C.R. (1983). Chemical and petrogenetic characteristics of Archaean tonalite-trondhjemite gneiss plutons in the Barberton Mountain Land. In: Anhaeusser C.R. (ed). Contributions to the geology of the Barberton Mountain Land. National Geodynamics programme, Barberton Project. Spec. Bull., **9**, Geol. Soc. South Afr.

Robb L.J., Barton J.M., Kable E.J.D. and Wallace R.C.(1986). Geology, Geochemistry and isotopic characteristics of the Archaean Kaap Valley pluton, Barberton Mountain Land, South Africa. Precambrian Res.,**31**,1-36

Saager R. and Meyer M. (1984). Gold distribution in the Archaean granitoids and supra crustal rocks from southern Africa: a comparison. 53-70. In: Forester R.P. (ed), Gold'82. The geology, geochemistry and genesis of gold deposits. Bolkema, Rotterdam, 1-753.

Saager R., Meyer M. and Muff R. (1982). Gold distribution from Archaean greenstone belts of southern Africa and from Paleozoic ultramafic complexes of the European Alps: metallogenic and geochemical implications. Econ. Geol., **77**, 1-24

Sheppard S.M.F. (1986). Igneous rocks:II. Isotopic case studies of magmatism in Africa, Eurasia and oceanic islands. In: Valley J.W., Taylor H.P Jr. and O'Neil J.R. (eds). Stable Isotopes in High Temperature Geological Processes. Mineral. Soc. of Am., Rev. in Mineral., **16**.

Sheppard S.M.F., and Harris C. (1985). Hydrogen and oxygen isotope geochemistry of Ascenion Island lavas and granites: variation with crystal fractionation and and interaction with sea water. Contr. Mineral. and Petrol., **91**,74-81.

Smith H.S. (1986). Evidence from $\delta^{13}C$ and ^{18}O isotopes in carbonate minerals for the origin of fluids in Archaean greenstone belt metamorphic and mineral processes. Geol. Soc. South Afr. Geocongress, '86, Abstracts

Smith H.S. and Erlank A.J. (1980). Geochemistry of some ultramafic komatiite flows from the Barberton Mountain Land, South Africa. Precambrian Res., 11, 399-415

Smith H.S. and Erlank A.J. (1982). Geochemistry and petrogenesis of komatiite from the Barberton greenstone belt, South Africa. In: Arndt N.T., E.G. Nisbet (eds). Komatiites. Allen and Unwin

Smith H.S., O'Neil J.R. and Erlank A.J. (1984). Oxygen isotopic compositions of minerals and rocks and chemical alteration patterns in pillow lavas from the Barberton greenstone belt, South Africa: In Kroner A. et al., Archaean Geochemistry. Springer-Verlag Berlin Heidelberg. 115-137

Smith P.M., Ayer J.S., Buck S., Morrice M.G., Sandborn-Borrie M., Blackburn R.E., Brown P.E. and Davis D.W.(1988). Style, controls and timing of gold mineralisation in the Lake of the Woods greenstone belt, Northwestern Ontario, Canada: Evidence for a plutonic connection. Gold

South African Committee for Stratigraphy (S.A.C.S.) (1980). Stratigraphy of South Africa Part 1 (Comp. L.E.Kent). Lithostratigraphy of the Republic of South Africa, South West Africa/Namibia, and the Republics of Bophuthatswana, Transkei and Venda: Handb. geol. Surv. S. Afr.,8

Stott G.M., Smith P.M. (1988). Development of gold bearing structures in the Archaean: the role of granite plutonism. Gold '88, Melbourne. Extended Abs., 48-50

Taylor H.P. Jr. (1968). Oxygen isotope geochemistry of igneous rocks. Contr. Mineral. Petrol., 19, 1-71

Taylor H.P. Jr. (1973). O^{18}/O^{16} evidence for meteoric-hydrothermal

alteration and ore deposition in the Tonopah, Comstock Lode, and Goldfield mining districts, Nevada. Economic Geol., **68**,p. 747-767

Taylor H.P. Jr. (1974). The application of oxygen and hydrogen isotope studies to problems of hydrothermal alteration and ore deposition. Econ. Geol., **69**,p. 843-883

Taylor H.P. Jr. (1977). Water/rock interaction and the origin of water in granite batholiths. J Geol. Soc. London, **133**, 509-508

Taylor H.P. Jr. (1986). Igneous rocks:II. Isotopic case studies of circumpacific magmatism. In: Valley J.W., Taylor H.P Jr. and O'Neil J.R. (eds). Stable Isotopes in High Temperature Geological Processes. Mineral. Soc. of Am., Rev. in Mineral., **16**.

Taylor H.P. Jr. (1988). Oxygen, hydrogen and strontium constraints on the origin of granites. Transactions Royal Soc. Edinburgh: Earth Sci., **79**, 317-338

Taylor H.P. Jr. and Epstein S. (1962). Relationship between $^{18}O/^{16}O$ ratios in coexisting minerals of igneous and metamorphic rocks. Part 2. Application to petrologic problems. Geol. Soc. Am. Bull., **73**, 675-694

Taylor H.P. Jr. and Forester R.W. (1979). An oxygen and hydrogen study of Skaergaard intrusion and its country rocks: a description of a 55 My old fossil hydrothermal system. J. Pet., **20**, 355-419

Taylor H.P. Jr. and Magaritz M. (1975). Oxygen and hydrogen isotopic studies of the 2.6-3.4 B.Y. old granites from the Barberton Mountain Land , Swaziland and Rhodesian Craton, South Africa. Geol. Soc. Am. Abs. Program, 7, 1293

Taylor H.P. Jr. and Sheppard S.M.F. (1986). Igneous rocks: I. Processes of isotopic fractionation and isotopic systematics, 227-272. In: Valley J.W., Taylor H.P Jr. and O'Neil J.R. (eds). Stable Isotopes in High Temperature Geological Processes. Mineral. Soc. of Am., Rev. in Mineral., **16**.

Taylor S.R. and McLennan S.M. (1985). The Continental Crust, its composition and evolution. Oxford, England, Blackwell. 1-312

Tegtmeyer A.R. and Kroner A. (1987). U-Pb zircon ages bearing on the nature of Early Archaean greenstone belt evolution, Barberton Mountain Land, South Africa. Precam. Res., **36**, 1-20

Tegtmeyer A.R., Kroner A. and Hoffman A.W. (1985). Isotopic systematics of early Archaean high-grade greenstones from Swaziland, southern Africa. Terra Cognita, **5**, 205 (abstract)

Turner F.J. (1981). Metamorphic Petrology Mineralogical, Field and Tectonic Aspects. (2nd Edition). McGraw-Hill Book Company, New York

Viljoen M.R. and Viljoen R.R. (1969a). The geology and geochemistry of the lower ultramafic unit of the Onverwacht Group and a proposed new class of igneous rocks. Spec. Publ. Geol. Soc. Afr., **2**, 55-85. Viljoen M.R. and Viljoen R.R. (1969b). A proposed new classification of the granitic rocks of the Barberton region. Spec. Publ. Geol. Soc. Afr. ,**2**, 153-188.

Viljoen M.R., Viljoen R.R., Smith H.S. and Erlank A.J. (1983). Geological, textural and geochemical features of komatiitic flows from the Komati Formation. In: Anhaeusser C.R (ed). Contributions to the geology of the Barberton Mountain Land. Geol. Soc. South Afr., Spec. Publ., **9**, 1-20

Visser D.J.L. (compiler) (1956). The geology of the Barberton area. Geol. Soc. South Afr. Spec. Publ. **15**, 1-253

Wenner D.B. and Taylor H.P. Jr. (1971). Temperatures of serpentinization of ultramafic rocks based on O^{18}/O^{16} fractionation between coexisting serpentine and magnetite. Contr. Mineral. Petrol., **32**, 165-185.

White A.J.R., and Chappell B.W. (1977). Ultrametamorphism and granitoid genesis. Tectonophysics, **43**, 7-22.

1. APPENDIX 1

1.1 STABLE ISOTOPE GEOCHEMISTRY

The terminology and mathematical rationale of stable isotope geochemistry is briefly summarised from O'Neil (1986).

1.1.1 *The Isotope Exchange Reactions*

Isotope exchange reactions are usually equilibrium reactions in which the isotopes of a single element are exchanged between two substances. For the general case of an isotope exchange reaction between two substances A and B, where the subscripts 1 and 2 refer to the molecules totally substituted by the light and heavy isotope, respectively,

$$aA_1 + bB_2 = aA_2 + bB_1 \quad (1)$$

The equilibrium constant for this reaction is written in the usual way:

$$K = \frac{(A_2/A_1)^a}{(B_2/B_1)^b} \quad (2)$$

1.1.2 *The Fractionation Factor α*

The isotopic fractionation factor between two substances A and B is defined as:

$$\alpha_{A\text{-}B} = R_A/R_B \quad (3)$$

In terms of δ values this expression becomes from (1):

$$\alpha_{A\text{-}B} = \frac{(1000 + \delta_A)}{(1000 + \delta_B)} \quad (4)$$

Table A.1: Fractionation Factors Used In This Study

Quartz-H_2O	References
$\Delta = 4.10*10^6*T^{-2} - 3.70$	1
Chlorite-H_2O	
$\Delta = -1.34*10^6*T^{-2} -2.07$	2
$\Delta = 1.56*10^6*T^{-2} -4.70$	3
Plagioclase-H_2O	
$\Delta = (3.13-1.04B)*10^6*T^{-2} -3.70$	1
B = An of plagioclase	
Quartz-Plagioclase	
$\Delta = (0.97+1.04B)*10^6*T^{-2}$	1
Quartz-Hornblende	
$\Delta = 3.15*10^6*T^{-2} -0.30$	1
Quartz-Biotite	
$\Delta = 3.69*10^6*T^{-2} -0.60$	1
Quartz-Chlorite	
$\Delta = 5.44*10^6*T^{-2} -1.63$	1
Quartz-Epidote	
$\Delta = 1.56*10^6*T^{-2}$	1

References

1. Bottinga and Javoy (1973 in Friedman and O'Neil, 1977; 1975)
2. Javoy (1977)

3. Wenner and Taylor (1971).

Fractionation factors for calcite used in this study are H_2CO_3-Calcite and HCO_3^--Calcite (Hoefs, 1987) and and Calcite-H_2O (Friedman and O'Neil, 1977).

KF21; tonalite, poor mineral lineation
KF22; tonalite, fine-grained, side of mountain
KF23; tonalite, no lineation
KF24; tonalite, very hard, silicified, large dolerite dykes nearby
KF25; tonalite, Graig Dune farm, dolerite dykes in area and few xenoliths
KF26; quartz vein 15cm wide
KF27; tonalite, xenoliths
KF28; tonalite
KF29; tonalite, no lineation
KF30; tonalite, road to farm house "castle", altered, Fe-rich, quartz veins
KF31; tonalite, altered as above
KF32; tonalite,
KF33; tonalite, fair mineral lineation
KF34; tonalite
KF35; tonalite
KF36; tonalite, no mineral lineation, quartz veins
KF37; quartz vein
KF38; tonalite,
KF39; tonalite, large biotite phenocrysts, near farm house
KF40; tonalite, good mineral lineation, waterfall
KF41; tonalite, fair mineral lineation, waterfall
KF42; tonalite, very light colour
KF43; tonalite, highly silicous and chlorite alteration
KF44; tonalite, equigranular, in riverbed
KF45; tonalite, equigranular, near weir wall
KF46; quartz vein near weir wall
KF47; tonalite, highly altered chl rich, green colour rock
KF48; tonalite, chl rich, near weir wall
KF49; tonalite, side of dolerite hill
KF50; tonalite, 2 m from dolerite dyke
KF51; tonalite, good mineral lineation,dolerite dyke nearby
KF52; tonalite, strong vertical mineral lineation,very altered, ~15m BGB contact,on Abbots road

KF53; quartz vein
KF54; tonalite, good mineral lineation
KF55; tonalite, highly chloritised
KF56; tonalite, under bridge,
KF57; tonalite, highly altered, ~2m from BGB contact
KF58; quartz vein
KF59; tonalite,
KF60; tonalite, good mineral lineation
KF61; tonalite, good mineral lineation
KF62; tonalite, fair to poor mineral lineation
KF63; tonalite, poor mineral lineation
KF64; tonalite,
KF65; tonalite, no mineral lineation, fresh sample, Kwa Thewane Pools
KF66; tonalite,
KF68; tonalite, near BGB contact
KF69; tonalite,
KF70; tonalite, chlorite alteration, near dolerite dyke
KF71; tonalite, 5m away from dolerite dyke, Devils Knuckels view point
KF72; tonalite, 3m away from dolerite dyke
KF73; tonalite, next to contact
KF74; tonalite,
KF75; tonalite,
KF76; tonalite,
KF77; tonalite, very altered, pink/red colour, Bekker plot 20
KF78; quartz veining lots
KF79; tonalite,
KF80; tonalite, very altered, chlorite
KF81; quartz vein within KF80
KF82; tonalite, altered chl
KF83; tonalite, altered
KF84; tonalite, altered,no dykes in the area
KF85; quartz vein in hematised tonalite, pit
KF86; tonalite, altered, no dolerite dykes

KF87; tonalite, near contact with Jamestown Schist Belt
KF88; tonalite, near contact, very altered, chlorite
KF89; tonalite, very altered, no dolerite dykes
KF90; tonalite, chlorite alteration, moderate mineral lineation
KF91; tonalite, poor mineral lineation
KF92; tonalite, altered, very hard, near dolerite dyke ridge
KF93; tonalite, plenty xenoliths in the area, some partially absorbed
KF94; tonalite,
KF95; carbonate Fe-rich veins
KF96; tonalite, hornblende mineral lineation subhorizontal, plenty of xenoliths in the area
KF97; tonalite, contact between fine and medium/coarse grained, fine grained tonalite that post dates the medium/coarse grained tonalite
KF98; tonalite,
KF99; tonalite, fine grained
KF100; tonalite,
KF101; tonalite,
KF102; tonalite,
KF103; tonalite, good outcrop
KF104; tonalite,
KF105; tonalite, good outcrop
KF106; quartz veining, shear zone?, pits probably exploring greenstone xenolith
KF107; tonalite, fine grained, Impombo waterfall
KF108; tonalite,
KF109; tonalite,
KF110; tonalite, fine grained post dates coarse,
KF111; tonalite,
KF112; tonalite, good outcrop
KF113; tonalite,
KF114; tonalite, good outcrop, no mineral lineation
KF115; tonalite,
KF116; tonalite,
KF117; tonalite, altered, pink colour, fair mineral lineation

KF118; tonalite,
KF119; tonalite, near dolerite dyke, lots chlorite veins, no mineral lineation
KF120; tonalite,
KF121; tonalite,
KF122; tonalite,
KF123; tonalite, 20m from dolerite dyke and appears relatively fresh
KF124; tonalite,
KF125; tonalite,
KF126; migmatite, direction of lineation 35°
KF127; migmatite, disseminated pyrite
KF128; tonalite, fine grained, slightly schistose, pyrite along subvertical bands
KF129; tonalite, fine grained
KF130; tonalite,
KF131; tonalite, weathered?, dolerite dykes nearby
KF132; tonalite, dolerite dyke ~20m away
KF133; tonalite, very near dolerite dyke, very hard
KF134; dolerite dyke with pyrite
KF135; tonalite, altered , chlorite
KF136; albitite and smoky quartz
KF137; vein
KF138; carbonate vein fracturing albitite vein
KF139; carbonate vein within greenstones
KF140; tonalite, fine grained, altered
KF141; tonalite, altered, chlorite, 50m from KF140
KF142; tonalite, good mineral lineation, 50m from KF141
KF143; tonalite, 70m from KF142
KF144; tonalite, 80m from KF143, near switchback of road

1. APPENDIX 3

1.1 MINERAL POINT-COUNTING RESULTS

The KVT mineral modal percentages determined by point-counting of 78 thin-sections at 900 counts per thin-section.

	QTZ	PLAG	HBL	BIOT	SERI	CHL	EPI	CARB
KF2	18.1	61.8	10.7	0.2	99	8.7	0.5	-
KF5	21.6	57.6	6.3	10.8	32	2.1	0.3	0.8
KF7	26.1	58.0	-	-	79	13.0	2.7	-
KF8	19.5	50.2	-	1.8	65	20.0	7.5	0.8
KF11	30.0	49.3	8.1	10.8	31	1.5	-	0.1
KF12	17.8	61.0	-	-	79	19.6	1.5	-
KF15	19.3	54.3	-	-	99	17.1	0.1	8.8
KF17	6.8	65.4	12.2	-	100	4.1	1.2	-
KF18	17.3	53.7	7.0	-	94	19.1	1.6	0.8
KF19	17.8	57.9	8.6	2.3	70	12.3	0.8	-
KF20	14.0	59.1	-	-	97	20.0	6.8	-
KF21	14.8	67.4	9.5	-	92	6.5	1.0	0.5
KF23	35.5	47.7	1.6	0.1	88	9.6	4.5	-
KF25	20.8	66.9	7.6	3.8	59	0.6	-	-
KF28	35.6	47.1	1.6	-	62	9.3	6.0	-
KF29	28.3	52.3	0.5	-	93	10.6	8.1	-
KF30	29.1	57.4	0.1	-	94	10.1	2.8	-
KF31	29.3	56.1	-	-	91	13.0	0.6	0.8
KF32	25.1	57.7	9.6	4.1	50	1.5	1.6	-
KF33	27.0	53.8	7.8	-	73	8.3	1.8	-
KF35	19.5	68.9	0.1	-	98	7.3	2.8	0.3
KF36	28.3	53.9	-	-	94	12.8	4.3	0.3
KF38	22.6	56.1	0.3	-	97	15.3	3.1	1.5
KF39	31.5	50.5	7.6	4.1	81	2.5	2.8	-
KF41	23.0	65.1	5.1	-	91	5.8	0.8	-
KF42	27.3	60.3	3.1	-	88	7.5	1.6	-
KF47	28.6	7.0	-	-	100	24.4	-	40.0

Table 1.1 continues.....

Table 1.1: continues....

	QTZ	PLAG	HBL	BIOT	SERI	CHL	EPI	CARB
KF49	25.0	60.8	-	-	80	11.3	2.3	0.1
KF51	18.8	55.7	10.3	-	78	14.5	0.3	-
KF55	11.8	56.8	15.5	0.5	85	9.5	5.8	-
KF59	12.5	51.1	1.6	-	97	32.6	1.8	-
KF60	30.8	59.1	4.5	-	88	4.5	1.0	-
KF62	23.1	46.1	12.5	-	94	10.0	10.0	0.8
KF64	21.5	53.7	11.2	-	99	11.5	1.8	-
KF65	16.32	35.6	20.28	10.02	17.78	-	-	-
KF66	16.5	58.6	16.0	-	85	7.0	1.8	-
KF67	25.8	46.6	-	-	88	19.5	5.0	2.6
KF68	22.0	60.2	7.1	-	50	8.8	1.3	-
KF69	23.3	60.2	8.1	6.5	24	0.5	0.5	-
KF70	25.6	53.1	4.0	-	88	14.0	2.8	-
KF72	15.1	73.2	-	-	77	6.6	4.8	-
KF74	29.5	52.4	6.8	-	59	9.8	0.8	-
KF75	25.5	56.8	5.1	-	82	11.5	1.0	-
KF76	28.0	63.6	4.1	-	82	2.5	1.6	-
KF77	21.3	70.2	-	-	99	8.0	0.3	-
KF79	25.3	62.8	0.1	-	90	6.5	5.0	-
KF80	20.1	63.5	-	-	100	16.3	-	-
KF84	29.0	58.8	-	-	98	10.8	1.3	-
KF88	29.1	53.8	6.0	-	72	10.1	0.3	0.3
KF89	17.1	60.6	9.3	-	84	9.3	1.8	-
KF90	29.3	49.9	3.1	-	96	12.6	3.8	0.8
KF91	27.3	55.3	6.1	-	96	6.8	3.6	0.6
KF94	20.3	60.0	6.0	-	89	9.5	3.8	-
KF96	20.8	59.2	7.5	5.6	88	4.8	1.8	-
KF100	19.5	61.0	4.5	-	94	11.3	3.6	-
KF102	21.1	64.2	3.0	-	84	10.8	0.5	-

Table 1.1: continues.....

Table 1.1: continues....

	QTZ	PLAG	HBL	BIOT	SERI	CHL	EPI	CARB
KF103	19.8	59.3	7.3	-	79	12.6	0.6	-
KF104	22.8	63.8	4.6	-	76	6.3	2.1	0.1
KF105	19.5	61.3	8.9	-	82	8.6	1.1	-
KF108	16.5	55.6	17.2	-	49	8.3	1.5	0.3
KF111	19.8	61.9	8.8	0.1	82	6.3	2.5	-
KF114	19.1	62.1	4.6	-	86	8.8	5.1	-
KF115	16.8	57.1	11.3	-	69	12.3	1.8	0.5
KF116	20.0	62.3	5.0	-	74	8.1	4.5	-
KF118	21.1	56.9	9.1	-	93	7.5	5.0	-
KF119	21.6	58.2	6.8	10.0	53	2.5	0.5	-
KF120	22.5	53.0	7.6	0.6	90	13.3	2.5	-
KF121	22.6	64.1	5.4	-	94	4.0	3.6	-
KF123	21.6	62.6	5.6	-	75	6.8	2.6	-
KF124	10.5	56.1	20.8	-	73	11.5	1.0	-
KF127	28.8	61.6	-	-	76	9.5	-	-
KF130	19.6	62.4	8.4	-	93	8.0	1.3	-
KF132	27.5	53.6	8.6	7.0	27	2.1	0.5	-
KF133	22.5	58.1	8.6	-	84	7.0	3.3	-
KF144	20.5	55.6	9.3	-	48.6	11.5	2.8	0.6

QTZ-quartz; PLAG-plagioclase + sericite; HBL-hornblende; BIOT-biotite; SERI-% plagioclase sericitised; CHL-chlorite; EPI-epidote; CARB-carbonate; SPH-sphene

3.2 KVT MINERAL MICROPROBE DATA

Mineral chemistry data is presented here for hornblende, biotite, chlorite and plagioclase. Most plagioclase minerals have been analysed within their cores, intermediate and rim portions. The average chlorite AL(IV) atomic proportions (based on 14 oxygens) are also presented. These values have been used to estimate temperatures of formation, using the Cathelineau and Nieva (1986) solid-solution geothermometer (Chapter 4).

KVT PLAGIOCLASE

	1	1	2	3	5	5	5	5	6	6
SIO2	63.32	63.85	61.23	61.20	60.80	61.24	61.85	61.88	61.04	61.10
TIO2										
AL2O3	21.83	22.38	23.74	23.63	24.41	23.64	23.73	23.79	24.31	23.66
CR2O3										
FE2O3										
FEO	.01	.15	.17	.01	.01	.18	.01	.21	.01	.01
MNO										
MGO	.01	.01	.01	.01	.01	.01	.01	.01	.01	.01
CAO	3.98	4.14	5.73	5.85	6.45	5.62	5.93	5.77	6.36	5.28
NA2O	8.72	8.75	8.01	7.79	7.58	8.04	7.83	7.92	7.67	7.95
K2O	.23	.17	.10	.39	.35	.38	.45	.44	.14	.48
NIO										
TOTAL	98.10	99.45	98.99	98.88	99.61	99.11	99.81	100.02	99.54	98.49
OXYGEN	8	8	8	8	8	8	8	8	8	8
SI	2.844	2.831	2.743	2.746	2.713	2.745	2.750	2.748	2.722	2.750
TI										
AL	1.156	1.170	1.254	1.250	1.284	1.249	1.244	1.245	1.278	1.255
CR										
FE3+										
FE2+		.006	.006			.007		.008		
MN										
MG	.001	.001	.001	.001	.001	.001	.001	.001	.001	.001
CA	.192	.197	.275	.281	.308	.270	.283	.275	.304	.255
NA	.759	.752	.696	.678	.656	.699	.675	.682	.663	.694
K	.013	.010	.006	.022	.020	.022	.026	.025	.008	.028
NI										
SUM	4.965	4.965	4.981	4.979	4.983	4.991	4.978	4.983	4.975	4.983
AN	19.9	20.5	28.2	28.7	31.3	27.3	28.7	28.0	31.2	26.1
AB	78.77	78.48	71.25	69.06	66.64	70.55	68.67	69.49	68.02	71.09
OR	1.37	1.00	.58	2.28	2.03	2.19	2.60	2.54	.82	2.82

*** ALL ZERO VALUES PRINTED AS BLANKS ***

SAMPLE DESCRIPTIONS :

1	:	PLG	CORE KF65
1	:	PLG	CORE "
2	:	PLG	CORE KF11
3	:	PLG	CORE KF93
5	:	PLG	CORE KF68
5	:	PLG	CORE "
5	:	PLG	CORE "
5	:	PLG	CORE "
6	:	PLG	CORE KF40
6	:	PLG	CORE "

KVT PLAGIOCLASE

	8	9	10	10	11	12	1	1	2	2
SIO2	61.27	58.93	61.87	61.17	63.60	61.87	59.47	60.16	62.95	60.49
TIO2										
AL2O3	23.77	24.93	23.43	23.98	22.24	22.78	24.69	24.04	22.70	24.02
CR2O3										
FE2O3										
FEO	.01	.16	.01	.01	.01	.20	.01	.01	.01	.01
MNO										
MGO	.01	.01	.01	.01	.01	.01	.01	.01	.01	.01
CAO	5.99	7.43	5.43	5.93	4.29	5.04	7.24	6.16	4.59	6.51
NA2O	7.94	7.01	8.06	7.92	8.75	8.30	7.02	7.44	8.74	7.61
K2O	.24	.36	.47	.34	.28	.46	.24	.37	.10	.11
NIO										
TOTAL	99.23	98.83	99.28	99.36	99.18	98.66	98.68	98.19	99.10	98.76
OXYGEN	8	8	8	8	8	8	8	8	8	8
SI	2.740	2.662	2.763	2.734	2.830	2.782	2.683	2.721	2.805	2.720
TI										
AL	1.253	1.328	1.233	1.263	1.166	1.207	1.313	1.281	1.192	1.273
CR										
FE3+										
FE2+		.006				.008				
MN										
MG	.001	.001	.001	.001	.001	.001	.001	.001	.001	.001
CA	.287	.360	.260	.284	.205	.243	.350	.299	.219	.314
NA	.689	.614	.698	.686	.755	.724	.614	.652	.755	.664
K	.014	.021	.027	.019	.016	.026	.014	.021	.006	.006
NI										
SUM	4.984	4.991	4.982	4.988	4.972	4.990	4.975	4.975	4.979	4.978
AN	29.0	36.2	26.4	28.7	21.0	24.5	35.8	30.7	22.4	31.9
AB	69.60	61.75	70.89	69.35	77.40	72.89	62.80	67.10	77.06	67.47
OR	1.38	2.09	2.72	1.96	1.63	2.66	1.41	2.20	.58	.64

*** ALL ZERO VALUES PRINTED AS BLANKS ***

SAMPLE DESCRIPTIONS :

8	: PLG	NEAR CORE KF96
9	: PLG	NEAR CORE KF112
10	: PLG	NEAR CORE KF119
10	: PLG	NEAR CORE "
11	: PLG	CORE KF110
12	: PLG	NEAR CORE KF32
1	: PLG	MID KF65
1	: PLG	MID "
2	: PLG	MID KF11
2	: PLG	MID "

KVT PLAGIOCLASE

	3	3	3	3	3	3	5	5	5	5
SIO2	62.00	62.43	62.19	62.15	62.42	62.19	62.31	62.51	61.93	60.91
TIO2										
AL2O3	22.55	22.60	23.43	22.78	23.11	23.28	23.61	23.19	23.87	24.47
CR2O3										
FE2O3										
FEO	.20	.17	.01	.21	.01	.01	.01	.01	.01	.01
MNO										
MGO	.01	.01	.01	.01	.01	.01	.01	.01	.01	.01
CAO	5.36	5.23	5.36	5.10	5.12	5.34	5.49	5.30	5.57	6.43
NA2O	8.15	8.27	8.17	8.04	8.29	8.13	8.22	8.39	8.13	7.64
K2O	.45	.46	.33	.43	.22	.44	.46	.26	.34	.29
NIO										
TOTAL	98.72	99.17	99.50	98.72	99.18	99.40	100.11	99.67	99.86	99.76
OXYGEN	8	8	8	8	8	8	8	8	8	8
SI	2.787	2.792	2.769	2.789	2.784	2.773	2.761	2.778	2.750	2.713
TI										
AL	1.195	1.191	1.229	1.205	1.215	1.223	1.233	1.215	1.249	1.285
CR										
FE3+										
FE2+	.008	.006		.008						
MN										
MG	.001	.001	.001	.001	.001	.001	.001	.001	.001	.001
CA	.258	.251	.256	.245	.245	.255	.261	.252	.265	.307
NA	.710	.717	.705	.699	.717	.703	.706	.723	.700	.660
K	.026	.026	.019	.025	.013	.025	.026	.015	.019	.016
NI										
SUM	4.984	4.984	4.979	4.971	4.974	4.980	4.988	4.984	4.985	4.982
AN	26.0	25.2	26.1	25.3	25.1	26.0	26.3	25.5	26.9	31.2
AB	71.44	72.15	71.99	72.17	73.60	71.50	71.13	73.02	71.12	67.11
OR	2.60	2.64	1.91	2.54	1.28	2.55	2.62	1.49	1.96	1.68

*** ALL ZERO VALUES PRINTED AS BLANKS ***

SAMPLE DESCRIPTIONS :

3	:	PLG MID KF93
3	:	PLG MID "
3	:	PLG MID "
3	:	PLG MID "
3	:	PLG XENO MID
3	:	PLG XENO MID
5	:	PLG MID KF68
5	:	PLG MID "
5	:	PLG MID "
5	:	PLG MID "

KVT PLAGIOCLASE

	6	6	6	6	7	8	8	9	9	9
SIO2	61.70	62.80	62.03	61.14	69.62	61.82	61.93	61.16	62.00	62.48
TIO2										
AL2O3	23.76	22.70	22.65	24.05	19.23	23.40	23.56	23.62	23.31	23.19
CR2O3										
FE2O3										
FEO	.01	.01	.01	.01	.01	.01	.01	.01	.17	.20
MNO										
MGO	.01	.01	.01	.01	.01	.01	.01	.01	.01	.01
CAO	5.57	4.68	4.68	5.97	.09	5.39	5.39	5.77	5.44	5.25
NA2O	8.33	8.66	8.54	7.74	11.70	8.19	8.10	8.10	8.20	8.11
K2O	.08	.20	.18	.23	.01	.35	.32	.35	.52	.54
NIO										
TOTAL	99.46	99.06	98.10	99.15	100.67	99.17	99.32	99.02	99.65	99.78
OXYGEN	8	8	8	8	8	8	8	8	8	8
SI	2.749	2.802	2.795	2.734	3.015	2.763	2.762	2.743	2.764	2.777
TI										
AL	1.248	1.194	1.203	1.268	.982	1.233	1.239	1.249	1.225	1.215
CR										
FE3+										
FE2+									.006	.007
MN										
MG	.001	.001	.001	.001	.001	.001	.001	.001	.001	.001
CA	.266	.224	.226	.286	.004	.258	.258	.277	.260	.250
NA	.720	.749	.746	.671	.983	.710	.700	.704	.709	.699
K	.005	.011	.010	.013	.001	.020	.018	.020	.030	.031
NI										
SUM	4.989	4.981	4.982	4.974	4.985	4.985	4.978	4.995	4.993	4.980
AN	26.9	22.7	23.0	29.5	.4	26.1	26.4	27.7	26.0	25.5
AB	72.68	76.11	75.95	69.17	99.52	71.85	71.75	70.32	71.01	71.35
OR	.46	1.16	1.05	1.35	.06	2.02	1.87	2.00	2.96	3.13

*** ALL ZERO VALUES PRINTED AS BLANKS ***

SAMPLE DESCRIPTIONS :

6	: PLG	MID	KF40
6	: PLG	MID	"
6	: PLG	MID	"
6	: PLG	MID	"
7	: PLG	MID	KF28
8	: PLG	MID	KF96
8	: PLG	MID	"
9	: PLG	MID	KF112
9	: PLG	MID	"
9	: PLG	MID	"

KVT PLAGIOCLASE

	10	10	10	10	10	10	11	11	11	12
SIO2	62.43	63.37	60.28	62.79	62.25	62.41	63.36	61.57	63.40	61.01
TIO2										
AL2O3	23.76	23.07	24.07	23.28	23.14	23.14	22.02	23.22	22.31	24.16
CR2O3										
FE2O3										
FEO	.19	.26	.01	.01	.01	.01	.01	.01	.01	.01
MNO										
MGO	.01	.01	.01	.01	.01	.01	.01	.01	.01	.01
CAO	5.27	4.92	6.22	5.28	4.98	5.29	4.34	5.46	4.31	6.47
NA2O	8.26	8.48	7.58	8.34	8.27	8.41	8.88	8.14	8.68	7.53
K2O	.29	.49	.26	.41	.46	.30	.39	.38	.45	.41
NIO										
TOTAL	100.21	100.60	98.43	100.12	99.12	99.57	99.01	98.79	99.17	99.60
OXYGEN	8	8	8	8	8	8	8	8	8	8
SI	2.761	2.792	2.720	2.779	2.781	2.777	2.829	2.764	2.824	2.723
TI										
AL	1.239	1.198	1.280	1.214	1.218	1.214	1.159	1.229	1.171	1.271
CR										
FE3+										
FE2+	.007	.010								
MN										
MG	.001	.001	.001	.001	.001	.001	.001	.001	.001	.001
CA	.250	.232	.301	.250	.238	.252	.208	.263	.206	.309
NA	.708	.724	.663	.716	.716	.726	.769	.709	.750	.652
K	.016	.028	.015	.023	.026	.017	.022	.022	.026	.023
NI										
SUM	4.982	4.985	4.979	4.983	4.981	4.987	4.987	4.987	4.978	4.979
AN	25.6	23.6	30.7	25.3	24.3	25.4	20.8	26.5	21.0	31.4
AB	72.69	73.60	67.75	72.35	73.03	72.94	76.98	71.36	76.42	66.20
OR	1.68	2.80	1.53	2.34	2.67	1.71	2.22	2.19	2.61	2.37

*** ALL ZERO VALUES PRINTED AS BLANKS ***

SAMPLE DESCRIPTIONS :

10	: PLG	MID	KF119
10	: PLG	MID	"
10	: PLG	MID	"
10	: PLG	MID	"
10	: PLG	MID	"
10	: PLG	MID	"
11	: PLG	MID	KF110
11	: PLG	MID	"
11	: PLG	MID	"
12	: PLG	MID	KF32

KVT PLAGIOCLASE

	5	5	6	6	7	8	9	10	10	10
SIO2	64.38	64.15	65.08	64.79	69.46	62.91	63.64	63.19	62.38	63.15
TIO2										
AL2O3	22.20	22.33	21.60	21.91	19.42	23.18	22.54	22.45	23.29	22.86
CR2O3										
FE2O3										
FEO	.01	.18	.01	.01	.01	.01	.01	.19	.01	.01
MNO										
MGO	.01	.01	.01	.01	.01	.01	.01	.01	.01	.01
CAO	3.69	3.91	3.19	3.52	.17	4.81	4.37	4.87	5.22	4.55
NA2O	9.21	9.23	9.32	9.57	11.52	8.52	8.88	8.87	8.52	8.73
K2O	.21	.19	.08	.11	.01	.27	.19	.15	.22	.25
NIO										
TOTAL	99.71	100.00	99.29	99.92	100.60	99.71	99.64	99.73	99.65	99.56
OXYGEN	8	8	8	8	8	8	8	8	8	8
SI	2.845	2.832	2.878	2.856	3.010	2.790	2.820	2.806	2.773	2.803
TI										
AL	1.156	1.162	1.126	1.139	.992	1.212	1.177	1.175	1.220	1.196
CR										
FE3+										
FE2+		.007						.007		
MN										
MG	.001	.001	.001	.001	.001	.001	.001	.001	.001	.001
CA	.175	.185	.151	.166	.008	.229	.207	.232	.249	.216
NA	.789	.790	.799	.818	.968	.733	.763	.764	.734	.751
K	.012	.011	.005	.006	.001	.015	.011	.008	.012	.014
NI										
SUM	4.978	4.987	4.960	4.986	4.979	4.979	4.979	4.993	4.990	4.982
AN	17.9	18.8	15.8	16.8	.8	23.4	21.1	23.1	25.0	22.0
AB	80.88	80.15	83.70	82.59	99.14	75.03	77.76	76.07	73.77	76.52
OR	1.21	1.09	.47	.63	.06	1.56	1.10	.85	1.25	1.44

*** ALL ZERO VALUES PRINTED AS BLANKS ***

SAMPLE DESCRIPTIONS :

5 : PLG EDGE KF68
5 : PLG EDGE "
6 : PLG EDGE KF40
6 : PLG EDGE "
7 : PLG EDGE KF28
8 : PLG EDGE KF96
9 : PLG EDGE KF112
10 : PLG EDGE KF119
10 : PLG EDGE "
10 : PLG EDGE "

	11	11	11	12	12
SIO2	64.44	63.20	64.87	65.32	64.19
TIO2					
AL2O3	21.35	22.10	21.51	21.28	21.72
CR2O3					
FE2O3					
FEO	.16	.01	.01	.01	.01
MNO					
MGO	.01	.01	.01	.01	.01
CAO	3.32	4.28	3.11	2.84	3.52
NA2O	9.58	8.94	9.43	9.84	9.41
K2O	.25	.26	.22	.21	.21
NIO					
TOTAL	99.11	98.80	99.16	99.51	99.07
OXYGEN	8	8	8	8	8
SI	2.867	2.826	2.877	2.887	2.856
TI					
AL	1.120	1.165	1.124	1.109	1.139
CR					
FE3+					
FE2+	.006				
MN					
MG	.001	.001	.001	.001	.001
CA	.158	.205	.148	.134	.168
NA	.827	.775	.811	.843	.812
K	.014	.015	.012	.012	.012
NI					
SUM	4.993	4.987	4.973	4.986	4.987
AN	15.8	20.6	15.2	13.6	16.9
AB	82.74	77.90	83.50	85.21	81.87
OR	1.42	1.49	1.28	1.20	1.20

*** ALL ZERO VALUES PRINTED AS BLANKS ***

SAMPLE DESCRIPTIONS :

11	:	PLG	EDGE KF110
11	:	PLG	EDGE "
11	:	PLG	EDGE "
12	:	PLG	EDGE KF32
12	:	PLG	EDGE "

KVT HORNBLENDES

	1	2	3	4	5	6	7	8	9	10
SIO2	48.24	50.28	48.44	48.67	47.42	48.80	48.61	50.07	48.44	50.52
TIO2	.85	.66	1.02	1.03	1.40	.92	1.18	.58	1.09	.70
AL203	5.84	5.33	6.47	6.40	7.25	6.12	6.53	5.29	6.39	5.42
CR203	.01	.01	.01	.10	.01	.01	.01	.01	.01	.01
FE203										
FEO	13.76	13.57	15.17	14.75	15.81	15.55	15.03	13.89	15.05	13.78
MNO	.44	.44	.39	.37	.40	.52	.41	.44	.35	.43
MGO	14.45	14.99	13.61	13.75	13.02	13.27	13.69	14.68	13.38	14.43
CAO	11.97	12.00	11.88	12.03	11.80	11.65	11.31	12.33	11.43	12.13
NA2O	.97	.92	1.17	1.13	1.35	1.18	1.41	.72	1.48	.80
K2O	.38	.37	.45	.45	.50	.54	.45	.42	.40	.39
NIO										
TOTAL	96.91	98.57	98.61	98.68	98.96	98.56	98.63	98.43	98.02	98.61
OXYGEN	23	23	23	23	23	23	23	23	23	23
SI	7.134	7.272	7.082	7.097	6.946	7.149	7.092	7.269	7.115	7.303
TI	.095	.072	.112	.113	.154	.101	.129	.063	.120	.076
AL	1.018	.909	1.115	1.100	1.252	1.057	1.123	.905	1.106	.924
CR	.001	.001	.001	.012	.001	.001	.001	.001	.001	.001
FE3+										
FE2+	1.702	1.641	1.855	1.799	1.937	1.905	1.834	1.687	1.849	1.666
MN	.055	.054	.048	.046	.050	.065	.051	.054	.044	.053
MG	3.185	3.231	2.965	2.988	2.842	2.897	2.977	3.176	2.929	3.109
CA	1.897	1.860	1.861	1.880	1.852	1.829	1.768	1.918	1.799	1.879
NA	.278	.258	.332	.319	.383	.335	.399	.203	.422	.224
K	.072	.068	.084	.084	.093	.101	.084	.078	.075	.072
NI										
SUM	15.437	15.365	15.456	15.436	15.511	15.439	15.458	15.354	15.459	15.306

*** ALL ZERO VALUES PRINTED AS BLANKS ***

SAMPLE DESCRIPTIONS :

1 : HBL-KF68 (4)
2 : HBL-KF39 (3)
3 : HBL-KF93 (6)
4 : HBL(xenolith)-KF93 (2)
5 : HBL-KF96 (5)
6 : HBL-KF112 (3)
7 : HBL-KF119 (3)
8 : HBL-KF32 (3)
9 : HBL-KF104 (4)
10 : H8L-KF87 (4)

	11	12	13	14
SIO2	48.20	47.09	47.89	48.95
TIO2	1.65	1.28	1.63	.85
AL2O3	6.93	6.97	7.30	6.15
CR2O3	.01	.01	.01	.01
FE2O3				
FEO	13.95	16.32	13.30	14.40
MNO	.24	.34	.21	.44
MGO	14.39	12.68	14.76	14.18
CAO	11.38	11.58	11.10	12.02
NA2O	1.45	1.38	1.72	1.06
K2O	.42	.51	.37	.38
NIO				
TOTAL	98.62	98.16	98.29	98.44
OXYGEN	23	23	23	23
SI	7.002	6.972	6.960	7.136
TI	.180	.143	.178	.093
AL	1.187	1.216	1.251	1.057
CR	.001	.001	.001	.001
FE3+				
FE2+	1.695	2.021	1.617	1.756
MN	.030	.043	.026	.054
MG	3.115	2.798	3.197	3.081
CA	1.771	1.837	1.729	1.878
NA	.408	.396	.485	.300
K	.078	.096	.069	.071
NI				
SUM	15.467	15.523	15.512	15.427

*** ALL ZERO VALUES PRINTED AS BLANKS ***

SAMPLE DESCRIPTIONS :

11 : HBL-KF 11 (2)
12 : HBL-KF65 (6)
13 : HBL-KF11 (2)
14 : HBL-KF14 (1)

KVT CHLORITE

	1	1	1	1	1	2	2	2	2	3
SIO2	29.11	27.35	28.38	28.38	27.04	27.66	27.76	28.05	26.65	27.60
TIO2	.01	.01	.18	.19	.12	.09	.31	.56	.10	.01
AL2O3	18.91	18.75	18.04	17.69	19.12	19.26	18.14	17.68	19.79	19.40
CR2O3	.01	.01	.01	.01	.01	.01	.01	.11	.01	.01
FE2O3										
FEO	17.79	22.76	23.53	22.78	23.08	24.74	23.50	22.79	24.96	21.82
MNO	.27	.37	.36	.31	.32	.37	.29	.36	.41	.36
MGO	21.80	17.90	18.19	18.07	17.05	17.02	17.32	17.40	16.70	18.89
CAO	.10	.01	.18	.15	.01	.01	.17	.49	.01	.10
NA2O	.01	.01	.01	.01	.06	.01	.01	.01	.01	.01
K2O	.01	.01	.01	.01	.01	.08	.13	.01	.01	.01
NIO										
TOTAL	88.02	87.18	88.89	87.60	86.82	89.25	87.64	87.46	88.65	88.21
OXYGEN	22	22	22	22	22	22	22	22	22	22
SI	4.594	4.493	4.583	4.633	4.468	4.476	4.556	4.599	4.356	4.453
TI	.001	.001	.022	.023	.015	.011	.038	.069	.012	.001
AL	3.518	3.630	3.434	3.404	3.724	3.673	3.509	3.417	3.813	3.689
CR	.001	.001	.001	.001	.001	.001	.001	.014	.001	.001
FE3+										
FE2+	2.348	3.127	3.178	3.110	3.190	3.348	3.225	3.125	3.412	2.944
MN	.036	.051	.049	.043	.045	.051	.040	.050	.057	.049
MG	5.127	4.382	4.378	4.397	4.199	4.104	4.236	4.252	4.068	4.542
CA	.017	.002	.031	.026	.002	.002	.030	.086	.002	.017
NA	.003	.003	.003	.003	.019	.003	.003	.003	.003	.003
K	.002	.002	.002	.002	.002	.017	.027	.002	.002	.002
NI										
SUM	15.648	15.693	15.680	15.643	15.665	15.686	15.666	15.619	15.727	15.703

*** ALL ZERO VALUES PRINTED AS BLANKS ***

SAMPLE DESCRIPTIONS :

1 : CHL-BIOT KF93
1 : CHL-BIOT
1 : CHL-BIOT
1 : CHL-BIOT
1 : CHL-HBL
2 : CHL-XENOLITH KF93
2 : CHL-XENOLITH
2 : CHL-XENOLITH
2 : CHL-XENOLITH
3 : CHL-BIOT KF68

KVT CHLORITE

	3	3	3	3	3	3	4	4	4	4
SIO2	29.24	27.75	27.97	27.72	28.20	25.20	27.76	34.89	30.00	33.80
TIO2	3.82	1.03	.01	.13	.53	.18	.01	.72	.13	.53
AL2O3	17.36	18.68	18.11	18.34	17.15	18.74	20.88	17.38	17.95	17.32
CR2O3	.01	.01	.01	.01	.01	.01	.01	.01	.10	.16
FE2O3										
FEO	19.62	21.35	20.77	21.26	19.60	20.59	20.27	20.62	22.55	20.83
MNO	.33	.37	.43	.44	.30	.44	.42	.24	.29	.31
MGO	17.12	17.88	19.21	19.07	17.96	18.93	20.17	14.78	17.72	15.58
CAO	3.59	.96	.01	.07	.62	.13	.06	.01	.14	.01
NA2O	.01	.01	.01	.01	.01	.01	.01	.07	.01	.01
K2O	.01	.01	.01	.13	.18	.01	.01	6.76	1.17	5.17
NIO										
TOTAL	91.11	88.05	86.54	87.18	84.56	84.24	89.60	95.48	90.06	93.72
OXYGEN	22	22	22	22	22	22	22	22	22	22
SI	4.562	4.491	4.579	4.524	4.710	4.272	4.365	5.277	4.766	5.184
TI	.448	.125	.001	.016	.067	.023	.001	.082	.016	.061
AL	3.193	3.563	3.495	3.528	3.376	3.745	3.870	3.098	3.362	3.131
CR	.001	.001	.001	.001	.001	.001	.001	.001	.013	.019
FE3+										
FE2+	2.560	2.889	2.844	2.902	2.738	2.919	2.666	2.608	2.996	2.672
MN	.044	.051	.060	.061	.042	.063	.056	.031	.039	.040
MG	3.981	4.312	4.687	4.638	4.470	4.783	4.727	3.331	4.196	3.561
CA	.600	.166	.002	.012	.111	.024	.010	.002	.024	.002
NA	.003	.003	.003	.003	.003	.003	.003	.021	.003	.003
K	.002	.002	.002	.027	.038	.002	.002	1.304	.237	1.012
NI										
SUM	15.395	15.604	15.674	15.711	15.556	15.835	15.701	15.754	15.651	15.686

*** ALL ZERO VALUES PRINTED AS BLANKS ***

SAMPLE DESCRIPTIONS :

3 : CHL-BIOT
3 : CHL-BIOT
3 : CHL-HBL
3 : CHL-HBL
3 : CHL-HBL
3 : CHL-HBL
4 : CHL-HBL KF39
4 : CHL-VEIN
4 : CHL-vein
4 : CHL-vein

KVT CHLORITE

	1	1	1	1	1	2	2	2	2	3
SIO2	29.11	27.35	28.38	28.38	27.04	27.66	27.76	28.05	26.65	27.60
TIO2	.01	.01	.18	.19	.12	.09	.31	.56	.10	.01
AL2O3	18.91	18.75	18.04	17.69	19.12	19.26	18.14	17.68	19.79	19.40
CR2O3	.01	.01	.01	.01	.01	.01	.01	.11	.01	.01
FE2O3										
FEO	17.79	22.76	23.53	22.78	23.08	24.74	23.50	22.79	24.96	21.82
MNO	.27	.37	.36	.31	.32	.37	.29	.36	.41	.36
MGO	21.80	17.90	18.19	18.07	17.05	17.02	17.32	17.40	16.70	18.89
CAO	.10	.01	.18	.15	.01	.01	.17	.49	.01	.10
NA2O	.01	.01	.01	.01	.06	.01	.01	.01	.01	.01
K2O	.01	.01	.01	.01	.01	.08	.13	.01	.01	.01
NIO										
TOTAL	88.02	87.18	88.89	87.60	86.82	89.25	87.64	87.46	88.65	88.21
OXYGEN	22	22	22	22	22	22	22	22	22	22
SI	4.594	4.493	4.583	4.633	4.468	4.476	4.556	4.599	4.356	4.453
TI	.001	.001	.022	.023	.015	.011	.038	.069	.012	.001
AL	3.518	3.630	3.434	3.404	3.724	3.673	3.509	3.417	3.813	3.689
CR	.001	.001	.001	.001	.001	.001	.001	.014	.001	.001
FE3+										
FE2+	2.348	3.127	3.178	3.110	3.190	3.348	3.225	3.125	3.412	2.944
MN	.036	.051	.049	.043	.045	.051	.040	.050	.057	.049
MG	5.127	4.382	4.378	4.397	4.199	4.104	4.236	4.252	4.068	4.542
CA	.017	.002	.031	.026	.002	.002	.030	.086	.002	.017
NA	.003	.003	.003	.003	.019	.003	.003	.003	.003	.003
K	.002	.002	.002	.002	.002	.017	.027	.002	.002	.002
NI										
SUM	15.648	15.693	15.680	15.643	15.665	15.686	15.666	15.619	15.727	15.703

*** ALL ZERO VALUES PRINTED AS BLANKS ***

SAMPLE DESCRIPTIONS :

1 : CHL-BIOT KF93
1 : CHL-BIOT "
1 : CHL-BIOT "
1 : CHL-BIOT "
1 : CHL-HBL "
2 : CHL-XENOLITH KF93
2 : CHL-XENOLITH "
2 : CHL-XENOLITH "
2 : CHL-XENOLITH "
3 : CHL-BIOT KF68

KVT CHLORITE

	3	3	3	3	3	3	4	4	4	4
SIO2	29.24	27.75	27.97	27.72	28.20	25.20	27.76	34.89	30.00	33.80
TIO2	3.82	1.03	.01	.13	.53	.18	.01	.72	.13	.53
AL2O3	17.36	18.68	18.11	18.34	17.15	18.74	20.88	17.38	17.95	17.32
CR2O3	.01	.01	.01	.01	.01	.01	.01	.01	.10	.16
FE2O3										
FEO	19.62	21.35	20.77	21.26	19.60	20.59	20.27	20.62	22.55	20.83
MNO	.33	.37	.43	.44	.30	.44	.42	.24	.29	.31
MGO	17.12	17.88	19.21	19.07	17.96	18.93	20.17	14.78	17.72	15.58
CAO	3.59	.96	.01	.07	.62	.13	.06	.01	.14	.01
NA2O	.01	.01	.01	.01	.01	.01	.01	.07	.01	.01
K2O	.01	.01	.01	.13	.18	.01	.01	6.76	1.17	5.17
NIO										
TOTAL	91.11	88.05	86.54	87.18	84.56	84.24	89.60	95.48	90.06	93.72
OXYGEN	22	22	22	22	22	22	22	22	22	22
SI	4.562	4.491	4.579	4.524	4.710	4.272	4.365	5.277	4.766	5.184
TI	.448	.125	.001	.016	.067	.023	.001	.082	.016	.061
AL	3.193	3.563	3.495	3.528	3.376	3.745	3.870	3.098	3.362	3.131
CR	.001	.001	.001	.001	.001	.001	.001	.001	.013	.019
FE3+										
FE2+	2.560	2.889	2.844	2.902	2.738	2.919	2.666	2.608	2.996	2.672
MN	.044	.051	.060	.061	.042	.063	.056	.031	.039	.040
MG	3.981	4.312	4.687	4.638	4.470	4.783	4.727	3.331	4.196	3.561
CA	.600	.166	.002	.012	.111	.024	.010	.002	.024	.002
NA	.003	.003	.003	.003	.003	.003	.003	.021	.003	.003
K	.002	.002	.002	.027	.038	.002	.002	1.304	.237	1.012
NI										
SUM	15.395	15.604	15.674	15.711	15.556	15.835	15.701	15.754	15.651	15.686

*** ALL ZERO VALUES PRINTED AS BLANKS ***

SAMPLE DESCRIPTIONS :

3	:	CHL-BIOT KF68
3	:	CHL-BIOT "
3	:	CHL-HBL "
3	:	CHL-HBL "
3	:	CHL-HBL "
3	:	CHL-HBL "
4	:	CHL-HBL KF39
4	:	CHL-VEIN "
4	:	CHL-vein "
4	:	CHL-vein "

KVT CHLORITE

	5	5	5	5	6	6	6	6	6	7
SIO2	33.93	35.77	29.25	27.03	27.79	29.51	27.58	28.05	27.21	28.90
TIO2	.65	2.33	.01	.01	.01	2.43	.01	.18	.33	1.61
AL2O3	17.20	15.85	18.21	20.62	19.44	17.75	19.67	19.59	20.80	18.14
CR2O3	.01	.01	.01	.01	.01	.01	.01	.01	.01	.01
FE2O3										
FEO	18.91	17.37	20.08	21.41	24.01	20.54	23.04	23.48	23.88	20.23
MNO	.34	.23	.32	.37	.27	.24	.28	.37	.36	.30
MGO	16.04	14.81	20.67	19.24	18.31	17.16	18.28	18.09	17.63	19.21
CAO	.01	1.16	.01	.01	.10	2.18	.01	.01	.29	1.35
NA2O	.01	.07	.01	.01	.01	.01	.01	.08	.01	.01
K2O	6.12	6.84	.18	.01	.01	.20	.01	.33	.05	.01
NIO										
TOTAL	93.22	94.44	88.75	88.72	89.96	90.03	88.90	90.19	90.57	89.77
OXYGEN	22	22	22	22	22	22	22	22	22	22
SI	5.213	5.407	4.639	4.326	4.440	4.654	4.437	4.464	4.319	4.555
TI	.075	.265	.001	.001	.001	.288	.001	.022	.039	.191
AL	3.115	2.824	3.404	3.890	3.661	3.300	3.730	3.675	3.891	3.370
CR	.001	.001	.001	.001	.001	.001	.001	.001	.001	.001
FE3+										
FE2+	2.430	2.196	2.663	2.866	3.208	2.709	3.100	3.125	3.170	2.667
MN	.044	.029	.043	.050	.037	.032	.038	.050	.048	.040
MG	3.673	3.336	4.885	4.589	4.360	4.033	4.383	4.291	4.170	4.513
CA	.002	.188	.002	.002	.017	.368	.002	.002	.049	.228
NA	.003	.021	.003	.003	.003	.003	.003	.025	.003	.003
K	1.200	1.319	.036	.002	.002	.040	.002	.067	.010	.002
NI										
SUM	15.755	15.586	15.677	15.730	15.730	15.429	15.698	15.722	15.702	15.571

*** ALL ZERO VALUES PRINTED AS BLANKS ***

SAMPLE DESCRIPTIONS :

5 : CHL-BIOT KF40
5 : CHL-HBL "
5 : CHL-HBL "
5 : CHL-vein "
6 : CHL-HBL KF 100
6 : CHL-BIOT "
6 : CHL-BIOT "
6 : CHL-BIOT "
6 : CHL-BIOT "
7 : CHL-HBL KF28

KVT CHLORITE

	7	7	8	8	9	9	9	10	11	11
SI02	27.79	28.38	27.77	28.11	27.25	27.12	26.30	27.06	26.49	27.26
TI02	.01	.01	5.95	.01	.01	.01	.01	.01	.01	.15
AL203	19.37	19.44	16.23	18.40	20.92	21.30	21.14	19.41	18.79	19.34
CR203	.01	.01	.01	.12	.01	.01	.01	.01	.01	.01
FE203										
FEO	22.40	21.33	20.91	24.45	20.88	22.08	21.98	24.22	26.11	25.28
MNO	.40	.29	.23	.34	.52	.53	.49	.43	.28	.40
MGO	18.82	19.66	14.27	18.38	19.72	18.54	18.56	17.67	16.48	16.59
CAO	.01	.12	4.87	.01	.01	.01	.01	.01	.01	.01
NA20	.01	.01	.01	.01	.01	.01	.01	.01	.01	.01
K20	.01	.01	.01	.01	.01	.01	.01	.01	.01	.13
NIO										
TOTAL	88.83	89.26	90.26	89.84	89.34	89.62	88.52	88.84	88.20	89.18
OXYGEN	22	22	22	22	22	22	22	22	22	22
SI	4.463	4.502	4.447	4.512	4.318	4.308	4.239	4.395	4.385	4.434
TI	.001	.001	.717	.001	.001	.001	.001	.001	.001	.018
AL	3.666	3.635	3.064	3.481	3.907	3.988	4.016	3.716	3.667	3.708
CR	.001	.001	.001	.015	.001	.001	.001	.001	.001	.001
FE3+										
FE2+	3.008	2.830	2.800	3.282	2.767	2.933	2.963	3.290	3.615	3.439
MN	.054	.039	.031	.046	.070	.071	.067	.059	.039	.055
MG	4.504	4.648	3.406	4.397	4.657	4.389	4.458	4.277	4.066	4.021
CA	.002	.020	.836	.002	.002	.002	.002	.002	.002	.002
NA	.003	.003	.003	.003	.003	.003	.003	.003	.003	.003
K	.002	.002	.002	.002	.002	.002	.002	.002	.002	.027
NI										
SUM	15.705	15.681	15.307	15.741	15.729	15.699	15.753	15.747	15.782	15.708

*** ALL ZERO VALUES PRINTED AS BLANKS ***

SAMPLE DESCRIPTIONS :

7	:	CHL-HBL KF28
7	:	CHL-HBL "
8	:	CHL-BIOT KF96
8	:	CHL-BIOT "
9	:	CHL-HBL KF112
9	:	CHl BIOT "
9	:	CHL-BIOT "
10	:	CHL-BIOT KF119
11	:	CHL-BIOT KF110
11	:	CHL-BIOT "

KVT CHLORITE

	11	12	13	13	14	14	14	15	15	16
SIO2	30.80	28.32	28.41	28.68	28.35	28.57	27.65	28.90	30.78	27.17
TIO2	.76	.45	.61	1.48	.25	.12	.01	3.64	1.24	.01
AL2O3	20.93	18.54	17.74	16.34	18.65	18.98	19.57	16.71	16.91	21.38
CR2O3	.01	.01	.01	.01	.01	.01	.01	.01	.01	.01
FE2O3										
FEO	22.08	18.89	24.23	23.44	20.99	21.30	21.67	19.82	20.69	20.59
MNO	.36	.48	.27	.20	.27	.37	.38	.33	.30	.35
MGO	13.00	19.89	17.33	17.34	19.36	19.38	19.13	16.99	18.34	19.66
CAO	.62	.42	.46	1.17	.21	.15	.08	3.18	.89	.09
NA2O	.08	.01	.01	.01	.01	.01	.01	.01	.09	.01
K2O	2.05	.23	.26	.19	.01	.01	.01	.08	.47	.01
NIO										
TOTAL	90.69	87.24	89.33	88.86	88.11	88.90	88.52	89.67	89.72	89.28
OXYGEN	22	22	22	22	22	22	22	22	22	22
SI	4.842	4.562	4.592	4.657	4.555	4.552	4.441	4.591	4.852	4.297
TI	.090	.055	.074	.181	.030	.014	.001	.435	.147	.001
AL	3.878	3.521	3.380	3.127	3.532	3.565	3.705	3.129	3.142	3.986
CR	.001	.001	.001	.001	.001	.001	.001	.001	.001	.001
FE3+										
FE2+	2.903	2.545	3.276	3.183	2.820	2.838	2.911	2.633	2.728	2.724
MN	.048	.066	.037	.028	.037	.050	.052	.044	.040	.047
MG	3.046	4.775	4.175	4.196	4.635	4.602	4.579	4.023	4.308	4.634
CA	.104	.072	.080	.204	.036	.026	.014	.541	.150	.015
NA	.024	.003	.003	.003	.003	.003	.003	.003	.028	.003
K	.411	.047	.054	.039	.002	.002	.002	.016	.095	.002
NI										
SUM	15.347	15.647	15.671	15.619	15.651	15.653	15.708	15.418	15.491	15.711

*** ALL ZERO VALUES PRINTED AS BLANKS ***

SAMPLE DESCRIPTIONS :

11 : CHL-BIOT KF110
12 : CHL-HBL KF32
13 : CHL-BIOT KF104
13 : CHL-BIOT "
14 : CHL-BIOT KF97
14 : CHL-BIOT "
14 : CHL-HBL "
15 : CHL-BIOT KF87
15 : CHL-HBL "
16 : CHL-HBL KF19

Table A.1: On the basis of 14 oxygen atoms, the average chlorite atomic proportions are presented.

	ATOMIC PROPORTION Al(IV)	STD DEV.	No. of CHLORITES ANALYSED
KF19	1.26	0.05	5
KF28	1.14	0.03	4
KF32	1.10	-	1
KF39	0.88	0.30	4
KF40	0.88	0.32	4
KF68	1.15	0.09	7
KF87	1.03	0.05	4
KF93	1.11	0.05	5
KF93-Xeno.	1.14	0.07	4
KF96	1.15	0.04	4
KF97	1.12	0.03	6
KF100	1.17	0.08	11
KF104	1.03	-	3
KF110	1.19	-	3
KF112	1.20	0.05	4
KF119	1.15	-	2

3.3 KVT MINERAL VARIATION CONTOURS

The following diagrams are contour plots of mineral volume percentages determined from point-counting. A total of 900 counts were done per thin-section and these values contoured using a SACLANTS graphics package (Chapter 3). The figures 4.14 have been constructed from these diagrams by copying the zones high-lighted by the contours.

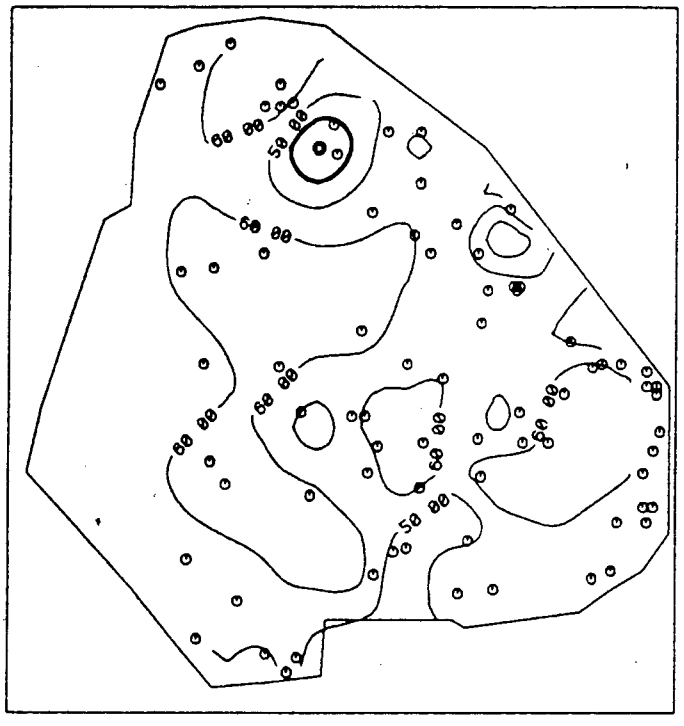

MODAL % PLAGIOCLASE

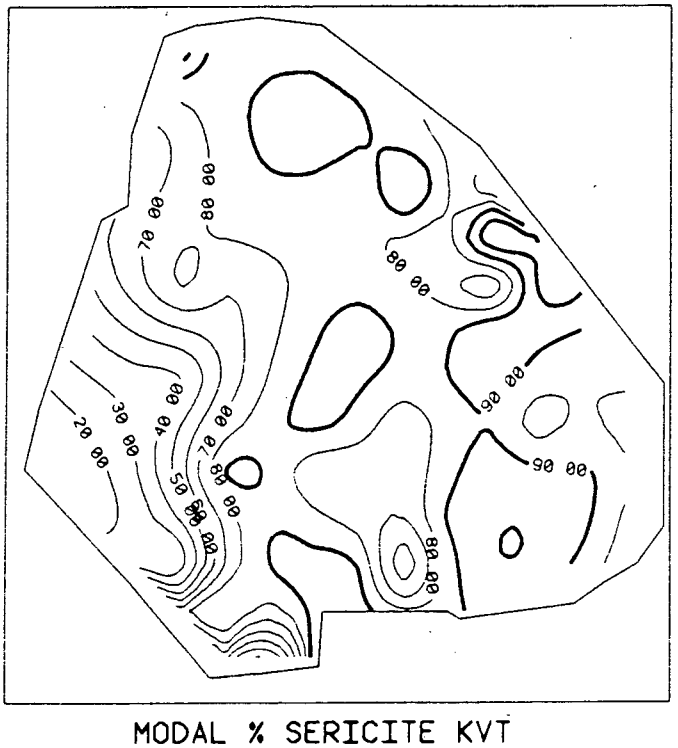

MODAL % SERICITE KVT

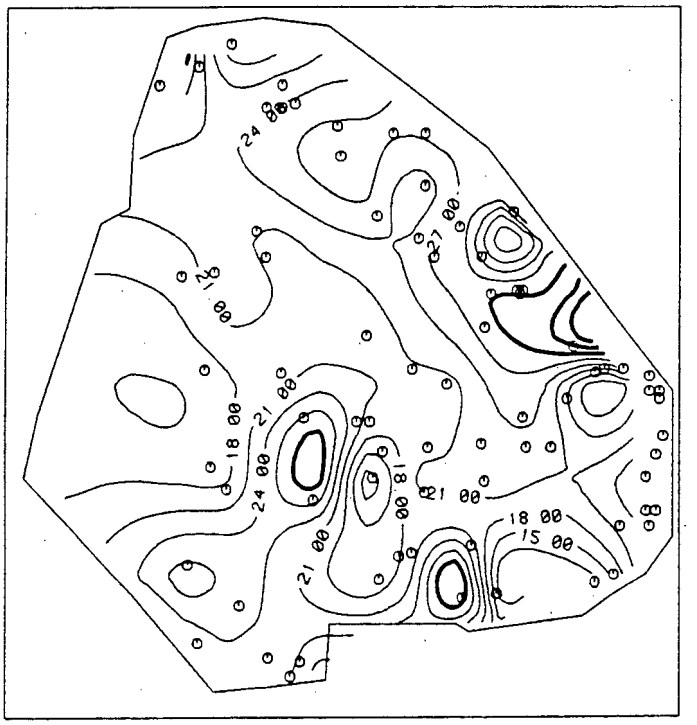

MODAL % QUARTZ

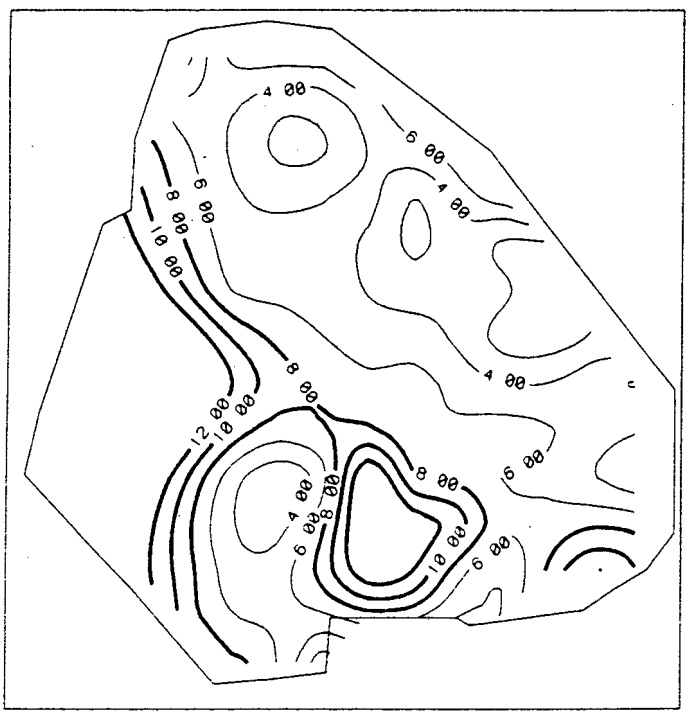

MODAL % HORNBLENDE KVT

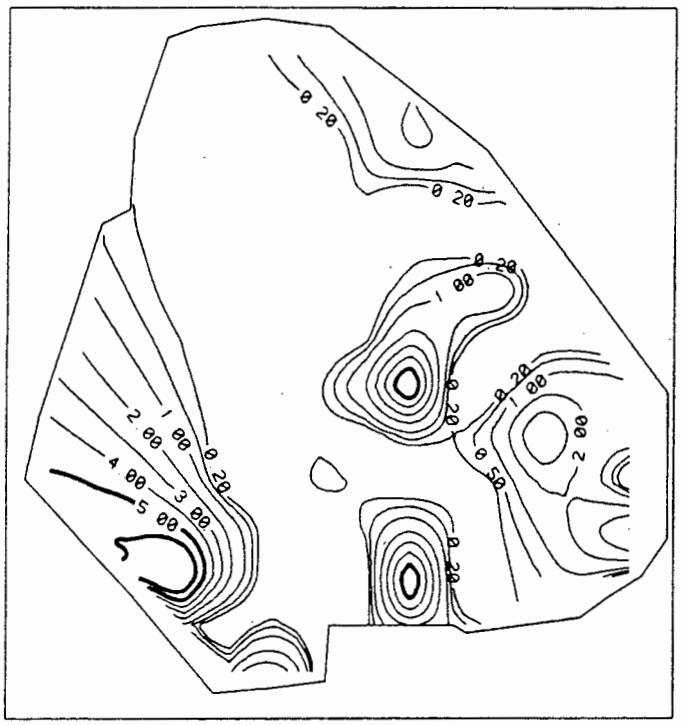

MODAL % BIOTITE KVT

MODAL % CHLORITE KVT

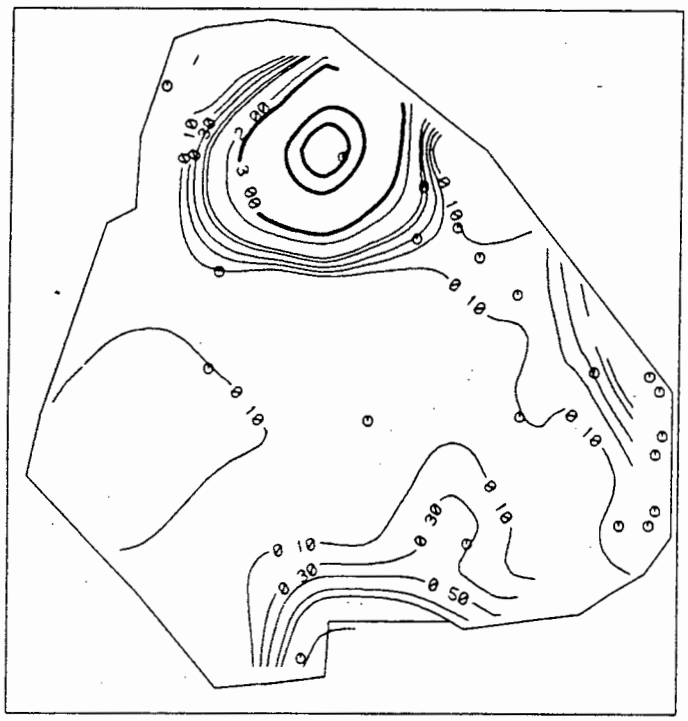

MODAL % CALCITE KVT

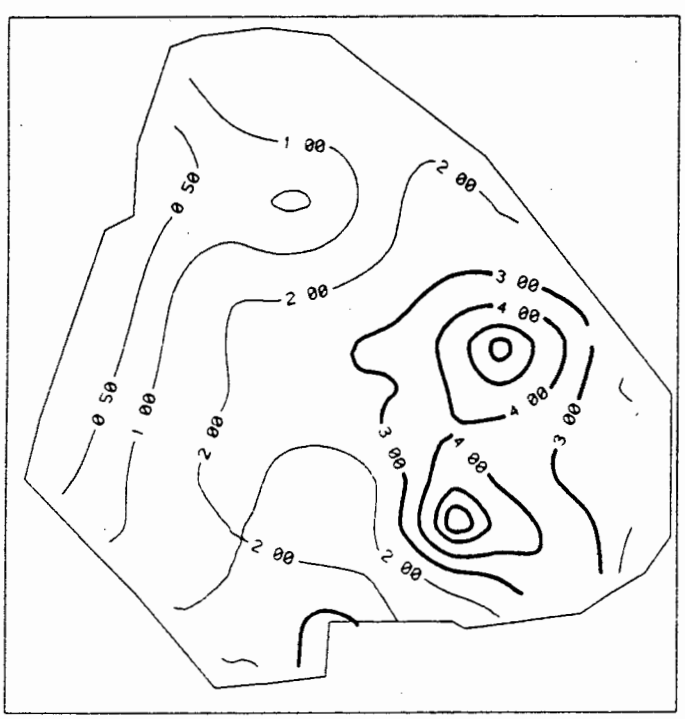

MODAL % EPIDOTE KVT

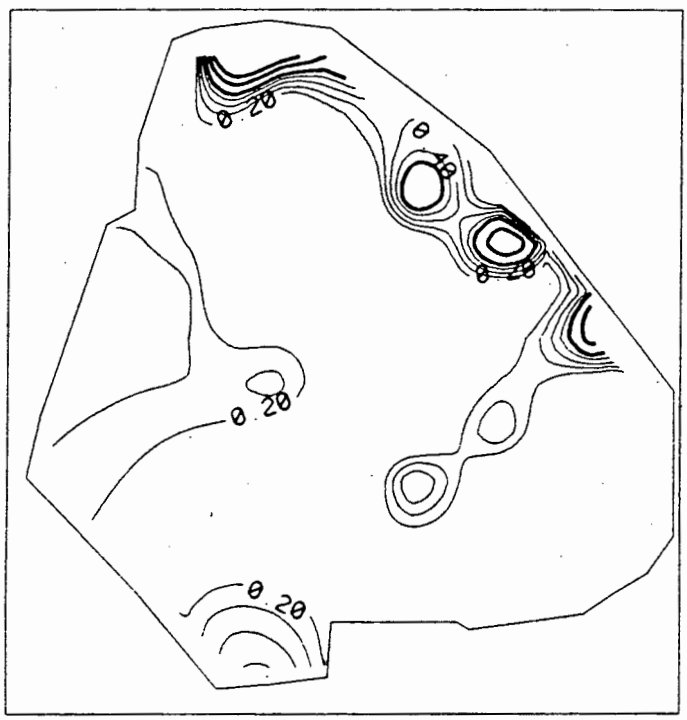

MODAL % SPHENE KVT

3.4 KVT $\delta^{18}O$ MINERAL CONTOURS

The $\delta^{18}O$ of the KVT minerals are contoured to establish the oxygen isotope variation of each mineral within the pluton. The $\delta^{18}O$ data is presented in Chapter 5, Table 5.1.

DELTA 18/16 OXYGEN-PLAGIOCLASE

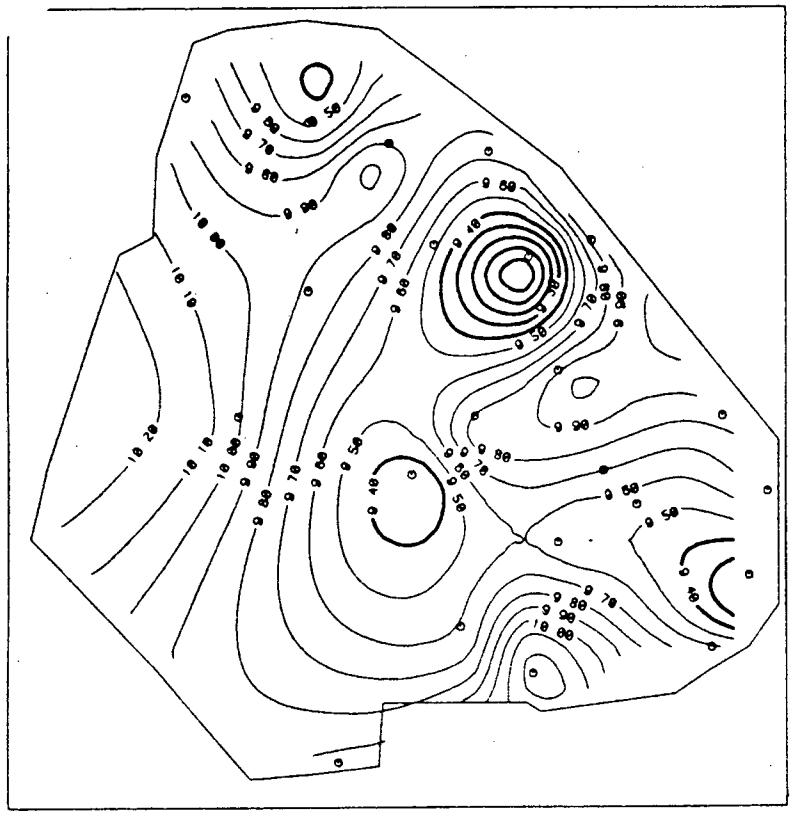

DELTA 18/16 OXYGEN QUARTZ

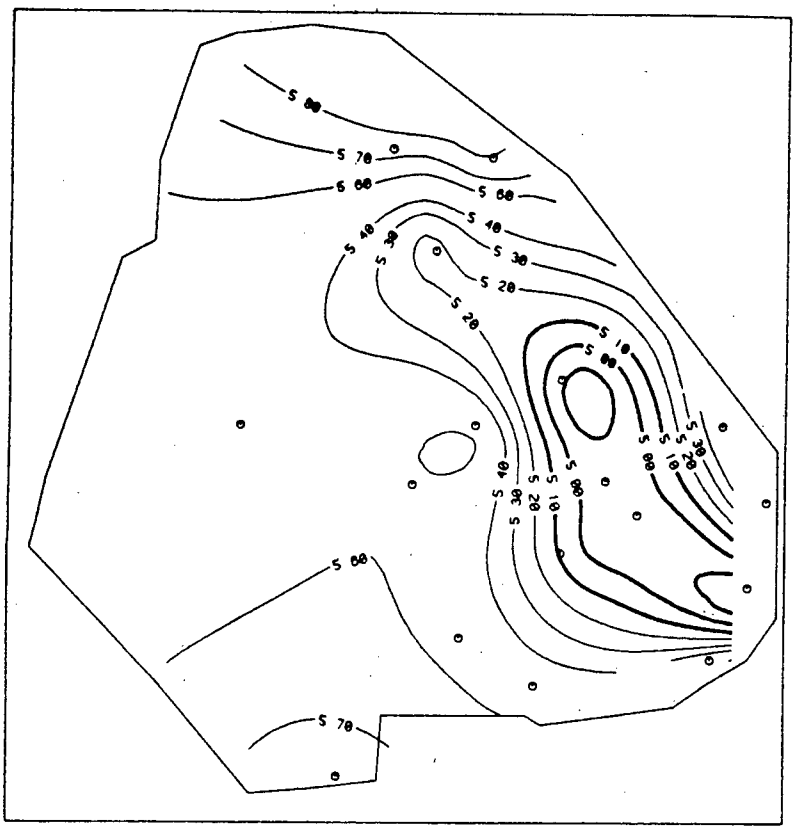

DELTA 18/16 OXYGEN-HORNBLENDE

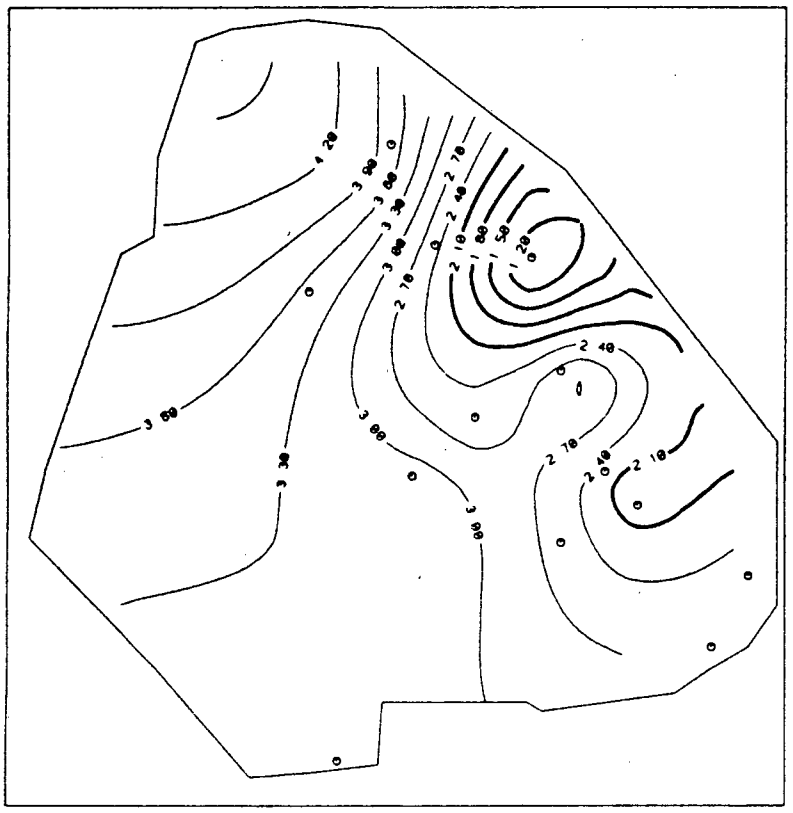

DELTA 18/16 OXYGEN-CHLORITE